Republic of Iraq
Ministry of Higher Education and Scientific Research
University of Babylon / College of Science for Women
Department of laser Physics

Theoretical Analysis of Nanocomposites Polymers' Properties for Optoelectronics Applications

A Thesis
Submitted to the Council of the College of Science for Women/

University of Babylon

In Partial Fulfillment of the Requirements for the Degree of Doctor of Philosophy in Laser Physics and its Applications

By

Wasan Mubdir Khilkhal

B.Sc. in laser physics / 2011

M.Sc. in Laser Physics and its Applications / 2015

Supervised by

Prof. Dr.

Ghaleb Ali Al-Dahash

2023A.D *1444 A.H*

يُؤْتِي الْحِكْمَةَ مَن يَشَاءُ ۚ وَمَن يُؤْتَ الْحِكْمَةَ فَقَدْ أُوتِيَ خَيْرًا
كَثِيرًا ۗ وَمَا يَذَّكَّرُ إِلَّا أُولُو الْأَلْبَابِ ﴿٢٦٩﴾

Supervisors Certification

I certify that this thesis entitled " **Theoretical Analysis of Nanocomposites Polymers' Properties for Optoelectronics Applications***" Was prepared by Wasan Mubdir Khilkhal under my supervision at University of Babylon , College of Science for Women, Laser Physics Department as Partial Fulfillment of the Requirements for the Degree of Doctor of Philosophy Science in Laser Physics and its applications.*

Signature

Supervisor: Dr.Ghaleb A. Al-Dahash

Title: Professor

Address: College of Science for Women-University of Babylon

Date: / /2023

In view of the available recommendations, I forwarded this thesis for debate by the examining committee.

Signature:

Name: Asst. Prof. Dr. Jinan Ali Abd

Title: Assistant Professor

Address: Head of Laser Physics

Department, College of Science for Women-University of Babylon

Date: / /2023

Examination Committee Certification

We certify that we have read this thesis entitled **" Theoretical Analysis of Nanocomposites Polymers' Properties for Optoelectronics Applications"** and as the examining committee, examined the student **" Wasan Mubdir Khilkhal"** in its contents and that, in our opinion meets of doctor of philosophy in laser physics and its application.

Signature
Name: **Dr. Enas M. Al-Robayi**
Title: **Professor**
Address: College of Science for women/ University of Babylon
Data: / / 2023
(Chairman)

Signature
Name: **Dr. Shorouk Sabah Abdul Abbas**
Title: **Professor**
Address: College of Education for Pure Sciences / University of Babylon
Data: / / 2023
(Member)

Signature
Name: **Sami Abdul Hussein Habana**
Title: **Asst. Professor**
Address: Hilla University College
Data: / / 2023
(Member)

Signature
Name **Oday Arkan Abbas Al-Owaedi**
Title: **Asst. Professor**
Address: : College of Science for women/ University of Babylon
Data: / / 2023
(Member)

Signature
Name: **Hussein Neama AL-Khegani**
Title: **Asst. Professor**
Address: : College of Science for women/ University of Babylon
Data: / / 2023
(Member)

Signature
Name: **Dr. Ghaleb Ali Al-Dahash**
Title: **Professor**
Address: : College of Science for women/ University of Babylon
Data: / / 2023
(Supervisor)

Approved by the University of Babylon a committee on graduate studies.

Signature
The Dean: **Dr. Abeer F. Al-Robayi**
Title: **Professor**
Address: College of Science for women/ University of Babylon
Date: / / 2023

Dedication

To the Shining stars that fill the sky with a faint smile to give me hope, power and support

All My Family Members especially My Gorgeous Daughter "Lian"

I dedicate this work.....

Wasan M. Khilkhal

Acknowledgements

All Praise and gratitude be to ALLAH, for His uncountable blessings, and best prayers and peace be upon His last messenger ***Mohammed****, his pure descendant and his noble companions .*

I wish to express my deepest gratitude and appreciation to my supervisors Dr. Ghaleb AliAl-dahash for proposing the title of the thesis and indeed for all the fruitful discussions and the constructing criticism all along,.

While I am writing the last stages of this work, I want to express my deep appreciation and sincere gratitude to all who helped me during the long phases of this work, for their skillful scientific guidance and discussions during the period time of this project .

Gratitude to all my professors in the Department of Laser Physics and who are the owners of the credit for what I've reached today

Last but not least, thanks to the members of my family and to all my friends who supported me a lot during study and were of great help especially my parents my husband and my daughter .

Wasan M. Khilkhal

Abstract

The electronic structure of newly proposed polymer nanocomposites was theoretically examined using density functional theory (DFT) at the B3LYP level. The DFT method was used in the Gaussian 09 program to calculate structural, electrical, and optical characteristics. The time-dependent (TD-DFT) method was used to calculate the ultraviolet-visible spectra of the structures under study.

The results showed that the polymer nanocomposite has a low LUMO-HOMO energy gap. This means that the electrons in the nanocomposite are more easily excited, which could lead to improved electrical and optical properties. The change in the Eg of the structure refers to different electronic behaviors. For example, adding nanoparticles to the polymer causes H to decrease and S to increase. This suggests that the nanoparticles are interacting with the polymer in a way that changes the electronic structure of the material.

The electronic and thermoelectric properties of Dye-polymer-Dye junctions were also demonstrated. This is important for the future of molecular electronics, as it could lead to the development of new devices with improved performance. To investigate this, the SIESTA code was used using a combination of DFT and the transport theory Green's function formalism.

In summary, this study used DFT to investigate the electronic structure of polymer nanocomposites and Dye-polymer-Dye junctions.

The results showed that these materials have potential for improved electrical and optical properties, as well as thermoelectric performance.

CONTENTS

LIST OF SYMBOLS

SYMBOL	**DESCRIPTION**
Ψ	Wave function
$\hat{H}$	Hamiltonian operator
$\hbar$	Reduce Dirac constant $(1.054571628 \times 10^{-34}\,\mathrm{J.S})$
$\hat{T}$	Kinetic energy
∇^2	Laplacian operator
$\hat{V}$	Potential energy
E	Energy of the system
$\vec{r}, R$	The electron and the nuclei spatial coordinates
$N_{elec.}$	Numbers of electrons
$N_{nucl.}$	Numbers of nuclei
$\hat{T}_{elec.}$	Kinetic energy of electron
$\hat{T}_{nucl.}$	Kinetic energy of nuclear
$\hat{V}_{nucl.\ elec.}$	Potential energy between nucleus-electronic
$\hat{V}_{elec.\ elec.}$	Potential energy between electronic-electronic
$\hat{V}_{nucl.\ nucl.}$	Potential energy between nucleus -nucleus
$\Psi_{tot.}$	Total wave function
$\Psi_{elec.}$	Wave function of electron
$\Psi_{nucl.}$	Wave function of nucleus
E_o	Energy of the ground state
Φ	Trial function
α	Spin up
β	Spin down
Ψ_i	The molecular orbitals

$\hat{F}$	Fock operator
$C_{\mu i}$	Molecular orbital expansion coefficients
ε_i	One-electron energy of the molecular
$S_{\mu\nu}$	Overlap matrix
$\rho(\vec{r})$	Electron density
$F_{HK}[\rho]$	Hohenberg-Kohn operator
$\hat{V}_{ext.}(\vec{r})$	External potential
$F_{HK}[\rho]$	Hohenberg-Kohn operator
$T_{KS}[\rho]$	Kohn-Sham Kinetic energy
$E_{XC}[\rho]$	Exchange-correlation energy
$\varepsilon_{XC}(\rho(\vec{r}))$	Exchange-correlation energy per particle of an electron gas
E_{gap}	Energy gap
fem	Emission oscillator strength
σem	Emission cross section
$g(z, z')$	Green's function
v_g	group velocity
μ_L, μ_R	chemical potential at the contacts
γ	Hopping Parameters
δI	the incident electric current
δV	Voltage
S	Scattering matrix
E_{HOMO}	Energy of HOMO
E_{LUMO}	Energy of LUMO
E_T	Total energy
I_E	Ionization Energy

E_A	Electron affinity
μ	Chemical potential
H	Hardness
S	Softness
ω	Electrophilicity index
E_N	Electronegativity
G	electrical conductance
E	Electrical field
G_0	quantum of conductance
f(E)	Fermi energy
$\boldsymbol{S}$	Seebeck coefficient
L	(C…C), molecule length
D	(Au…Au), is the molecular length
X	the bond length (Au…C)
Z	theoretical electrodes separation
T(E)	Transmission coefficient

LIST OF ABBREVIATIONS

ABBREVIATION	SYMBOL
TMO	Transition Metal Oxides
OSSLs	Organic Solid-State Lasers
PVA	Poly (Vinyl Alcohol
PEG	Polyethylene glycol
PS	Polystyrene
PMMA	Poly Methyl-Methacrylate
ZnO	Zinc Oxide
Br	Bromine
B3LYP	Becke three parameters Lee-Yang-Par
BO	Born-Oppenheimer
DFT	Density Function Theory
DOS	Density of States
GGA	Generalized Gradient Approximation
G09	Gaussian 2009
GS	Ground State
GTO	Gaussian Type Orbital
HF	Hartree-Fock
HOMO	Higher Occupied Molecular Orbital
HK	Hohenberg-Kohn
IR	Infrared Radiation
KS	Kohn-Sham
LUMO	Lowest Unoccupied Molecular Orbital
LDA	Local Density Approximation
LSDA	Local Spin Density Approximation

MO	Molecular Orbitals
SD	Slater Determinant
SCF	Self-Consistent-Field
STO	Slater Type Orbital
TD-SCF	Time-Dependent Self-Consistent-Field
TD-DFT	Time Dependent Density Functional
UV-Vis.	Ultraviolet-Visible

LIST OF FIGURES

LIST OF TABLES

Chapter one

Introduction

1.1. Nanotechnology

A branch of applied science and technology known as nanotechnology deals with materials with large surfaces at the nanoscale [1]. It is broad range of applications in the sciences, industries, biotechnology, and nanoscience are what are driving the field's rapid development.

When a material is limited to nano level, it acts differently and shows novel characteristic that it does not have in its macro scale or bulk form. As a bridge between solid materials and atomic and/or molecular structures, nanoparticles are of tremendous interest [2,3]. Recently, there has been a significant interest in nanoparticles in the fields of diets, farming, and pharmaceuticals[4]. Polymer science has long used nanotechnology, as evidenced by earlier studies that involved nanoscale dimensions but were not yet known as nanotechnology [5].

Nanocomposites is a multiphase solid material where one of the phases has one, two or three dimensions in nanoscale; less than 100 nanometers (nm) [6].

Nanoparticles, nanotubes, nanosheets, nanofibers, and other nanofillers enhance the polymer matrix in polymer nanocomposites. To a large

extent, the interaction between nanofillers and polymer molecules determines physical properties of these composites [7].

Matrix-nanoparticle interactions, as well as the geometry, size distribution, aggregation, and surface chemistry of organic/inorganic nanoparticles , play a crucial role in the polymer nanocomposites. Nonetheless, it was discovered that the properties of nanocomposites depend on the type of nanoparticles used, the amount of nanofillers used, as well as the way in which the nanoparticles chemically and physically bridge with the polymer matrix[8].

Polymer matrix nanocomposites (PMNC), metal matrix nanocomposites (MMNC), and ceramic matrix nanocomposites (CMNC) are the three main categories of nanocomposites based on their matrix materials [9].

Many different uses can be found for nanocomposites made from organic and inorganic materials because they combine the best properties of both types of materials. Organic polymers can be dielectric, ductile, and flexible, while inorganic materials can be rigid, strong, have a high refractive index, and be hard[10]. if the qualities of individual nanoparticles are not quite right, perhaps creating nanocomposites is the key. Nanocomposites, which are made up of two or more different

materials, are frequently utilized in the field of semiconductors to modify their electrical and optical properties[11].

1.2. Transition Metal Oxides (TMO)

Because transition metal compounds can spur on so many different processes, it can be tricky to get just one to take hold[12]**.** The wide range of physical and chemical features found in transition metal oxides is well-known. The structural, electrical, and magnetic properties of many of these materials change dramatically during phase transitions[13]. Over the past decade, the surface science of metal oxides has matured in response to a wide range of technological obstacles. [14]. Incorporating metal oxides including zinc oxide, titanium dioxide, tin oxide, and tin dioxide, as well as other semiconductors, into organic matrices results in increased physical and chemical stability. Nanocomposites made from a combination of inorganic nanoparticles used as filler and organic polymers used as matrices can exhibit remarkable electrical, optical, and mechanical capabilities . The advantages of metal oxides are combined with the processability and adaptability of polymers in these nanocomposites [15].

1.3. Polymer Structure

The term polymerization refers to the process by which monomers are repeatedly joined to form larger organic molecules (complexes). The thousands of atoms that make up each molecule are held together by chemical bonds, and the forces that draw two molecules together in a polymer apart are specific to that polymer [16]. Polymers, when in a solid state, have both crystalline and non-crystalline parts. The non-crystalline polymers are nearly totally non-crystalline, whereas the crystalline polymers contain at least 90% crystalline areas [17].

1.3.1 Poly (Vinyl Alcohol) (PVA)

The unique features of poly (vinyl alcohol) (PVA)—including high dielectric strength, strong charge storage capacity, commercial availability, cheap, high optical and mechanical characteristics piqued the curiosity of numerous scientists [18].

PVA is a great host material because of the high flexibility and superb film morphology it displays. However, its great solubility in water means that its electrical and mechanical qualities degrade quickly when exposed to moisture, limiting the polymer's usefulness except as a dielectric material, membrane, or adhesive [19]. PVA is a synthetic polymer that is non-toxic and safe; it is also highly transparent, has a high dielectric strength, and allows for rapid charge transfer at the electrode-

nanocomposite interface [20]. One example of a hydrophilic polymer is poly (vinyl alcohol), or PVA. According to its utility, it can be combined with other substances to produce a more effective composite [21]. PVA's semi crystalline nature is a key distinguishing property; this is defined as the existence of both crystalline and amorphous regions, which results in crystal-amorphous interfacial effects that boost the material's physical qualities [22].PVA has hydroxyl groups connected to methane carbons along its carbon chain backbone , Figure (1.1).

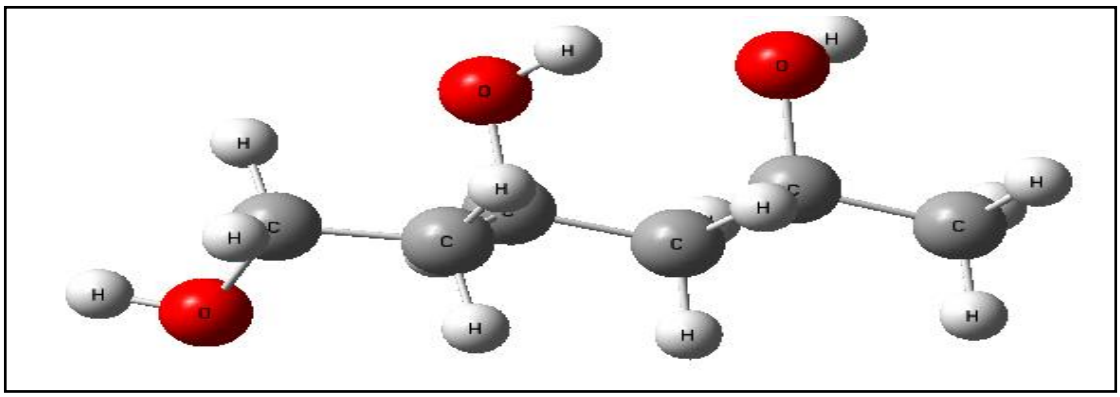

Figure(1.1):The structure of Poly (vinyl alcohol) .

1.3.2.Poly-methyl-methacrylate (PMMA)

Poly-methyl-methacrylate (PMMA) , widely used, low-cost thermoplastic polymer with a surprising number of practical applications. As the most widely used acrylic polymer, PMMA is commonly known by its brand names Plexiglas, Lucite, and Acrylite [23]. Structured poly(methyl methacrylate) chemical formula is:

-[CH_2-C(CH_3)($COOCH_3$)]-

Methyl methacrylate is the monomer from which this synthetic polymer is constructed. In the early 1930s, British chemists discovered PMMA, Polymers of this sort have unique optical features, including excellent weather resistance and extreme sensitivity to electron radiation while still being transparent at 92% transmission (the theoretical limit for the incident visible region) [24], Figure (1.2).

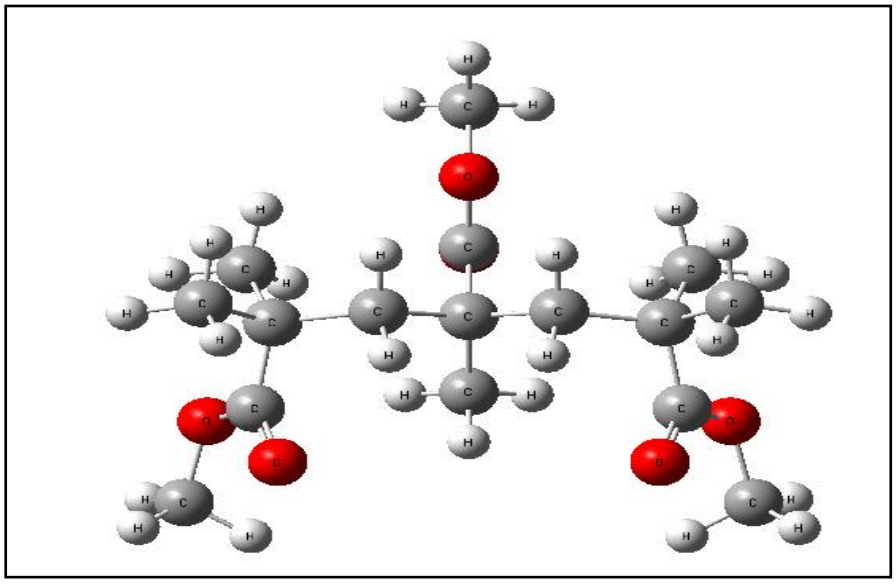

Figure (1.2): The structure of Poly methyl-methacrylate

PMMA is a transparent polymer with a glass transition temperature around (100-130) degrees Celsius. At room temperature, its density might be 1.20 g/cm^3. Because of its transparency and high compatibility with human tissue, PMMA is a vital material in the fields of ophthalmology and transplantation. It has an optical refractive index of 1.490 [25]. PMMA has a high Young's Modulus and a low elongation at breakage ,

In the field of mechanical strength. Consequently, it does not break apart into shards when it is broken, and it is also one of the hardest thermoplastics, with exceptional scratch resistance [26]. This polymer exhibits respectable chemical resistance it is stable in the presence of aqueous solutions of most commonly used laboratory chemicals [27].

1.3.3 Polystyrene (PS)

Styrene is a monomer that is used to create a synthetic polymer called polystyrene [5] .solid or foamed are the available forms of polystyrene. transparent, rigid, and breakable best describe general-purpose polystyrene. When measured in terms of weight, this resin is quite cheap. It has a low melting point and is a poor oxygen and water vapour barrier. Naturally, polystyrene is clear, however it can be colored with additives [28].

Polystyrene is a long series of hydrocarbon with phenyl groups bonded to alternate carbon centers along the chain (a derivative of benzene). Polystyrene is a synthetic polymer made up of carbon and hydrogen, with the molecular formula $(C_8H_8)n$ [29] ,Figure(1.3).

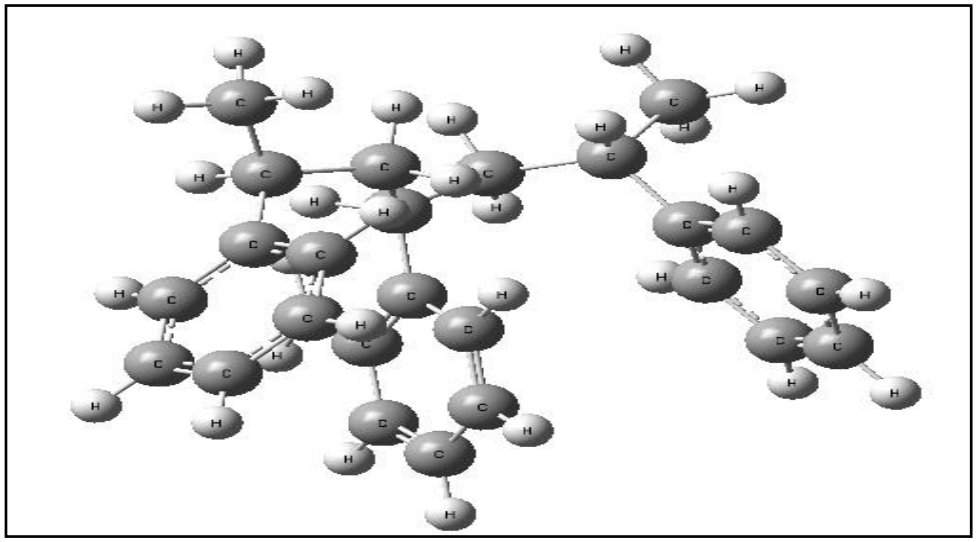

Figure(1.3): The structure of Polystyrene

Short-range van der Waals attractions between polymer chains affect the material's characteristics. Attraction between molecules is strong because each molecule contains thousands of atoms . When heated (or deformed at a rapid rate, due to a combination of viscoelastic and thermal insulation properties), the chains can take on a higher degree of confirmation and slide past each other . This intermolecular weakness (versus the high intramolecular strength due to the hydrocarbon backbone) confers flexibility and elasticity . The ability of the system to be readily deformed above its glass transition temperature allows polystyrene (and thermoplastic polymers in general) to be readily softened and moulded upon heating[30].

1.3.4 Polyethylene glycol (PEG)

A petroleum-based polyether molecule having a wide range of potential uses from industry to medicine. Depending on its atomic weight, polyethylene glycol (PEG) can alternatively be referred to as polyethylene oxide (PEO) or polyoxyethylene (POE). $H-(O-CH_2-CH_2)n-OH$ is a chemical structure of PEG's [31],Figure(1.4)

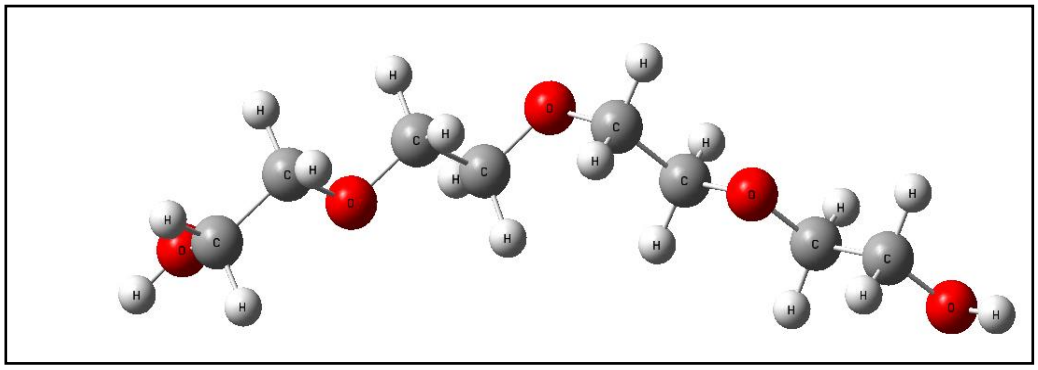

Figure(1.4):The structure of Polyethylene glycol.

PEG can be dissolved in both aqueous and organic media. PEG, meanwhile, has been shown to be hydrophilic and biocompatible [32], To prevent proteins from randomly adhering to glass slides during single-molecule fluorescence experiments, the hydrophilic molecule PEG has been employed to passivate the surfaces of microscope slides[33], Polyethylene glycol has several applications due to its low toxicity[34].

1.4. Para-quaterphenyl

P-quaterphenyl, or para-quaterphenyl, is an organic molecule with four phenyl groups linked in a straight chain at the para position. After benzene and biphenyl and para terphenyl, it is the next natural progression. Both a chromophore and an aromatic hydrocarbon [35], Figure (1.5)

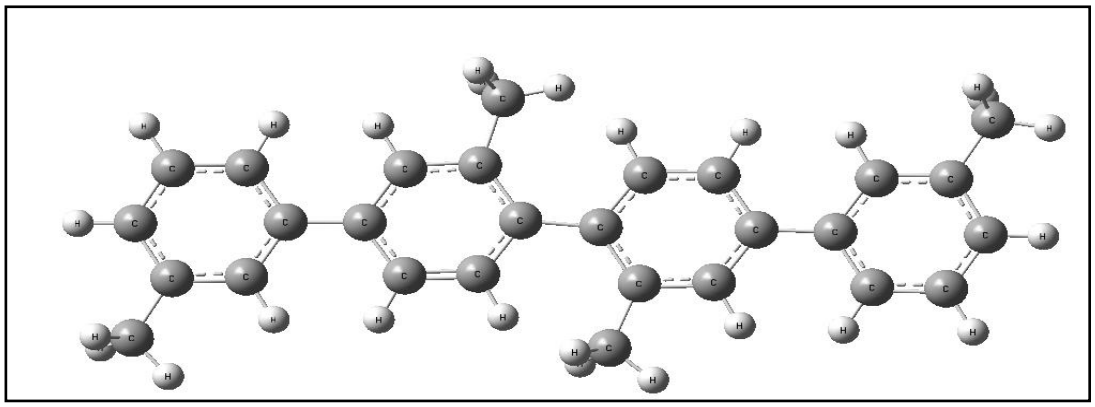

Figure (1.5):The structure of the p-quaterphenyl.

Among the organic semiconducting materials with a band gap (2.85) eV, p-quaterphenyl ($C_{24}H_{18}$) stands out. Those materials' thin films have several uses, including those of laser dye and a light blue emitter diode. [36-38]. Over the course of the last few decades, poly-p-phenylenes have attracted researchers' attention due to their promising and nonlinear optical coefficients, as well as their fluorescence and absorption, spectroscopic features, and laser-pumping abilities[39-42].

Many dyes based on the p-phenylene component are now commercially accessible as a result of these studies and find use as laser dyes[43]. This class of laser dyes is well suited for this purpose because of its high molar absorption, efficiency at short wavelengths, and stability under laser excitation. The benefits listed above, in addition to the fact that these qualities can be modified relatively easily, and that a wide range of information, including results from recent quantum-chemical investigations, is already accessible for these dyes, [44] Molecular engineering is most suited to the poly-p-phenylene family.

1.5 Organic Solid State Laser

The use of lasers has expanded into many fields. Miniaturization, portability, and increased integration are all on the rise in the industry of laser, so new laser technologies are in extremely popular.

Gain media made from organic semiconductors wield considerable promise for future generations of novel laser devices because of their many desirable properties, such as their low refractive indices, mechanical flexibilities, low thresholds, etc., which make them simple to process and spectrum and chemistry tuning. organic solid-state lasers (OSSLs) open up a new horizon of simple, low-cost, time-saving, versatile and environmental-friendly manufacturing technologies for new

and desirable laser structures (micro-, asymmetric, flexible, etc.) to unleash the full potential of semiconductor lasers for future electronics. Besides the development of optical feedback structures, the design and synthesis of robust organic gain media is critical as a vigorous aspect of OSSLs[45]. The first record of organic gain media using OSSLs was in 1967, when rhodamine 6G doped in (PMMA) was reported [46] . The Adachi laboratory announced their success with electrically pumped OSLs in 2019 [47].

1.6. Literature Review

Bahaa H. Rabee. *et.al*.[48] (2014) have investigate the effect of Zinc chlorides on optical and electrical properties of (PS-PMMA) copolymer. by using casting technique the samples of composites were prepared . The experimental results presented anincreasing in the absorbance, absorption coefficient, energy band gap, extinction coefficient, refractive index and real and imaginary parts of dielectric constants with increase of the Zinc chloride perecentage. temperature range from 300 $^{\circ}$C to 800 $^{\circ}$C the electrical properties were measured. also with the increasing of the weight percentages of Zinc chloride and temperature D.C electrical conductivity (PSPMMA) copolymer is increased . with increase of Zinc chloride concentration the activation energy of composites decreases .

Attia A.A. *et.al.* (2016)[49] Para-quaterpheny1 (p-4pheny1) thin films were deposited on glass/quartz surfaces using the thermal evaporation process for structural and optical studies . X-ray diffraction analysis of p-4 phenyl thin films confirmed their monoclinic structure as deposited. The surface morphology of p-4phenyl thin film was studied using scanning electron microscope . The absorption spectrum of p-4phenyl thin film recorded in the wavelength range (200-2500)nm . Photoluminescence measurements revealed two emission peaks at 435 and 444 nm using N_2-laser (337.1 nm).The energy gap obtained from the absorption and photoluminescence data was found to be 2.87 eV and 2.74 eV respectively with Stokes shift value of 0.13eV . The current-voltage characteristics of p-4phenyl/p-Si heterojunction have been recorded in the dark and under illumination of laser (337.8 nm) . Responsivity, Detectivity, External quantum efficiency and Response speed of (Au/p-4pheny1/p-Si/Al) photodetector have been determined using different laser sources.

Hegedűs, P *et.al.* [50] (2017) had been investigated TiO_2 photocatalyst with the application of Poly (Vinyl Alcohol) (PVA). The study showed that Despite the favourable effect of the immobilized TiO_2 on the crosslinking of the polymer, the stability of the PVA support was too low for a practical use, due to its still considerable water-solubility.

The stability of the PVA-based foils could be significantly enhanced by a thermal treatment . Before a photocatalytic application, however, the water-soluble products of the heating process had to be removed from the surface of the PVA-TiO_2 composite foil . Three cycles of irradiation and rinsing proved to be sufficient for this purpose.

Xiang, A. *et.al*. [51] (2018) have prepared PVA/SiC composites by melt blending, and the effect of surface modification of SiC by silane coupling agent was investigated in detail . The results showed that the properties of the materials have been greatly improved . It is aimed to produce environmentally friendly composite materials with excellent mechanical properties and wear resistance.

Pham, N. K *et. al.* [52](2018) have investigate the resistive switching behaviour of a nanocomposite composed of (TiO_2 nanotubes) TNTs embedded in PVA matrix. Density functional theory calculations illustrated that TiO_2/PVA system could form stable structures through strong bonds between the O atoms in PVA's OH groups and the Ti atoms on the surface of TiO_2 . Both analysis of the charge transport mechanism and the theoretical calculation results confirmed that the bipolar resistive switching mechanism of the nanocomposite device was governed by the trapping-detrapping process of carriers under an external electric field.

Sihama Issa Salih and *et.al.* [53](2018) have study two groups of PMMA nano composites samples were fabricated by using hand lay-up method at laboratory temperature used for manufacturing of the maxillary complete or partial denture base . These samples consist of (PMMA) resin as a matrix material, was strengthen by two different natural powder in nanometresize (pomegranate peels (PPP) and seed powder of dates Ajwa (SPDA)) in individually form, with selected weight fraction ratio (0, 0.4, 0.8, 1.2 & 1.6 wt. %).Some mechanical properties and analytical physical properties (FTIR, SEM) were investigated . The result showed a considerably improvement in the values of these properties for both groups of bio composite specimens comparing with neat PMMA . All bio composite specimens reinforced with pomegranate peels powder in nanometre size showed the highest properties as compared with the bio composite specimens strengthened by nano seed powder of dates ajwa.

S. Ahmed *et.al.* [54](2019) have investigate the influence of thickness on the optical properties for poly methyl methacrylate (PMMA), that the films were prepared by spin coating method . Some of optical properties of poly(methyl methacrylate) film have studied, this study shows that having different properties due to the difference in thickness . Effect of thickness variation and number of rotations on optical measurements .

Also notice the value of the energy gap is as high as possible and reaches to (3.08 eV) at 5000 rpm with thickness (47 nm) and have the highest refraction at the value that the thickness(206 nm) .

Angham Hazimand *et.al*.[55] (2019) have study the geometrical parameters, electronic and optical properties of the (PMMA-ZrO_2-Ag) nanostructures. The electronic properties include electrochemical hardness and electronic softness while the optical properties include absorbance**,** transmittance, absorption coefficient**,** extinction coefficient, refractive index, real and imaginary parts of dielectric constants and optical conductivity . The properties calculated by using Gaussian 0.9 program with Gaussian View 0.5 using density function theory (DFT). The results showed that the addition of Ag nanoparticles lead to decrease the chemical hardness and increase in the softness . optical properties for (PMMA-ZrO_2-Ag) nanocomposites showed that the absorbance**,** absorption coefficient**,** extinction coefficient, refractive index, real and imaginary parts of dielectric constants and optical conductivity of (PMMAAl_2O_3) nanocomposites increase while the transmittance and energy band gap decrease with increase in Ag nanoparticles concentrations . antibacterial results showed that the (PMMA-ZrO_2-Ag) nanocomposites have good antibacterial for positive and negative gram organisms .

S. A. Hussain and *et.al*. [56] in (2020) were studied the effect of nanoparticle of Silver on the optical properties of Polymethylmethacrylate (PMMA) films prepared by using casting technique at a temperature (50 ^{o}C) with thickness (8±1 μm) . The results of measurement showed that the transmittance of the films decreased with increasing the addition of silver nanoparticle due to increasing of attenuation of incident light with a clear increase of absorption and a decrease in optical reflectivity .

Hind Ahmed and Ahmed Hashim [57] (2020) studied the electronic structure of PVA-PEG-Y2O3 (54 atom) is to present a theoretical study based on the hybrid function of three parameters Lee-Yang-Parr B3LYP of the density functional theory DFT quantum mechanical approach together with LanL2DZ basis sets for optoelectronics applications. The results state that the yttrium oxide has low HOMO -LUMO energy gap, and have more biological activity ratios. The obtained results indicated that the PVA-PEG-Y_2O_3 can be used in different fields for electronics and photonics applications such as sensors, transistors, diodes, solar cell, electronic gates, and lasers .

Angham Hazim *et. al*.[58] (2021) they study the quantum mechanical treatment of the geometrical optimization and the electronic structure problems of a nanomaterial PMMA and nanocomposites . The hybrid functional B3LYP/6-31G level of DFT was used to investigate four

molecules divided into two groups, it was PMMA as an original basis molecule and (PMMA–Au), (PMMA–Al_2O_3–Au), (PMMA–ZrO_2–Au) nanocomposites as the two group . One of the important results was obtain in this study, is the decreasing of the energy gap. This states that these nanocomposites are the nearest to semiconductor due to the both HOMO and LUMO levels become more adjacent. These consequences mention to construct new structures with new electronic properties. All nanocomposites need small energy to become cationdue to ionization potential is decrease with addition nanoparticles to the pure PMMA, but the electronic affinity is an increase with addition nanoparticles to the pure PMMA. The total ground state energy of the PMMA have largest value of total energy compared for other nanocomposites, where E_T decreased with addition nanoparticles to pure PMMA. The hardness decrease with addition nanoparticles to the pure PMMA, therefore all the nanocomposites are softer, and this reduces the resistance of a species to lose electrons. Good relax for the structures of the studied PMMA was obtained theoretically, in which, the angles C–C, C=O and C–H in pure PMMA are remain in the same ranges for other nanocomposites. In general, most of the studied nonocomposites direct electronic transition from the valence to conduction band with wave length lies in the range of solar spectrum. The obtained results showed that the (PMMA–ZrO_2–Au)

and (PMMA–Al_2O_3–Au) nanocomposites have huge applications in electronics and photo-electronics fields.

Ameen Alwan Mohaimeed [59] (2022) have investigated how titanium dioxide nanoparticles affected the optical properties of polyvinyl alcohol. Polymer nanocomposites ($PVATiO_2$) created via stirring and casting. results demonstrate that transmittance improves from 75% to 95% while titanium dioxide concentration enhances the absorbance of nanocomposites. Nanocomposite films made of PVA and TiO_2 had reflectance values of 12 and 16 percent (weight percent=0.15 and 0.85%). The refractive index and coefficient of extinction increased with increasing density, and optical absorption and photon dispersion in the nanocomposite ($PVATiO_2$) also increased as the concentration of titanium dioxide nanoparticles increased . Real dielectric (r) and imaginary dielectric I constants also increased as titanium dioxide nanoparticle concentration does. The results show that when the weight of (TiO_2) nanoparticles increased, the energy gap decreased from 3.32 to 2.23 . Additionally, optical conductivity. increased with the concentration of (TiO_2) NPs. Nanocomposites of PVA and TiO_2 are essential for optical applications .

Ameen Alwan Mohaimeed *et.al*. [60] (2023) they prepared nanocomposite (PVA/TiO_2/Berry dye) films with a solid state thin layer

and the optical and calculated some structural properties . There was an increase in absorbance in the prepared films as a result of a higher concentration of Berry dye the dyeing process reduced the transmittance (79%) of these films. Incorporating an increase in Berry dye concentration, the energy gap was reduced from (3.64 to 3.54) eV. The electrons in the valence band can more easily access the conduction band localized levels due to the natural Berry dye's generation of new levels in the band gap . image of optical microscopy showed the dispersion of TiO_2 nanoparticles formed a network to move electrons faster inside Polyvinyl Alcohol (PVA). FE-SEM images the morphology of TiO_2 exhibits the creation of tiny clusters, as well as the morphology of PVA/TiO_2 agglomerates with porous irregular cauliflower-like characteristics, making it useful for various optoelectronic applications such as an photovoltaic, solar cells, light filters, UV detectors .

1.6. Aims of the Study

The main goal of this work is

1. Formulation of new types of (polymer- P-quaterphnyle –metal oxide), (polymer-metal oxide) and (P-quaterphnyle-metal oxide) structures that could be used in a variety of applications.

2.Study optical and electrical properties of the new structures.

3.Charstraization of the Nanocomposites as laser active medium .

4.Compared some properties obtained theoretically of these Nanocomposites.

Chapter two

Theoretical Background

2.1.Introduction

It is a continuing aim of the computational community to accurately predict molecule structure and characteristics. Furthermore, there is great potential for computational precision to aid experimental. Enhancing experimental data with computational predictions of important molecular events. Computational findings, for instance, can be directly connected to values determined experimentally [61].

Many examples of how computational chemistry may be used to elucidate on events observable in the physical world are presented in this thesis.

An essential and foundational technique used in molecular science research is computational chemistry, commonly known as molecular modelling [62]. Many physical properties of biological, inorganic, organometallic, polymeric, catalytic drug, and other molecular systems are now investigated computationally using molecular modeling methods and physicians. These properties include energies of molecules, molecular

geometries, electronic structure, electron and charge distributions, infrared (IR), ultra-violet (UV), and nuclear magnetic resonance (NMR) spectra [63]. in this chapter computational chemistry techniques discussed are derived from combined methodology. The Hartree-Fock technique is an ab initio method, which means it is based on fundamental principles. A variety of methods are being explored in an effort to determine a molecule's structure and energy using the Schrödinger Equation [61].

2.2.Schrödinger Equation

Erwin Schrödinger is given credit as the namesake of the Schrödinger equation for his contributions to the derivation and discovery of the equation in 1925 and its subsequent publication in 1926 [64],. This equation, known as the Schrödinger equation, was developed to describe the behaviour of systems ranging in size from the smallest subatomic particles to the largest macroscopic systems, including the universe. Schrödinger time dependent equation in is written as [65,66]

$$\hat{\mathrm{H}}(\vec{\mathrm{r}},\mathrm{t})\Psi(\vec{\mathrm{r}},\mathrm{t}) = \mathrm{i}\hbar\frac{\partial}{\partial \mathrm{t}}\Psi(\vec{\mathrm{r}},\mathrm{t}) = -\frac{\hbar^2}{2\mathrm{m}}\nabla^2\Psi(\vec{\mathrm{r}},\mathrm{t}) + \mathrm{V}(\vec{\mathrm{r}},\mathrm{t})\Psi(\vec{\mathrm{r}},\mathrm{t}) \qquad (\mathbf{2.1})$$

Where $\Psi(\vec{r},t)$ denotes the wave function, ($\hbar$) is the reduced Dirac constant, $\nabla^{\wedge 2}$ is the laplacian operator and $V(\vec{r},t)$ is potential energy depending on the position of the particle and the time.

The Schrödinger equation then reduces to the famous time-dependent equation written for a molecular system that is shown in Eq. (2.2)

$$\hat{H}\Psi(\vec{r},t) = E\Psi(\vec{r},t) \qquad (\mathbf{2.2})$$

Where $\hat{H}$ is represented the Hamiltonian operator, which includes the kinetic energy ($\hat{T}$) of the electrons and the nuclei and potential energy components ($\hat{V}$) as in Eq. (2.3). In addition, E denotes the energy of the system obtained as an eigenvalue to the Hamiltonian operator [67,68]

$$\hat{H} = \hat{T} + \hat{V} \qquad (\mathbf{2.3})$$

When the operator $\hat{H}$ is independent of time, the Schrödinger equation then reduces to the well-known time-independent equation written for a molecular system is as the following equation [69,70].

$$\hat{H}\Psi(\vec{r},R) = E\Psi(\vec{r},R) \qquad (\mathbf{2.4})$$

In Eq. (2.4) the $\Psi(\vec{r}, R)$is the molecular wave function depending on both $(\vec{r})$ and (R), where $(\vec{r})$ and R are the electron and the nuclei spatial coordinates, respectively.

The total Hamiltonian of the molecular system $\hat{H}$ contains numbers of electrons ($N_{elec.}$) and nuclei ($N_{nucl.}$), respectively, and can be expressed as follows [71,72]:

$$\hat{H}_{total} = \hat{T}_{elec.} + \hat{T}_{nucl.} + \hat{V}_{nucl.\ elec.} + \hat{V}_{elec.\ elec.} + \hat{V}_{nucl.\ nucl.} \qquad (\mathbf{2.5})$$

In Eq. $(\mathbf{2.5})$, the total kinetic energy is the amount of the electronic $(\hat{T}_{elec.})$ and nuclear $(\hat{T}_{nucl.})$ kinetic energies; this is the total potential energy that is the sum of three components: the attractive interactions between nuclei and electrons $(\hat{V}_{nucl.\ elec.})$, the repulsive electron-electron interactions $(\hat{V}_{elec.\ elec.})$ and the repulsive interactions between the nuclei $(\hat{V}_{nucl.\ nucl.})$.

Born-Oppenheimer (BO) Approximation is one of the essential and central approximation of the quantum chemistry. Employment of these approximation assumes that the electronic motion and the nuclear motion in the molecules can be separated, and the total wave function $\Psi_{tot.}$ of a

molecule could be divided into two components expressed as in the following equation [72,73]:

$$\Psi_{\text{tot.}} = \Psi_{\text{elec.}} \times \Psi_{\text{nucl.}} \qquad (\mathbf{2.6})$$

Since the nucleus is much heavier than the electrons, the nuclei moves much more slowly than the electronic movement. It could be considered as fixed. The kinetic energy of nuclei is decreased and the potential energy of nuclei-nuclei could be taken as fixed. In terms of this, the kinetic energy of nuclei and the potential energy of nuclei-nuclei can be eliminated from the Hamiltonian operator, and the Hamiltonian operator $\hat{H}$ is simplified as in the form [69,71,72]:

$$\hat{H}_{\text{elec.}} = \hat{T}_{\text{elec.}} + \hat{V}_{\text{nucl. elec.}} + \hat{V}_{\text{elec. elec.}} \qquad (\mathbf{2.7})$$

Where the system can actually be described only when all electrons move in a potential field of nuclei with fixed positions.

2.3 Hartree-Fock Methods

For all electrons in systems the quantum mechanical behavior could be describe using the time-independent Schrödinger equation, to solve the Schrödinger equation for all electrons in systems r it is necessary to calculate the many-electron wave functions esquires solving

many of simultaneous differential equations[72]. Performing such a calculation is extremely challenging and requires for the simplification of both the methodologies and the problem itself.

Hartree (1928) reduced the complexity of the problem by approaching an assumption about the form of the many-electron wave functions from the product of a set of single-electron wave functions [73]. Having this assumption, it was possible to proceed using the variational principle. From the variational principle, the lowest energy eigenvalue E_Φ of the trial function Φ can be expressed as in the following [72,73]:

$$E_\Phi = \frac{\langle \Phi | \hat{H} | \Phi \rangle}{\langle \Phi | \Phi \rangle} \geq E_o \qquad (2.8)$$

Where: E_o denotes the ground state energy . Using this theorem, is by approximated from the trial function that gives the lowest energy. Hartree examined the Hamiltonian equation of the many-electron system in which it was possible to treat each electron separately as a single-particle.

In Hartree-Fock (HF) method, approximation can write the wave function Ψ in a determinant called the "Slater determinant" (SD). The SD considers the spin of all the electrons and the Pauli exclusion principle.

The electrons can have a spin up (α) or a spin down (β). For N-electrons system, the SD is as in the following [74,75]:

$$\Psi = \frac{1}{\sqrt{N!}} \begin{vmatrix} \Psi_1(1)\alpha(1) & \Psi_1(1)\beta(1) & \Psi_2(1)\alpha(1) & \Psi_2(1)\beta(1) \dots \dots & \Psi_N(1)\alpha(1) & \Psi_N(1)\beta(1) \\ \Psi_1(2)\alpha(2) & \Psi_1(2)\beta(2) & \Psi_2(2)\alpha(2) & \Psi_2(2)\beta(2) \dots \dots & \Psi_N(2)\alpha(2) & \Psi_N(2)\beta(2) \\ . & & . & & . & \\ . & & . & & . & \\ \Psi_1(N)\alpha(N) & \Psi_1(N)\beta(N) & \Psi_2(N)\alpha(N) & \Psi_2(N)\beta(N) \dots \dots & \Psi_N(N)\alpha(N) & \Psi_N(N)\beta(N) \end{vmatrix} \quad (2.9)$$

where Ψ is the electronic wave function, α and β are the spin up and spin down of electrons, respectively, and $\frac{1}{\sqrt{N!}}$ is a normalization factor.

The molecular orbital expansion introduction is the main step in HF method, based on the variational principle the corresponding coefficients is determining [84]. By using the iterative process of the self-consistent-field (SCF) producer the molecular orbitals $\Psi_i$solves the HF equation yields the HF equation as in the form [76,77]:

$$\hat{F}\Psi_i(\vec{r}) = \varepsilon_i\Psi_i(\vec{r}) \quad (2.10)$$

In Eq. $(\mathbf{2.10})\,\hat{F}$ represent the Fock operator and ε_i is the spin orbital Ψ_i.energy

2.4 Density Functional Theory (DFT)

The Density Functional Theory (DFT), has influnced on the evolution of quantum mechanical method , to investigate the electronic structure and properties of many-electron systems its showed a wide applicability in physics and chemistry fields. knowledge of the electron density distribution by using functional DFT shows that ground state (GS) and other properties of a many-electron system could be determined[78]. In the fields of computational physics and chemistry, DFT is by far the most widely used and flexible technique. In addition, it has been shown to be highly effective at calculating the ground state properties of materials. [69,76].

Thomas and Fermi model(1927) is thought to be the foundation of density theory. They made the first attempt to describe the property of a system with electron density[79]. the energy of an atom were computed by expressing the kinetic energy of the atom as a functional of electron density by Thomas-Fermi model [73].

The density-functional theory (DFT) approach calculates features of a many-particle system as a function of electron density or probability density $\rho(\vec{r})$. $\rho(\vec{r})$ that means the probability of finding any of electrons (N) in volume element $d\vec{r}$ with any spin for a given state. It is

independently of the number of electrons of the system dependent only on three coordinates [65,80]:

$$N = \int \rho(\vec{r})d\vec{r} \qquad (\mathbf{2.11})$$

DFT's fundamental ideas are predicated on the fact that the electron density uniquely determines the ground state energy and all other electronic properties. More so, the electronic density at minimum total energy matches precisely to the system's ground state..

1964 proof two theorems by Hohenberg and Kohn (HK) that DFT could be considered a credible quantum chemical approach[34]. by the ground state electron density the ground state $\rho(\vec{r})$. of a many electron system can be determined has been proved by them [81,82].

Theorem I: "The ground state energy of a many-electron system is a unique, universal functional of ground state electron density $\rho(\vec{r})$".

Theorem II: "The functional of ground state energy is minimized by the ground state electron density $\rho(\vec{r})$. for a many-electron system".

According to above theorems, the ground state energy functional $E_V[\rho]$ can be described as in the following [79,83]:

$$E_V[\rho] = \int \rho(\vec{r})\, V_{ext.}(\vec{r})d\vec{r} + F_{HK}[\rho] \qquad (\mathbf{2.12})$$

The F_{HK} [ρ] in Eq. (2.12) denotes a functional of $\rho(\vec{r})$ to be determined which contains kinetic energy and all the electron-electron interactions. F_{HK} [ρ] is the HK universal functional of density independent of the external potential $\hat{V}_{ext.}(\vec{r})$.

2.5 Time Dependent- Density Functional Theory (TD-DFT)

Time-Dependent Density functional theory (TD-DFT) extends the fundamental idea of the ground-state DFT which can be used to investigate the excited-state properties and dynamics of a system in the attendance of time-dependent potentials, such as electric or magnetic fields. The impact of fields on molecules can be studied with TD-DFT as an implementation for demonstrating excitation energies, oscillator strength, wavelength, molecular orbital character and electronic transitions from spectroscopic (UV-Vis.) of the molecules. An example of this is the computing of excited states of metal complexes by TD-DFT that becomes a very significant accompaniment to spectroscopic techniques [84-87].

The theoretical of TD-DFT traced back to the Runge-Gross theorem (RG theorem) in 1984. The RG theorem explicated the relationship between the time-dependent external potential $\hat{V}_{ext.}(\vec{r}, t)$ and $\rho(\vec{r}, t)$of the system. RG theorem indicated that when two external

potentials $\hat{V}_{ext.}(\vec{r},t)$ and $\hat{V}_{ext.}{}'(\vec{r},t)$ have a variance of more than a time-dependent function, their own electron densities $\rho(\vec{r},t)$and $\rho'(\vec{r},t)$are also different [88-90].

Runge and Gross discussed how excited states are obtained using TD-DFT. The starting point of studying time-dependent systems is the time-dependent Schrodinger equation. The TD-DFT is directly related to the Schrodinger equation $[\, i\frac{\partial}{\partial t}\Psi(\vec{r},t) = \hat{H}\Psi(\vec{r},t)]$where the Hamiltonian is known to be [86,88, 89]:

$$\hat{H} = \hat{T} + \hat{V}_{elec.\ elec.} + \hat{V}_{ext.}(\vec{r},t) \qquad (\mathbf{2.13})$$

Here, $\hat{H}$ consists of the kinetic energy operator $\hat{T}$, electron-electron repulsion $\hat{V}_{elec.\ elec.}$ (Coulomb operator) and the external potential $\hat{V}_{ext.}(\vec{r},t)$.

Where $\hat{V}_{ext.}(\vec{r})$is given in the following operators:

$$\hat{V}_{ext.}(\vec{r}) = \sum_{i=1}^{N} V_{ext.}(\vec{r}_i,t) \qquad (\mathbf{2.14})$$

The densities of the system increase from a fixed initial state $\Psi(t_0)=\Psi(0)$.

The initial state, $\Psi(0)$, is arbitrary; it must not be the ground-state or some other eigen state of the initial potential $\hat{V}_{ext.}(\vec{r},t_0) = \hat{V}_0(\vec{r})$. The RG theorem indicates that there exists an one-to-one correspondence

between the time-dependent external potential, $\hat{V}_{ext.}(\vec{r},t)$, and the time-dependent electron density, $\rho(\vec{r},t)$. for systems evolving from a fixed initial many-body state. According to it, the density determines the external potential, and subsequently helps in obtaining the time-dependent many-body wave functions [89,90].

As this wave-function determines all observables of the system; as a consequence, the remarking point is that all observables are functionals of $\rho(\vec{r},t)$.

2.6 Kohn-Sham Equations

Depending on Hoherberg-Kohn theorems, the energy functional FHK[ρ] of an interacting many-electron system can be expressed as[91-94]:

$$F_{HK}[\rho] = T[\rho] + \frac{1}{2}\iint \frac{\rho(\vec{r})\rho\left(\vec{r'}\right)}{\left|\vec{r}-\vec{r'}\right|} d\vec{r}d\vec{r'} + E_{xc}[\rho] \qquad (\mathbf{2.15})$$

Where T[ρ] is the kinetic energy of a system, the second term is the classical Coulomb energy and the third term Exc[ρ] is the exchange-correlation energy which describes the non-classical interaction of electrons including all the many-body effects. Because the concrete

expression of functional T[ρ] and E_{xc}[ρ] were not given, one could not carry out a first principle calculation. In order to solve this problem, Kohn and Sham assuming that, a non-interacting many-electron system which has the same electron number N and ground state electron density ρ($\vec{r}$) under an external potential V_{ext} ($\vec{r}$) with those of an interacting many-electron system[79,91].

The key point of the DFT is to find the exchange-correlation energy EXC; if the exact exchange-correlation function is known, the system will be solved exactly. This function results from the difference of the Hamiltonian between the interacting many-electron systems to the non-interacting single electron system. Thus, this comprises all the impacts of exchange and correlation interactions, such as "Pauli exclusion" between electrons with same spin orientations, and the instantaneous reaction of electrons with opposite spins [92,93].

2.8 Exchange-Correlation Functionals

2.8.1 The Local-Density Approximation (LDA)

The local density approximation (LDA) is the simplest approximation to $E_{\times c}[\rho(\vec{r})]$, which assumes the system is a homogenous

electron gas and $E_{\times c}[\rho(\vec{r})]$, depends only on the local value of electron density. Therefore, $E_{\times c}[\rho(\vec{r})]$, can be written in a simple form[74]:

$$\mathrm{E_{XC}^{LDA}}[\rho] = \int \rho(\vec{r})\, \varepsilon_{\mathrm{XC}}\big(\rho(\vec{r})\big)\mathrm{d}\vec{r} \qquad (\mathbf{2.16})$$

Compared to LDA, the local spin density approximation LSDA defines the exchange correlation potential in terms of the density of α and β spins and was developed for calculating the properties of open-shell systems[74].

$$E_{XC}^{LSDA}[\rho_\alpha, \rho_\beta] = \int \rho(\vec{r})\varepsilon_{XC}\big(\rho(\vec{r})_\alpha, \rho(\vec{r})_\beta\big)d\vec{r} \qquad (\mathbf{2.17})$$

Where ε_{XC} is the exchange correlation energy per particle. The LSD approximation provides better results than HF for certain properties such as equilibrium structures, vibrational frequencies and dipole moments.

In general, the LSDA provides reliable information for those systems that closely resemble a uniform electron gas, namely those in which the density varies slowly with position. However, in reality, atomic and molecular systems do not possess uniform electron densities and thus more sophisticated models are required.

2.8.2 The Generalized Gradient Approximation (GGA)

The electron density in a real molecule varies greatly from position to position. To get a more accurate approximation of the exchange-correlation energy, functional which include not only the electron density, but also the gradient of the electron density were developed[80,83-86]:

$$E_{XC}^{GGA}[\rho_\alpha, \rho_\beta] = \int f(\rho_\alpha, \rho_\beta, \nabla\rho_\alpha, \nabla\rho_\beta) d\vec{r} \qquad (\mathbf{2.18})$$

This functional generally offer an improvement over the LSDA since they account for the variation of density with position. To simplify the problem, E_{XC} is often written as the sum of an exchange (E_X) and correlation (E_C) terms[95]:

$$E_{XC} = E_X + E_C \qquad (\mathbf{2.19})$$

The exchange-energy functional can then be obtained from the HF exchange term with the Kohn-Sham orbitals in place of the HF orbitals, and approximate solutions for EC are sought. Various exchange and correlation functional have been developed independently and can be combined in various ways. For instance, one popular GGA functional is BLYP, where Becke's 1988 exchange functional is paired with the Lee-Yang-Parr correlation functional[96].

2.8.3 Hybrid Functional

The hybrid exchange-correlation functionals occupy a privileged location in the molecular applications of the DFT and nowadays its very popular used in computational physics and chemistry fields [94,97].

These functionals combine the exchange-correlation GGA functionals and an exact exchange functional, lastly yielding a method that is somewhere between HF and GGA. The most widely hybrid functional, B3LYP uses Becke's 1988 exchange functional (E_X^{B88}) and Lee, Yang and Parr's correlation functional (E_C^{LYP}) as gradient corrections to the LSDA exchange and correlation functionals. The exchange-correlation term of B3LYP is shown as the in following form [78,91, 98,99]:

$$E_{XC}^{B3LYP} = (1-a)E_X^{LSDA} + aE_{XC}^{HF} + bE_X^{B88} + cE_C^{LYP} + (1-c)E_C^{LSDA} \qquad \textbf{(2.20).}$$

In Eq. (2.20) the three parameters; a =0.20, b=0.72 and c=0.81, where this values were found by fitting the experimental data. The first parameter (a) specified the amount of exact exchange, while (b) and (c) control the contribution of exchange and correlation.

2.9 Theory of Quantum Transport

The purpose of molecular electronics is to gain an understanding of the electrical properties and behavior of molecular junctions. One of the difficulties is delivering molecular structures of electrode blocks for the purpose of examining their electrical properties. Connection In general, the force between the molecule and the metal electrode has a significant role. In determining the transport properties of a lead | molecule | lead frame as a result of scattering processes within the lead | molecule | lead frame. The primary theoretical way for understanding scattering in this System is using the Green's function formalities [100].

Our objective in this section is to gain a general understanding of Landauer's formalism, and we will begin with a simple derivation of the Landauer formula. A one-dimensional construction is presented to demonstrate the overall methods utilized in the description. Transport in arbitrarily complex-geometry intermediate conductors. Assume this procedure. The interaction between carriers and inelastic processes is negligible, which is a well-known fact for molecules less than 3nm in length at ambient temperature [101].

2.9.1 Green's Function Scattering Formalism

We apply a Green function scattering formalism to determine the transmission coefficient of a molecule coupled to semi-infinite leads. This is a continuation of the next chapter's discussion of calculating the electronic structure of an isolated molecule using DFT. The isolated molecule's properties and the interaction between the molecule and the electrodes have an effect on the open system's electronic properties. As a result, transport models must account for both aspects in order to comprehend the electron scattering process between the two electrodes [102].

2.9.1.1 Perfect One-Dimensional Lattice

In this section will discuss what the Green's function looks like for a simple one dimensional lattice with on-site energies ε_o and real hopping parameters as shown in Fig. (2-1).

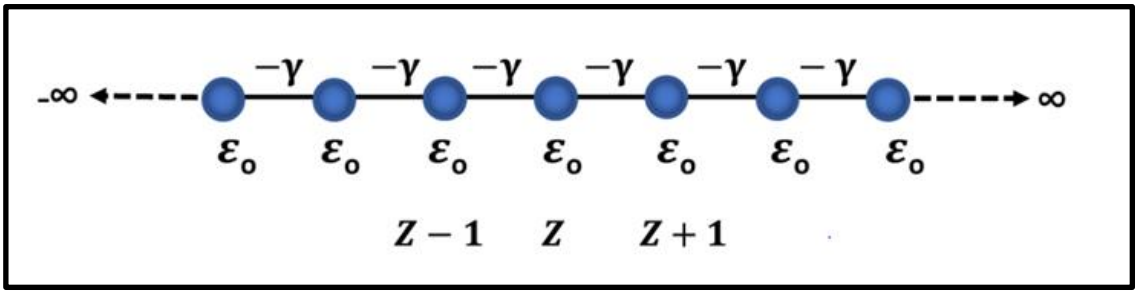

Figure (2.1): One-dimensional periodic lattice tight-binding approximation with on-site energies ε_o and hopping parameters γ[102].

The Schrödinger equation describes the wave function of the system with Hamiltonian H [100,102],

$$\hat{H}\,\psi = E\,\psi \qquad (\mathbf{2.21})$$

Wave function Ψ_z it is expanded into a one-dimensional orthogonal localized basis set $|z'\rangle$:

$$|\psi\rangle = \sum \psi_{z'}|z'\rangle \qquad (\mathbf{2.22})$$

Substituting equation (2.22) in equation (2.21) and multiply the result by $|z\rangle$ we get:

$$\sum H_{z,z'}\psi_{z'} = E\psi_z \qquad (\mathbf{2.23})$$

Hence,

$$H_{z,z'} = \langle z|\hat{H}|z'\rangle \qquad (\mathbf{2.24})$$

The matrix form of the Hamiltonian can be simply written:

$$H = \begin{pmatrix} \ddots & -\gamma & 0 & 0 \\ -\gamma & \varepsilon_o & -\gamma & 0 \\ 0 & -\gamma & \varepsilon_o & -\gamma \\ 0 & 0 & -\gamma & \ddots \end{pmatrix} \qquad (\mathbf{2.25})$$

the Schrödinger equation (equation 2.21) can be expanded at a lattice site z in terms of the energy and wave function ψ_z equation (2.22).

$$(E - H)\psi = 0 \quad \textbf{(2.26)}$$

$$\varepsilon_o \psi_z - \gamma\psi_{z+1} - \gamma\psi_{z-1} = E\psi_z \quad (\mathbf{2.27})$$

By using the wave function as given by Block's theorem for the perfect lattice chain which has the form $\psi_z = \frac{1}{\sqrt{v_g}}\, e^{ikz}$, where $-\pi \leq k < \pi$. The Schrödinger equation (eq. 2.27) can be solved to give the dispersion relation:

$$E = \varepsilon_o - 2\gamma\, cosk \quad (\mathbf{2.28})$$

Where we introduced the quantum number, k, commonly referred to as the wavenumber [103,102].

To calculate the retarded Green's function $g(z, z')$, which is closely related to the wave function, the following equation is solved:

$$(E - H)g(z, z') = \delta_{z,z'} \quad (\mathbf{2.29})$$

Physically, the lagging Green's function, $g\ (z,\ \acute{z})$, describes the response of a system at point z due to a source at point $\acute{z}$. Intuitively, we would expect such excitation to give rise to two waves, which travel outward from the excitation point, with amplitudes A and B as shown in Figure (2.2).

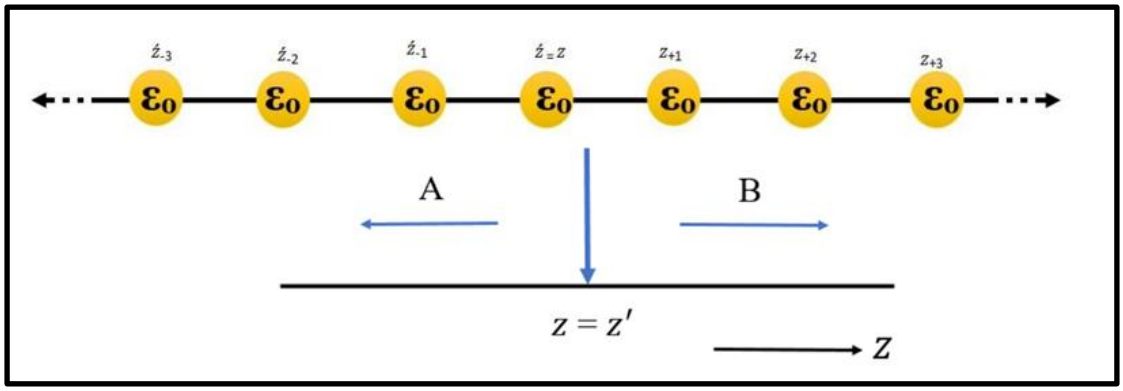

Figure (2.2): Retarded Green's function of an infinite one-dimensional lattice. The excitation at z = z ′ causes waves to propagate left and right with amplitudes A and B respectively[102].

These waves can be expressed simply as:

$$g(z,z') = Be^{ikz} \qquad z > z'$$

$$g(z,z') = Ae^{-ikz} \qquad z < z' \qquad \textbf{.(2.30)}$$

In this equation, the solution satisfies equation (2.58) at every point except $z = z'$. To overcome this, the Green's function must be continuous equation (2.31), so the two are equal at $z = z'$:

$$[g(z,z')]_{z=z'\ left} = [g(z,z')]_{z=z'\ right} \qquad \textbf{(2.31)}$$

$$Be^{ikz} = Ae^{-ikz} \Longrightarrow A = Be^{2ikz} \qquad \textbf{(2.32)}$$

By substituting equation (2.32) into the Green's function equation (2.30), we will find as shown:

$$g(z,z') = Be^{ikz} = Be^{ikz'}e^{ik(z-z')} \; z > z'$$

$$g(z',z) = Be^{2ikz'}e^{-ikz} = Be^{ikz'}e^{ik(z'-z)} \; z < z' \qquad (2.33)$$

We can rewrite equation (2.33) as:

$$g(z',z) = Be^{2ikz'}e^{ik|z-z'|} \qquad \textbf{(2.34)}$$

To find the value of the constant B, we use equation (2.29) and use equation (2.27) which for $z = z'$ given:

$$(\varepsilon_o - E)B - \gamma Be^{ik} - \gamma Be^{ik} = 1 \qquad \textbf{(2.35)}$$

$$\gamma B\left(2cosk - 2e^{ik}\right) = 1$$

$$B = \frac{1}{2i\gamma sink} = \frac{1}{i\hbar v_g}$$

where the group velocity, found from the dispersion relation equation (2.28), is:

$$v_g = \frac{1}{\hbar}\frac{\partial E(k)}{\partial k} = \frac{2i\gamma sink}{\hbar} \qquad \textbf{(2.36)}$$

We can rewrite the retarded Green's function as shown:

$$g^R(z-z') = \frac{1}{i\hbar v_g} e^{ik|z-z'|} \quad \textbf{(2.37)}$$

The literature [104,105] shows a more extensive derivation. The next step is to submit a file defect in the lattice to create a scattering area and then the transmission coefficient can be calculated.

To Calculate the Green's function for in this problem, we can get the scattering amplitudes. So, form a solution equation (2.29), which is given as follows:

$$G = (E - H)^{-1} \quad \textbf{(2.38)}$$

This equation can be singular if the energy E is equal to the Hamiltonian eigenvalues H, to deal with this, it is practical to consider the limit:

$$G_{\mp} = \lim_{\eta \to 0}(E - H \pm i\eta)^{-1} \quad \textbf{(2.39)}$$

Here η is a positive number and G+, G- is the retarded (advanced) Green's function. The sign of the positive infinitesimal η determines the type of solution which is either a retarded (-) or advanced (+) Green function. Generally, the methodology of computing electron transport is

focused on computing a Green function for the infinite system, which includes the leads and the scattering region [104,105].

In the case where there is no coupling between the molecule and the leads, α = 0, the Green's function can be given as:

$$g = \begin{pmatrix} -\frac{e^{ik}}{\gamma} & 0 \\ 0 & -\frac{e^{ik}}{\gamma} \end{pmatrix} = \begin{pmatrix} g_L & 0 \\ 0 & g_R \end{pmatrix} \quad \textbf{(2.40)}$$

If we consider a switch on of the interaction, then to obtain the Green's function of the coupled leads of this system, G, Dyson's equation is written:

$$G^{-1} = (g^{-1} - V) \quad \textbf{(2.41)}$$

where V is the operator that describes the interaction connecting the leads, which has the form:

$$V = \begin{pmatrix} 0 & V_c \\ V_c^{\dagger} & 0 \end{pmatrix} = \begin{pmatrix} 0 & \alpha \\ \alpha^* & 0 \end{pmatrix} \quad \textbf{(2.42)}$$

The solution to Dyson's equation, (Eq. 2.41) reads:

$$G = \frac{1}{|\alpha|^2 - \gamma^2 e^{-2ik}} \begin{pmatrix} \gamma e^{-ik} & \alpha \\ \alpha^* & \gamma e^{-ik} \end{pmatrix} \quad \textbf{(2.43)}$$

The only step left is to calculate the transmission, t, and reflection, r, amplitudes from the Green's function equation (2.42). This is done by taking advantage of the Fisher-Lee relation [102] that relates the scattering amplitudes of a scattering problem to Green's function of the problem. Since $A = B = 1/i\hbar vg$, the equation (2.43) gives a definition for the transmission and reflection coefficients, equations (2.44) and (2.45): The Fisher-Lee relations in this case state that:

$$G_{1,1} = \frac{1}{i\hbar v_g}\,(1 + r)$$

$$G_{2,1} = \frac{1}{i\hbar v_g}\,t\,e^{ik} \qquad \textbf{(2.44)}$$

$$r = i\hbar v_g\,G_{1,1} - 1 \qquad \textbf{(2.45)}$$

and

$$t = i\hbar v_g\,G_{2,1}e^{ik} \qquad \textbf{(2.46)}$$

Therefore, these amplitudes will be corresponded to particles incident from the left. On the other hand, particles are travelling from the right side, which means these expressions could be used for transmission t' and reflection r' amplitudes. According to these coefficients above, the

probability can be defined: T = tt*, R = rr*. Consequently Thus, the transmission probability for this case can be given as:

$$T = \frac{\sigma^2}{(\gamma^2 - \alpha^2)^2 + \sigma^2} \quad \textbf{(2.47)}$$

The parameters in this equation are $\sigma = 2\gamma\alpha sink$, and if α = γ that means the transmission T=1. In the case when α is greater or smaller than γ, which leads to create scattering region, and could be resulted to the transmission T ≤ 1.

2.9.2 The Landauer formula

Standard theoretical model to describe the transport phenomenon in ballistic mesoscopic the systems are Landauer's formula [106], a method applicable to phase cohesive systems. First of all, we assume that the system connects two large Scattering tanks, as shown in Fig. (2-3), in this case all are inelastic relaxation processes are limited to tanks [102]. Therefore, the electron is transferred passage through the system is formed as a quantum mechanical scattering problem. The second important assumption is that this system is connected to external tanks by an ideal quantum wire, which acts as a waveguide for electron waves.

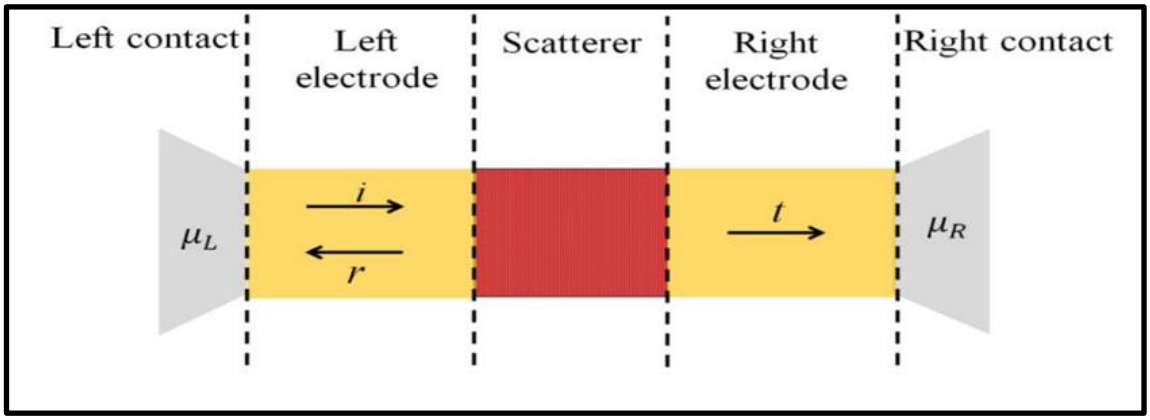

Figure (2.3): Shows a mesoscopic scatterer connected to the contacts by ballistic filaments. The μ_L and μ_R represent the chemical potential at the contacts. When the incident wave packet hits the scatterer on the left, it will be sent with probability $T = tt^*$, it is reflected with probability $R = rr^*$ where, t, t^* , r and r^* represent the transmission and reflection amplitudes from left to the right and vice versa. It requires the conservation of charges T + R = 1[107].

Mesoscopic scattered as shown in Figure (2.3), connected to two electron tanks, and these reservoirs have slightly different chemical potentials $\mu_L - \mu_R = \delta E > 0$, and it causes electrons to move from the left to the right tank. We will discuss the solution to one channel open to one electron: the incident electric current δI which is generated by the chemical potential gradient, as indicated by:

$$\delta I = e v_g \frac{\partial n}{\partial E} \delta E = e v_g \frac{\partial n}{\partial E} (\mu_L - \mu_R) \qquad \textbf{(2.48)}$$

The charge of the electron is (e), the group velocity is v_g. i.e. the velocity of electron, and $\partial n/\partial E$ is density of states per unit length in the lead in the energy window that can be determined by the chemical potentials from contacts:

$$\frac{\partial n}{\partial E} = \frac{\partial n}{\partial k}\frac{\partial k}{\partial E} = \frac{\partial n}{\partial k}\frac{1}{v_g \hbar} \qquad \textbf{(2.49)}$$

As in one-dimension, after including a factor of 2 of the rotation dependency $\frac{\partial n}{\partial k} = \frac{1}{\pi}$. When we substitute into equation (2.49), we will find that $\frac{\partial n}{\partial E} = \frac{1}{\pi}\frac{1}{v_g \hbar}$, which simplifies the equation (2.48) to:

$$\delta I = \frac{2e}{h}(\mu_L - \mu_R) = \frac{2\,e^2}{h}\,\delta V \qquad \textbf{(2.50)}$$

Where δV is the voltage generated by the chemical potential mismatch. From Eq.(2.50) it is clear that in the absence of a scattering region, the conductance of a quantum wire with one open channel is $\frac{2\,e^2}{h}$. If now we consider a scattering region, the current collected in the right contacts will be:

$$\delta I = \frac{2\,e^2}{h}\,T(\mu)\delta V \implies \frac{\delta I}{\delta V} = G = \frac{2\,e^2}{h}\,T(\mu) \qquad \textbf{(2.51)}$$

This equation is the Landauer formula, which relates the conductivity G of a mesoscopic scatterer to the transmission probability T of the electrons passing through it. Where $T(\mu)$ is the transmission coefficient as a function of the chemical potential μ and the quantum conductance G_0 represented by $2e^2/h$. The quantity G_0 includes the factor of 2 in the formula to include spin degeneracy [102,108].

Landauer's formula has been generalized in more than one open case Buttiker channel [106]. In this case, the transmission coefficient is replaced by the sum of all the transmission amplitudes describing electrons coming from the left-hand contact and arriving to the right contact. Landauer's formula equation (2.51) for many open channels and then it becomes:

$$\frac{\delta I}{\delta V} = G = \frac{2\,e^2}{h} \sum_{i,j} \left|t_{i,j}\right|^2 = \frac{2\,e^2}{h}\, Tr(tt^{\dagger}) \qquad \textbf{(2.52)}$$

Here, $t_{i,j}$ represents the transmission amplitude that describes the scattering from j^{th} channel from the left leads to i^{th} channel is for the right lead and G is the electric conductance. According to the definition of transmission amplitude, reflection amplitudes $r_{i,j}$ can be entered to describe the scattering processes where the particle is scattered to the

same lead from which it came, here $r_{i,j}$ distinguish probability a particle arriving at channel j is reflected back on channel i of the same lead. By combining the transmission and reflection amplitudes, we can produce the scattering matrix we call the S matrix, which connects the states coming from the left lead to the right and vice versa as follows:

$$S = \begin{pmatrix} r & t' \\ t & r' \end{pmatrix} \qquad \textbf{(2.53)}$$

In this equation, r and t denote left-handed electrons, while r' and t' denote right-handed electrons. When we return to equation (2.52), we see that r, t, r', and t' are matrices of multiple open channels that can be complicated in the presence of a magnetic field. The following section calculates S for the system's retarded Green function G(E). G(E) is derived by coupling the Green function of the leads to the Green function of the scattering region using Dyson's equation. The S matrix is an important component of scattering theory. In other words, it is useful not only in describing linearity transport, but also in other problems such as adiabatic pumping [107,108].

2.10 Computation of Molecular Properties

The computation of molecular properties in this study are carried out by Koopmans theorem (KT) as shown in the following description.

2.10.1 Energy of HOMO, LUMO and Band Gap

In quantum physics and chemistry, HOMO and LUMO are two most significant of molecular orbitals, where the HOMOs denotes highest occupied molecular orbitals and the LUMOs represents lowest unoccupied molecular orbitals. These orbitals are called "Frontier molecular orbitals (FMOs)" and as they lie at the outmost boundaries of the electrons of the molecules. The HOMO, which is the highest energy (outermost) orbital containing electrons, is the orbital acting as an electron donor. Contrariwise the LUMO is the lowest energy (innermost) orbital having space to accept electrons. The energy gap regards the difference of the energies between the HOMO and LUMO levels as in the following [109,110]:

$$E_{gap} = E_{LUMO} - E_{HOMO} \qquad (\mathbf{2.54})$$

Here E_{gap} indicates the energy gap, E_{LUMO} and E_{HOMO} denotes the energies of HOMO and LUMO in consecution.

FMOs and their resulting energy gap did not only decide the path of the molecule interacts with other species, but their energy gap helps to describe the chemical reactivity and kinetic stability of the molecules such as in metal complexes. In addition, FMOs play an significant role in UV-Vis spectra and electrical properties of molecular systems [96,111].

2.10.2 Total Energy, Ionization Potential and Electron Affinity

The total energy (I_E) represented the sum of total kinetic and potential energy of the system, at the optimized structure where the total energy of the molecule must be at the lowest value because the molecule is at the equilibrium position, which means the resultant of the effective forces is zero [111-113].

The ionization potential (I_E) for a molecule is the quantity of energy necessary to remove an electron from an isolated atom or molecule and expressed as the energy difference between the positive charged energy (E_+) and the neutral ($E_{(n)}$) as the relation: $I_E=E_+-E_n$. In addition, the HOMO energy was also used to compute I_E in the framework of Koopmans theorem as in the following form [114-116]:

$$I_E = -E_{HOMO} \qquad (2.55)$$

The electron affinity (E_A) of a molecule or atom is the energy change when an electron added to the neutral atom to form a negative ion and expressed as the energy difference between the neutral energy (E_n) and the negative charged energy (E_-) according to the relation: $E_A=E_n-E_-$. Furthermore, the LUMO energy was also used to calculate E_A according to Koopmans theorem as in the following [96,114,116]:

$$E_A = -E_{LUMO} \qquad (\mathbf{2.56})$$

2.10.3 Chemical Potential, Chemical Hardness and Softness

Within the outline of the DFT, measures the escaping tendency of an electronic cloud is the meaning of the chemical potential(μ); which is one example of a global quantity. through all space, for the ground state of an atom, molecule or solid it is a constant, and equals the slope of the energy versus N curve at constant potential $v_{(\vec{r})}$ as in the following formula

$$\mu = \left[\frac{\partial E}{\partial N}\right]_{v_{(\vec{r})}} \qquad (\mathbf{2.57})$$

Also, μ is related, experimentally, to two known quantities, I_E and E_A, as in the following relationship [96,117,118]:

$$\mu \approx \frac{1}{2}(E_{HOMO} + E_{LUMO}) \approx -\frac{1}{2}(I_E + E_A) \qquad (\mathbf{2.58})$$

Hardness (H) is a measurement of molecule resistance towards the deformation or polarization of the electron cloud of the atoms, ions or molecules under small perturbation n of chemical response and defined as the form [117]:

$$H = \frac{1}{2}\left(\frac{\partial \mu}{\partial N}\right)_{v_{(\vec{r})}} \qquad (\mathbf{2.59})$$

In terms of I_E and E_A, the hardness is half of the energy gap between two frontier orbitals as in the following [117,119]:

$$H = \frac{I_E - E_A}{2} \qquad (\mathbf{2.60})$$

The hard molecule has a large energy gap. The theoretical definition of chemical hardness has been provided by the DFT as the second derivative of electronic energy with respect to the number of electrons N, for a constant external potential $V(\vec{r})$ as in the Eq. (2.60) [117,118]:

$$H = \frac{1}{2}\left[\frac{\partial^2 E}{\partial N^2}\right]_{V(\vec{r})} = \frac{1}{2}\left[\frac{\partial \mu}{\partial N}\right]_{V(\vec{r})} \qquad (\mathbf{2.61})$$

The soft molecule has a small energy gap and this means small excitation energies to the manifold of excited states, the electron density of soft molecule changes more easily than a hard molecule, and due to that, soft molecules will be more reactive than hard molecules. The global chemical softness S is a property of molecules that measures the extent of chemical reactivity. It is the inverse with hardness as shown in equation [117,120]:

$$S = \frac{1}{2H} = \left(\frac{\partial^2 N}{\partial E^2}\right)_{V(\vec{r})} = \left(\frac{\partial N}{\partial K}\right)_{V(\vec{r})} \qquad (\mathbf{2.62})$$

2.10.4 Electrophilicity and Electronegativity

The electrophilicity index (ω) is a measure of energy lowering due to maximal electron flow between donor and acceptor. In which the electrophilicity index given as follow [121]:

$$\omega = \frac{\mu^2}{2H} \qquad (\mathbf{2.63})$$

Electrophilicity is built up from the electronic structure of molecules, independent of the nucleophilic. The electrophiles are species that stabilize upon receiving on additional amount of electronic charge from the environment [121,122].

The electronegativity (E_N) is a measure of the tendency to attract electrons by an atom in a chemical bond and defined as the negative of the chemical potential (E_N=-μ) in DFT and given by the following [112,120]:

$$\mathrm{E_N} = \frac{1}{2}(\mathrm{I_E} + \mathrm{E_A}) \qquad (\mathbf{2.64})$$

To evaluate the electronegativity according to Koopmans theorem, it can be defined as the negative value for average of the energy levels of the HOMO and LUMO as in the following equation [114,120]:

$$\mathrm{E_N} = -\frac{1}{2}(\mathrm{E_{HOMO}} - \mathrm{E_{LUMO}}) \qquad (\mathbf{2.65})$$

2.10.5 Electrical Conductivity

Electrical conductivity is an simplicity expression of which an electric current flows through a material. When a current of one Ampere passes through a component across which a voltage of one Volt exists, then the electrical conductance of the component is one Siemens (S) [123,124]:

$$G = I/E \qquad (\mathbf{2.66})$$

Where $f(\mathrm{E})$ is the Fermi function:

$$G = G_0 \int_{-\infty}^{\infty} dE\, T(E) \left(-\frac{df(E)}{dE}\right) \quad (\mathbf{2.67})$$

Where f(E) is the Fermi function:

$$f(\mathrm{E}) = [e^{\beta(E-E_F^{DFT})} + 1]^{-1} \quad (\mathbf{2.68})$$

E_F is the Fermi energy and β=1/kBT

G_0 in equation (2.38) is the quantum of conductance:

$$G_0 = \left(\frac{2e^2}{h}\right) \quad (\mathbf{2.96})$$

Since the quantity $(-\frac{df(E)}{dE})$ is a probability distribution at $E=E_F$, with a width of order k_BT [125].

2.10.6 Thermal conductivity

Thermal conductivity is the measured of conduct heat in a material, it depends on temperature. Principally, it is calculated according to Fourier's Law of heat conduction. Heat transfer across materials of low thermal conductivity (used as thermal insulation) occurs at a lower rate in comparison to the materials of high thermal conductivity (used in heat sink applications). Thermal conductivity is measured in watts per meter Kelvin (W/m•K) in SI units. The thermal resistivity is defined as the reciprocal of thermal conductivity [124].

2.10.7 Seebeck Coefficient

Seebeck coefficient is a measure of a magnitude of an induced thermoelectric voltage in response to a temperature difference across a material. Seebeck coefficient is also defined thermoelectric power and thermoelectric sensitivity of a material, it is measured in volts per kelvin (V/K) in SI units. Seebeck coefficient of a material is calculated when a small temperature gradient is applied to a material as [126]:

$$S = -\frac{\Delta V}{\Delta T} \qquad (\mathbf{2.70})$$

Where ΔT is a small temperature difference between the two ends of a material and ΔV is the thermoelectric voltage seen at the ends.

2.10.9 Transmission Coefficient

If the wave propagation is considered in a discontinues medium, then the transmission coefficient is describe the amplitude and intensity of a transmitted wave comparative to an incident wave [125]. The transmission coefficient and the associated reflection coefficient in non-relativistic quantum mechanics are used to describe the waves incident behavior on a barrier, the transmission coefficient is used to refer to the probability of tunneling of a particle through a barrier. The probability flux of the transmitted wave comparative to that of the incident wave is

represented in terms of transmission coefficient [127,128]. The transmission coefficient of the structure was placed between two electrodes. The transmission coefficient T(E) describes the propagation of electrons of energy E from one electrode to the other. T(E) was calculated by finding the Hamiltonian $\hat{H}$ and the matrices of overlap S [128].

2.11 The Software

All calculations and results in this study have been performed by using the Gaussian 09, Gauss View, Gauss Sum 3.0 , SIESTA and GOLLUM Programs. Those programs are described as in the following.

2.11.1 Building of Atomic Configuration: Avogadro Software

To obtain the structure of all the systems in the thesis, the Avogadro program was used. Avogadro is an advanced molecular editor and visualizer designed for cross-platform use in computational chemistry, molecular modeling, bioinformatics, materials science and related fields see Figure. (2-4). It provides high-quality flexible rendering and a robust additional structure [130]. Avogadro offers a semantic chemical generator and platform for visualization and analysis. For users, it offers an easy-to-use generator, integrated support for downloading from popular databases such as Pub-Chemistry and Protein Data Bank, extraction of chemical

data from a variety of formats, including computational chemistry output, and native semantic support for the CML file format. For more theoretical details about Avogadro and what it offers, see [131].

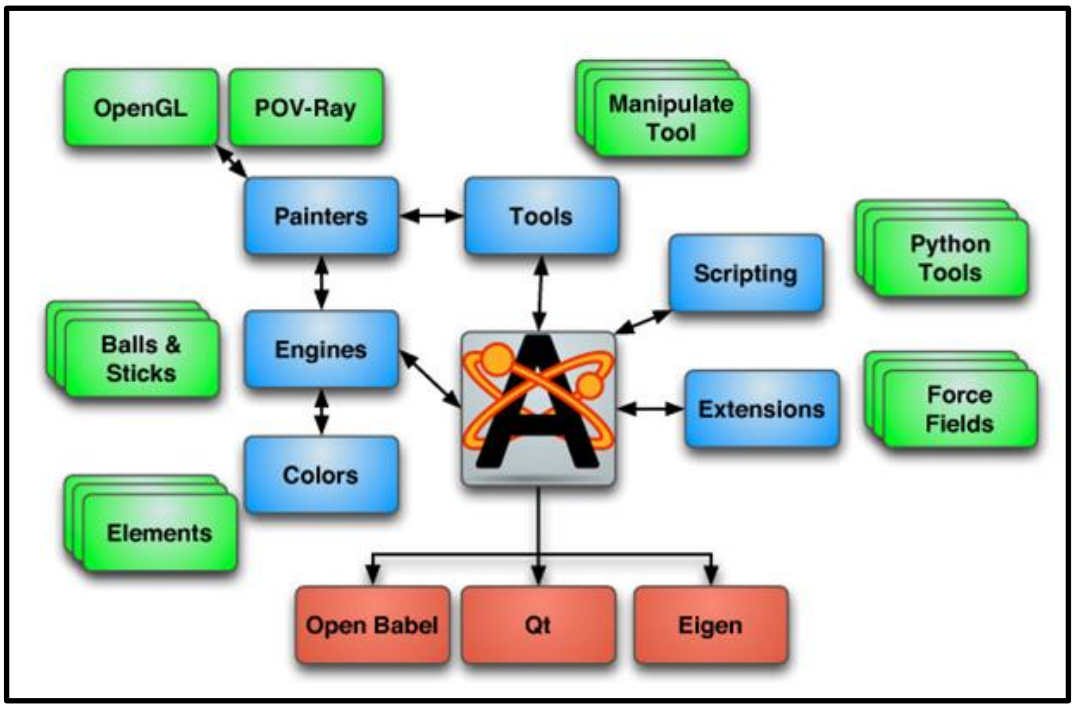

Figure (2.4): Atomic building capabilities and tools using Avogadro[130].

2.11.2 Gaussian 09 (G09) Program

The Gaussian program, one of the most widely computational chemistry software package initially released in 1970 by John Pople.

Gaussian program is a very high-end quantum chemical software package, available commercially through Gaussian, Inc.. The "09" refers to the year 2009 in which the software was published [129].

Gaussian is capable of running all of the major methods in molecular modeling, including molecular mechanics, ab initio, semi-empirical, HF and DFT. Moreover, excited state computes can be done by different methods in this program [132].

The name originates Gaussian come from the use of the Gaussian Type Orbital's that Gaussian's originator, John Pople, used to try to overcome the computational difficulties that arise from the use of Slater Type Orbital's [129,132].

2.11.3 SIESTA program

SIESTA (Spanish Initiative for Electronic Simulations with Thousands of Atoms) is both a method and its computer program implementation, to perform efficient electronic structure calculations and ab initio molecular dynamics simulations of molecules and solids. SIESTA's efficiency stems from the use of strictly localized basis sets and from the implementation of linear-scaling algorithms which can be applied to suitable systems. SIESTA is main characteristics are use the standard Kohn-Sham self-consistent density functional method in the local density approximations (LDA-LSDA) and GGA, as well as in a non-local functional that includes Van der Waals interactions. It uses norm-conserving pseudo potentials in their fully nonlocal (Klein man-

Bylander) form. It uses atomic orbitals as a basis set, allowing unlimited multiple-zeta and angular momenta, polarization and on site orbitals. Finite-support basis sets are the key for calculating the Hamiltonian and overlap matrices in the operations. Projects the electron wave functions and density onto a real-space grid in order to calculate the Hartree and exchange-correlation potentials and their matrix elements [133]

2.11.4 GOLLUM 1.0 Program

GOLLUM is a program written by Fortran that computes the electrical and thermal transport properties of multi-terminal nano-scale systems. The program can compute transport properties of either user-defined systems described by a tight-binding (or Huckel) Hamiltonian. The program has been created to interface easily with any DFT code and uses a localized basis [134]. It currently reads information from SIESTA [135]. Plans to produce interfaces to other codes like FIREBALL are underway. GOLLUM is based on equilibrium transport theory, meaning that it consumes much less memory than NEGF (non-equilibrium Greens function) codes. The program has been designed for user-friendliness and takes a considerable leap towards the realization of ab initio multi-scale simulations of conventional and more sophisticated transport functionalities. GOLLUM delivers functionalities, reads either Tight-

Binding or DFT Hamiltonians, simulates multi-terminal devices, computes the full scattering matrix and charge transport, number of open scattering channels, transmission and reflection coefficients, shot-noise, computes heat transport, thermal conductance and thermo power (Seebeck coefficient), peltier coefficient, computes spin transport, computes zero-voltage as well as I-V curves, computes band-structure of the leads and DOS in the scattering region [134].

Chapter Three

Results and Discussion

Electronic and Spectroscopy Properties

3.1 Introduction

The results and discussion of structural, electronic and optical properties for pure (Polymeres), (Polymeres-ZnO_2), (Polymers-Dye) and (Polymers-Dye-ZnO_2) nanocomposites in our work, as well as pure Dye were demonstrated.

The Becke's three parameter exchange with Lee, Yang, and Parr correlation functional (B3LYP) Density Functional Theory (DFT) basis sets are theoretically used to calculate the ground state. By employing the time-dependent DFT(TD-SCF) methods with (B3LYP) functional and (DFT) basis sets the excited state calculations are carried out .

3.2 The Structural Properties of pure Polymers and its Nanocomposites.

3.2.1 Geometrical Properties of pure polymers and their nanocomposite.

By using Avogadro program the suggested nanocomposites were designed and then relaxed at the Gaussian 09 package of programs by using the three-parameter hybrid functional of Becke,s (B3LYP) with density functional theory (DFT) basis set.

The relaxed geometries of all nanocomposites in varied polymer type are illustrated in Figure (3-1) for PVA and its nanocomposite , while the Figure (3-2)for PEG Polymer and its nanocomposite, Additionally Figure(3-3) for PMMA polymer and its nanocomposite .

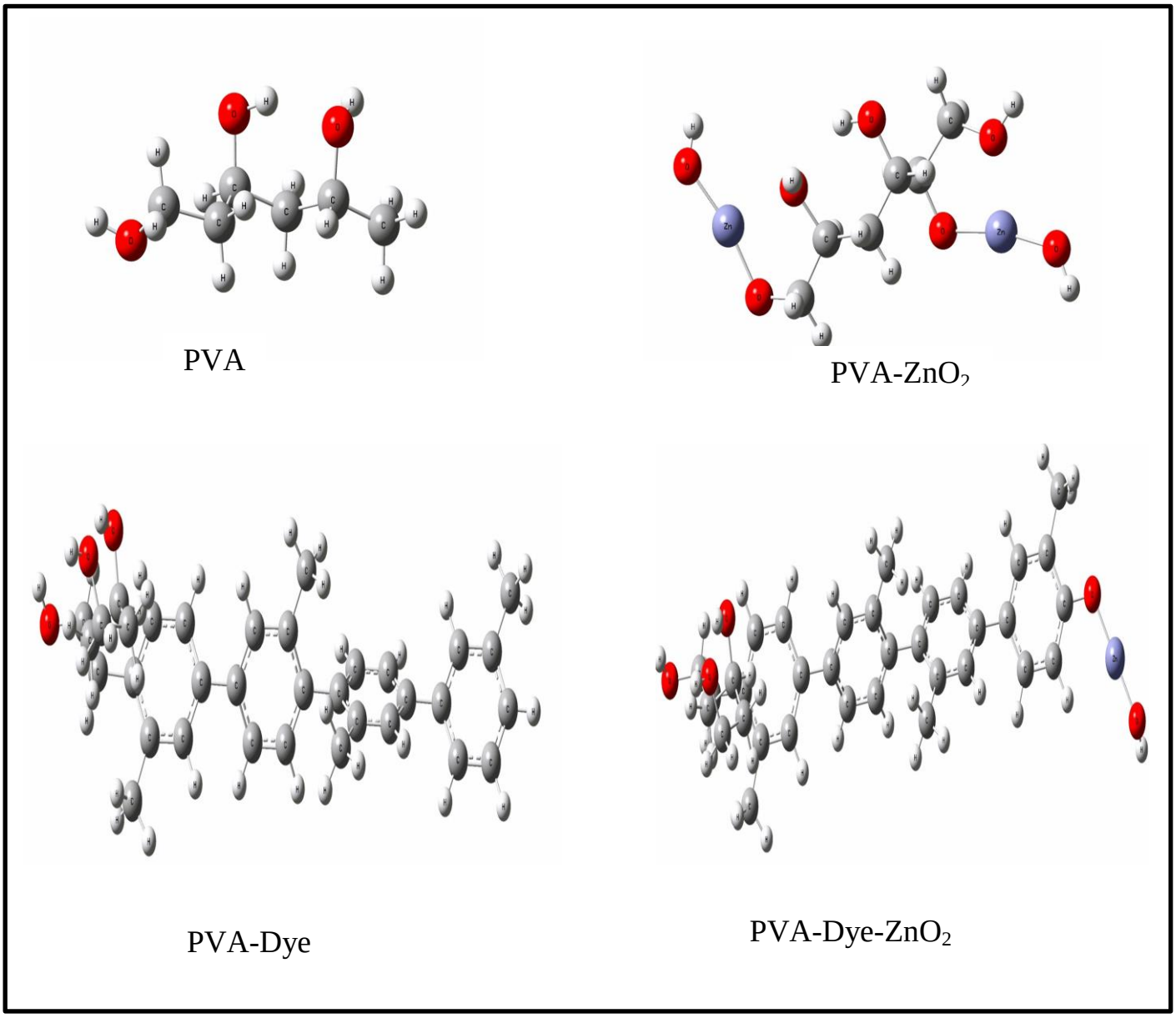

=Carbon , =oxygen , =Hydrogen and = zinc.

Figure (3.1): The relax structures of the pure PVA and its nanocomposite.

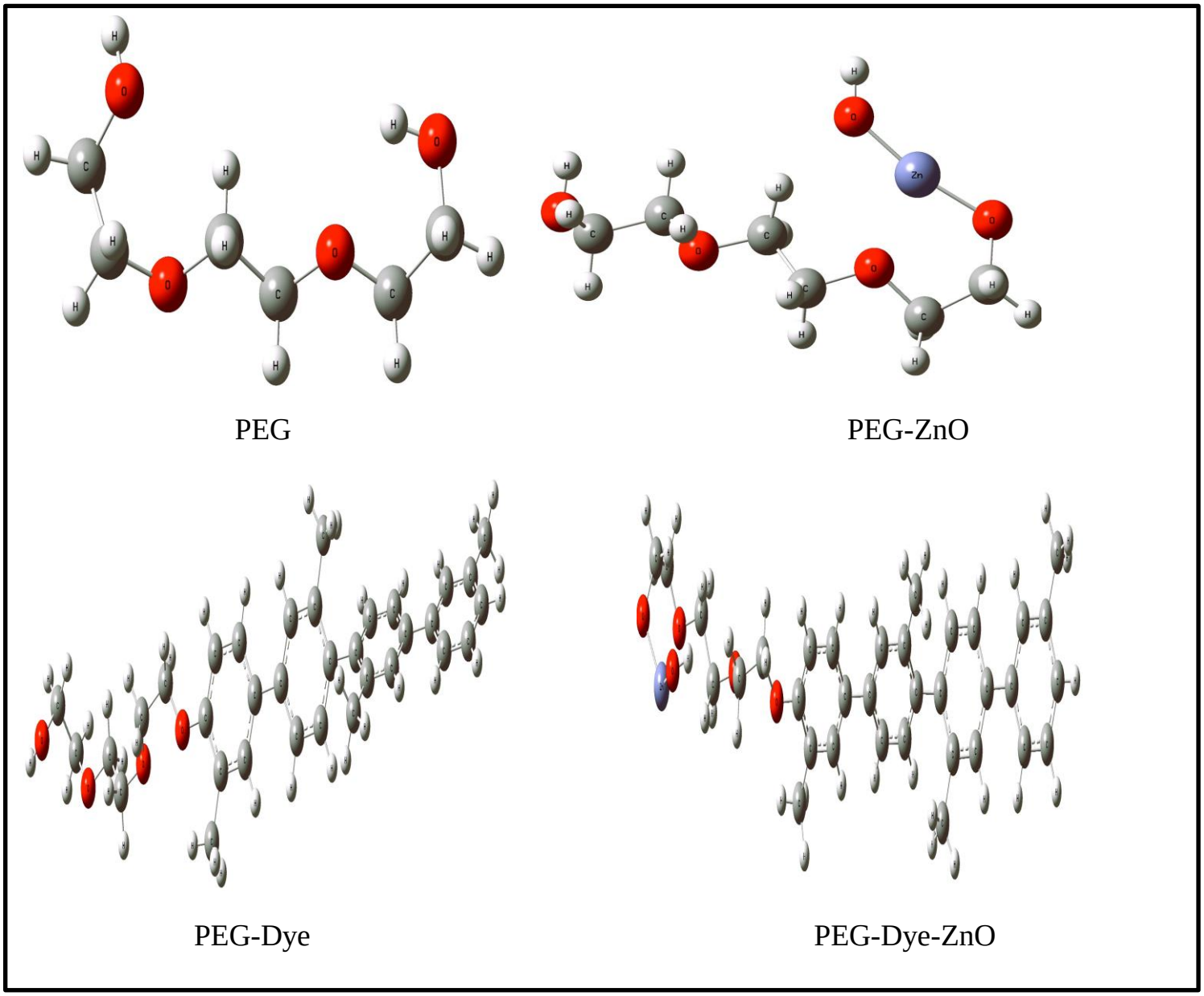

Figure (3.2): The relax structures of the pure PEG and its nanocomposite.

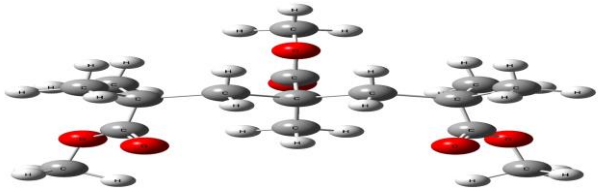

PMMA

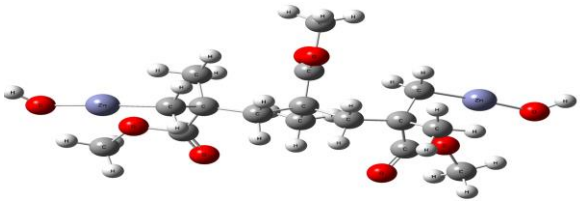

PMMA-ZnO

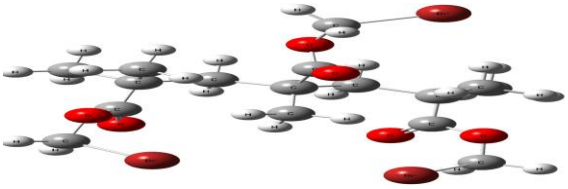

PMMA-3Br

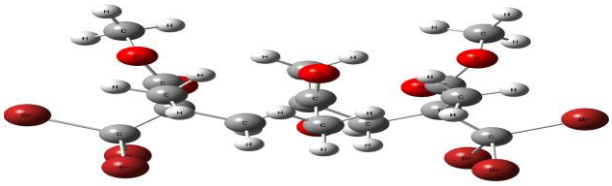

PMMA-6Br

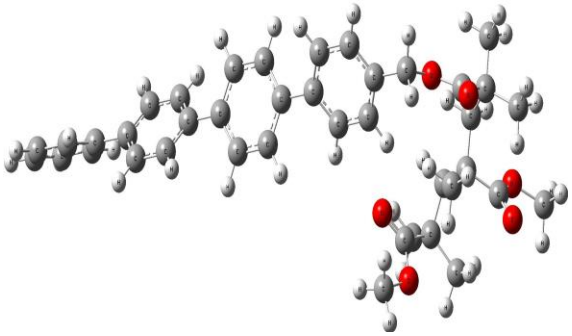

PMMA-Dye

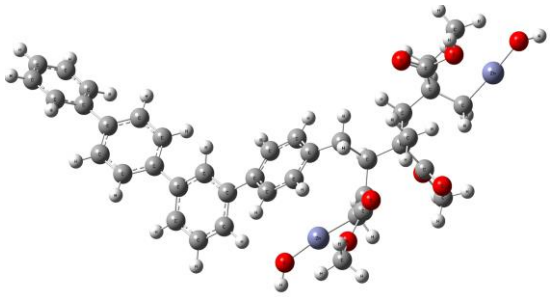

PMMA-Dye-ZnO

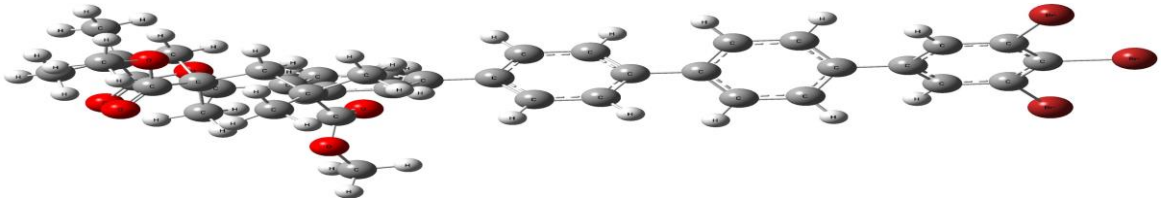

PMMA-Dye-Br

Figure (3.3): The relax structures of the pure PMMA and its nanocomposite

Tables (3.1), (3.2) and (3.3) presented the optimized parameters (bonds in Angstroms and angles in Degrees) for the polymer and its nanocomposite after the relaxation of each structure. Values of bonds in PVA which calculated are in a good agreement with theoretical study [118], this indicates to a good relax was obtained for composites from the suitable DFT basis sets. The included result in this table show that the addition of nanoparticle to pure Polymers has effect on the values of the optimize properties (bonds and angles) of the original structure, which showed that the added of nanoparticales (Zinc oxide , Br and Dye) cause a simple changing in the bond length and angle which means good relax for the structures of the studied nanocomposite was obtained theoretically[58] ; Also from the same table can be note variation in the values of the angles (C-C-C, C-C-H) because of different atomic numbers which cause the strong of interaction between them.

Table 3.1. Average bond lengths in (Å) and angles in degree for PVA nanocomposite.

linear	The optimization parameters	Pure PVA	PVA-ZnO_2	PVA-ZnO_2-Dye
Bond Length (Å)	C-C	1.52	1.54	1.539
	C-H	(1.08-1.09)	1.1	1.09
	C-O	1.48	1.51	1.47
	Zn-O	-	1.84	1.795
Bond Angle (degree)	C=C=C	-	-	118-120
	C-C-C	(111-114)	(112-116)	115
	C-C-H	(108-110)	110	111.8
	C-C=C	-	-	112
	C-O-Zn	-	114.11	118.9

Table 3.2. Average bond lengths in (Å) and angles in degree for PEG nanocomposite.

linear	The optimization parameters	purePEG	PEG-ZnO	PEG-ZnO`-Dye
Bond Length (Å)	C-C	1.51	1.53	1.52
	C-H	1.1	1.1	1.1
	C-O	1.45	1.43,1.47	1.38
	Zn-O	-	1.8	1.8
Bond Angle (degree)	C=C=C	-	-	118-120
	C-C-C	-	-	118
	C-C-H	108	110	111.8
	O-Zn-O	-	168	109.9
	C-C=C	-	-	112
	C-O-Zn	-	111	105

Table 3.3. Average bond lengths in (Å) and angles in degree for PMMA nanocomposite.

linear	The optimization parameters	purePMMA	PMMA-3Br	PMMA-3Br-Dye	PMMA-ZnO	PMMA-ZnO-Dye
Bond Length (Å)	C-C	1.53,1.56	1.56	1.55	1.55	1.566
	C-H	1.087,1.0916	1.09	1.09	1.09	1.09
	C-O	1.47	1.43	1.48	1.472	1.465
	C=O	1.23	1.22	1.22	1.226	1.244
	Zn-C				1.92	1.816
	Br-C		2	1.9		
Bond Angle (degree)	C=C=C	-	-	118		
	C-C-C	108	108	112	-	110.7
	C-C-H	110	108	109	109.6	113
	C-O-C	116	125	112	112	110
	O-C-H	104	107	105	104	104
	O-C-Br	-	111	-		
	O-C-Zn				176	173
	H-C-Br	-	105			
	C-C-O	111		112		
	Br-C-C			121		
	Br-C-Br	-	106	-		

3.2.2 Geometrical Properties of pure P-quaterphynel Dye.

Figure(3.4) shows the relaxed structure of pure P-quaterphyneldye, as well as table 3.4 presented the optimized parameters (bonds in Angstroms and angles in Degrees) for the pure Dye.

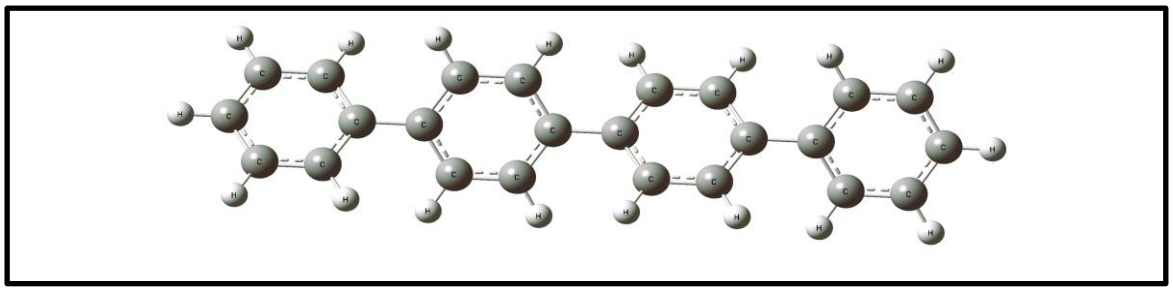

Figure (3.4): The structures of the pure Dye (P-Quaterphyneldye).

Table 3.4. Average bond lengths in (Å) and angles in degree for Dye(P-Quaterphyneldye).

linear	The optimization parameters	pureDye
Bond Length (Å)	C-C	1.5
	C=C	1.4
	C-H	(1.06-1.09)
Bond Angle (degree)	C=C=C	117
	C=C-C	121.16
	C-C-H	(108-110)
	H-C=C	119.79
	H-C-C	111.28

(3-3) Infrared Radiation (IR) of Polymers Nanocomposites and pure Dye .

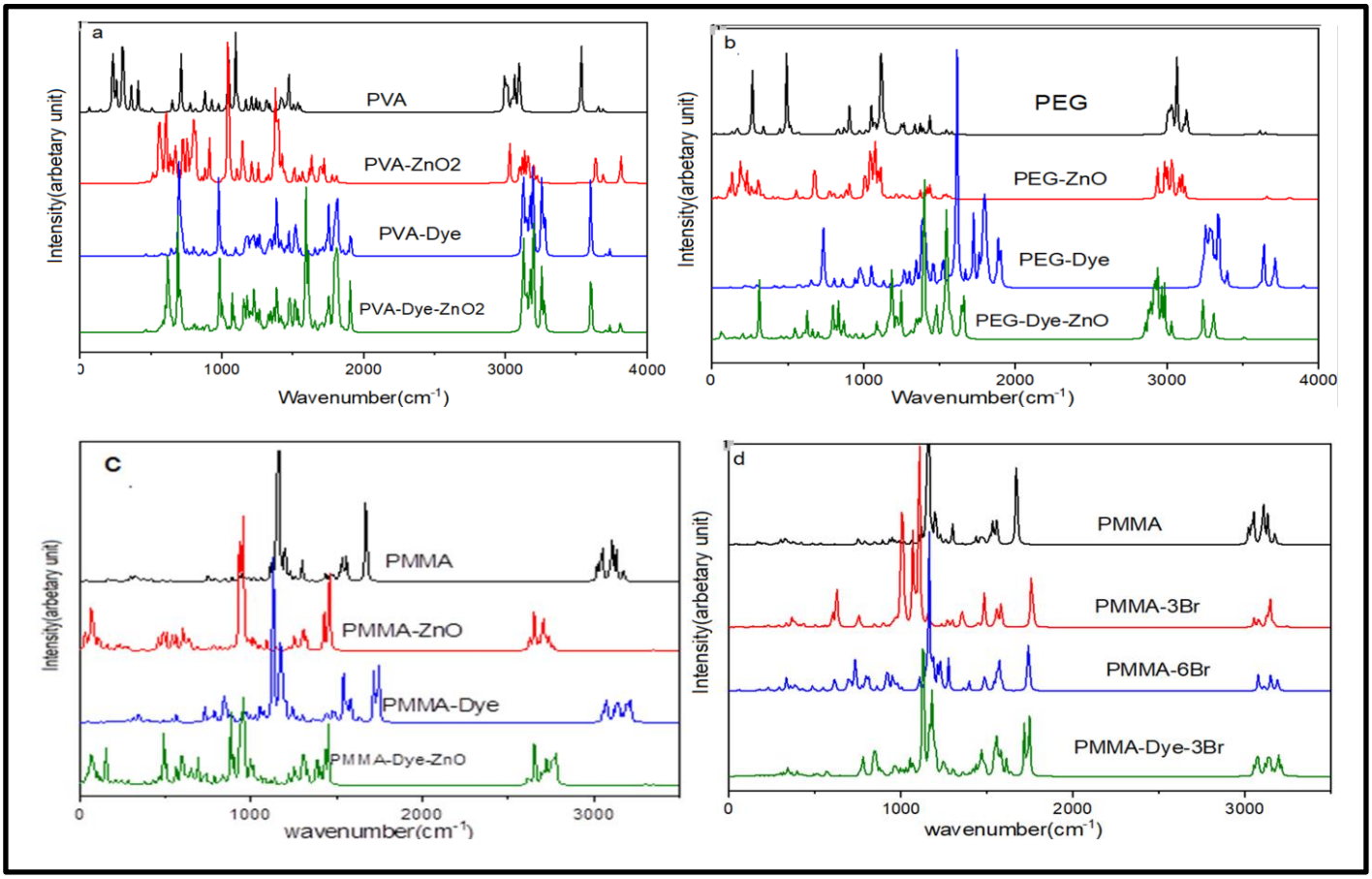

Figure (3.5): IR spectra of (a) PVA,(b) PEG,(c) PMMA-ZnO, and(d) PMMA-Br and their Nanocomposites.

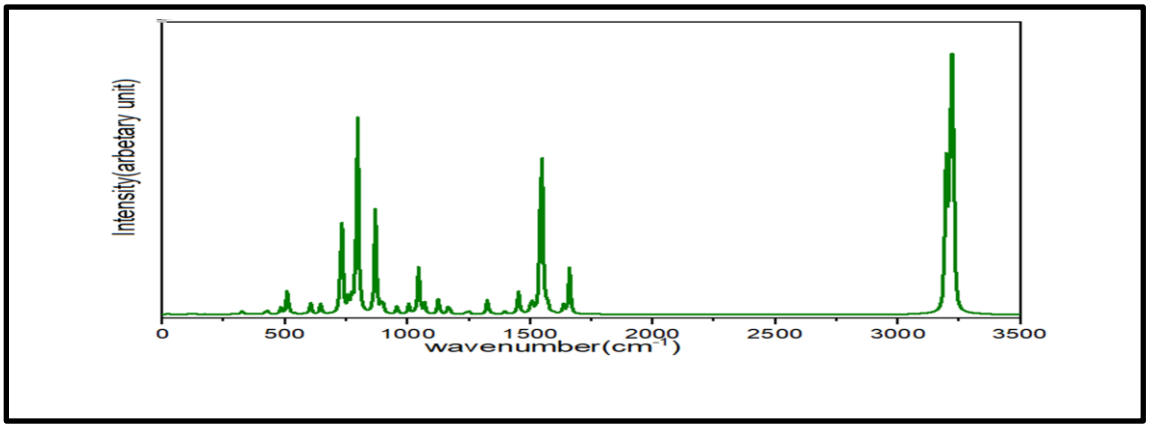

Figure (3.6): The IR spectra the pure Dye.

IR spectra of (PVA, PVA-ZnO_2,PVA-Dye-ZnO_2, PVA-Dye and PVA-Dye-ZnO_2) nanocomposites theoretically are shown in Figure (3-5) respectively and Tables (3-5). Two main regions are noticed, the diagnostic region which lie between (1500-4000)cm^{-1} and the fingerprint region lie between (400-1500)cm^{-1} pointed to functional group region, the left region specially close to (4000) cm^{-1} it is for the high energy bonds.

The result for PVA and its nanocomposite demonstrated that the band of absorption at (545) cm^{-1} related to Zn-O[**2**], (C–O) stretching band illustrated(1097)cm^{-1}. C-C stretching is related to the region (700-1056) cm^{-1} it is a stretching vibration of (CH and CH_2) that causes the peak at (470) cm^{-1}. There is a prominent band between (3019 and 3073) cm^{-1}, which is due to (-CH_3) symmetric stretching vibration, and a peak between (3069 and 3073) cm^{-1}, which is due to (-CH) symmetric stretching vibration. (-CH_2) symmetric stretching vibration is represented by the peak at (2878) cm^{-1}, while (-CH_2) asymmetric stretching vibration is represented by the peak at (3093-3144) cm^{-1}[1] .

On the other hand, for PEG Polymer, the absorption bands at (3117 -3662)cm^{-1} was due to the O–H stretching band, (2920) cm^{-1} was due to the C–H stretching, (1442, 1374) cm^{-1} were due to the C-H bending vibrations, in the region from (1011-1111) cm^{-1} and 700 cm^{-1} due to respectively the C–O and C–C groups' [3].

For PMMA polymer the result showed that the band of absorption at (1147) cm^{-1} represents stretching and bending of (C–C). The (C-O) stretching vibration is reflected by the peak at (1299) cm^{-1}. There is a peak at (1671) cm^{-1}, which is indicative of a stretching vibration in the molecule (C=O). The prominent band at 3042 cm^{-1} ($–CH_3$) stretching vibration with a symmetric peak at (3069–3073) cm^{-1} ($–CH_2$) Vibrations of stretched symmetry. The peak at (3111) cm^{-1} represents ($–CH_3$) asymmetric stretching vibration and the peak at (3144) cm^{-1} represents ($–CH_2$) asymmetric stretching vibration[4,59], The vibration modes due to C-C stretching appear at (985.66 and 965.14) cm^{-1}. The peaks at (911.13) cm^{-1} and at (810.42 and 749.14)cm^{-1} are due to the CH_2 rocking in plane and out of plane bending, respectively[59]. (840.69) cm^{-1} are assigned to CH_2 rocking, and the peaks.

Some bond shifts and intensity variations are inevitable outcomes. Changes in the IR spectra of polymer have been triggered by the presence of metal oxides ZnO, Br and Dye (P-Quaterphynel), leading to a rearrangement of certain bonds and a modification of the intensities [1].

Table 3.5. IR frequency with their assignment of (PVA-PEG AND PMMA) polymers nanocomposite.

Assignment	Type of vibrational mode	Wavenumber(cm^{-1})
PVA		
ZnO	**-**	**400-700**
C−C	**Stretching and bending**	**700-1056**
C−O	**Stretching**	**1097**
$-CH_2$	**in–plane bending**	**1470**
C−C	**Stretching and bending**	**1543-1561**
C−H	**Symmetric stretching**	**3000-3081**
O−H	**Stretching**	**3535**
PEG		
C−C	**Stretching and bending**	**700**
C−O	**Stretching**	**1011-111**
C-H	**bending**	**1422**
C-H	**Stretching**	**2920**
O-H	**Stretching**	**3117,3662**
PMMA		
C-C	**Stretching and bending**	**1147.9**
C-O	**stretching**	**1210-1299**
C=O	**stretching**	**1671.6**
$-CH_3$	**Symmetric stretching**	**3042**
$-CH_3$	**Asymmetric stretching**	**3111**
CH_2	**Symmetric stretching**	**3144**
Br-C	**-**	**400**

3-4 UV-Vis Spectrum and Oscillator strength of Polymers and its nanocomposite.

The Ultraviolet-Visible of the Nancomposites under research were investigated and evaluated using the time dependent- TD approach with the same hybrid functional and basis sets as in the B3LYP/ DFT method. The critical factor in determining if the Nanocomposite can be used as an active medium for laser is their emission oscillator strength.

3-4-1 PVA Polymer and its Nanocomposites.

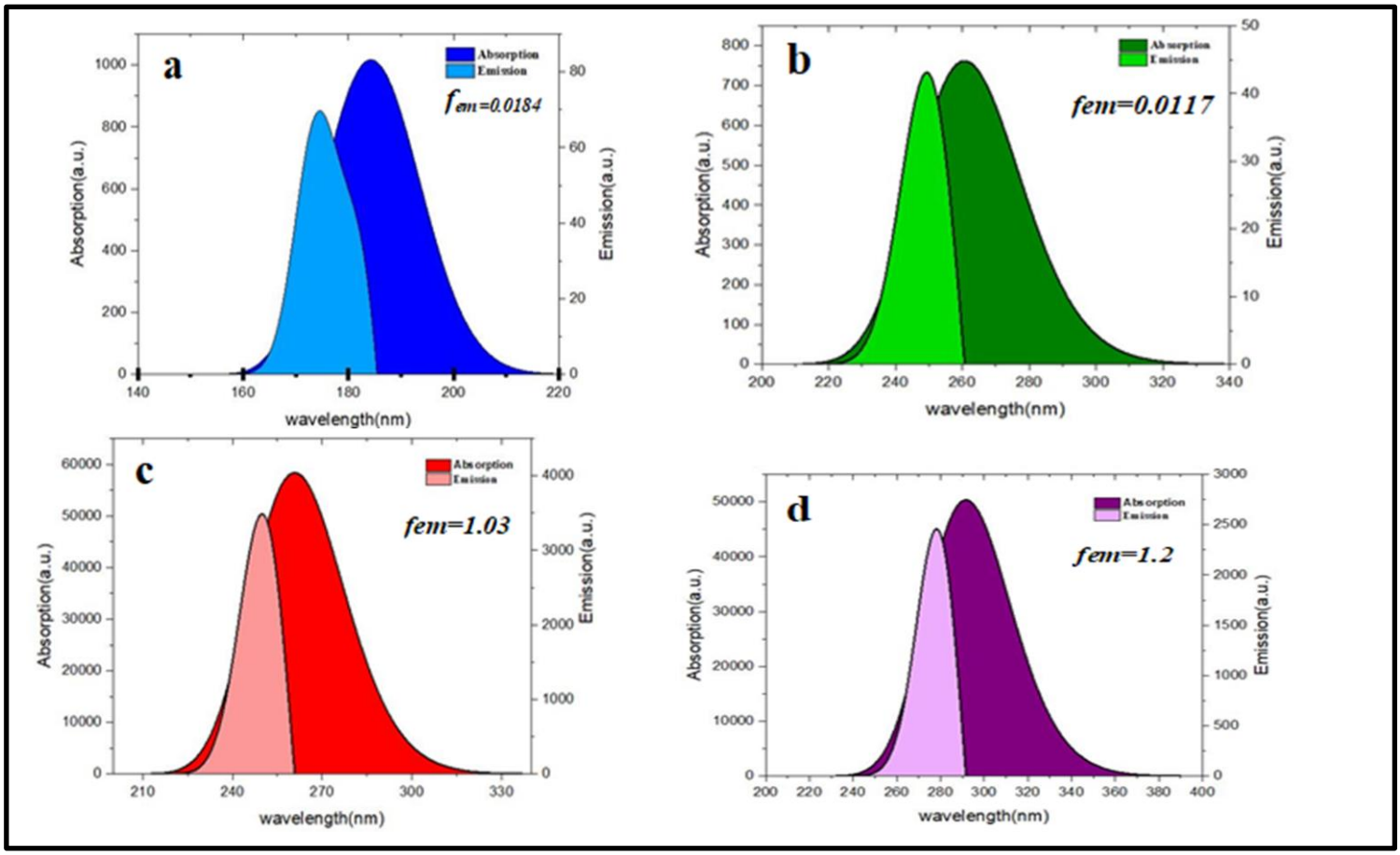

Figure (3.7): UV-Vis spectra for (a) pure PVA,(b) (PVA- ZnO_2), (c)(PVA- Dye)and(d) (PVA-ZnO_2-Dye).

Figure (3.7) and Table(3.6) shows that the absorption peak of PVA shifted from 190 nm to 260nm(red shift) noticeably with added ZnO_2, as well as in the case of PVA-Dye and PVA-ZnO_2-Dye (Tetramethylp-quaterphynel) since When the atoms number that formate the nanocomposites increases, also the spectrum shifted to longer wavelength [7].

The value of the absorption intensity (ε) has an increasable enhancement in the presence of dye , for the PVA is 1000 a.u., PVA-ZnO_2 is 750a.u. while it increased for the PVA-Dye $5.5*10^4$ a.u. and PVA-ZnO_2-Dye its $5 *10^4$a.u. Furthermore displacement of the absorption peaks can be noted, where the maximum absorption of the PVA-Dye at 260nm and PVA-ZnO_2-Dye at 291.6nm, it can be conclude altering the intensity of the absorption, and effective shifting in wavelengths were a result of increasing the number of atoms that formation the nanocomposites [66], Figure 3.7 displays the emission oscillator strength (*fem*) as a function of the wavelengths, which is the second significant outcome. Intriguingly, the presence of Dye dramatically increasing the Oscillator strength of PVA which produces the maximum *fem* (1.2), while the PVA-ZnO_2 gives the minimum *fem* (0.011). The sequence of the absorption intensity and *fem* , is PVA-ZnO_2-Dye (1.2) > PVA-Dye (1.03) > PVA(0.018) >PVA-ZnO_2(0.0117).

Based on these outcomes, a theoretically sound approach to selecting the (PVA-Dye and PVA-ZnO_2-Dye) that can be used as an active laser medium. These results can formulate a promising theoretical strategy for choosing the (PVA-Dye and PVA-ZnO_2-Dye) that can serve as an active laser medium. Since, the accomplishment of laser in terms of the threshold energy, output energy, maximum gain, etc can impact by the emission cross section (σem) of a laser transition. which means, the high gain lase is due to high value of emission cross section (σem).

3-4-2 PEG Polymer and its Nanocomposites

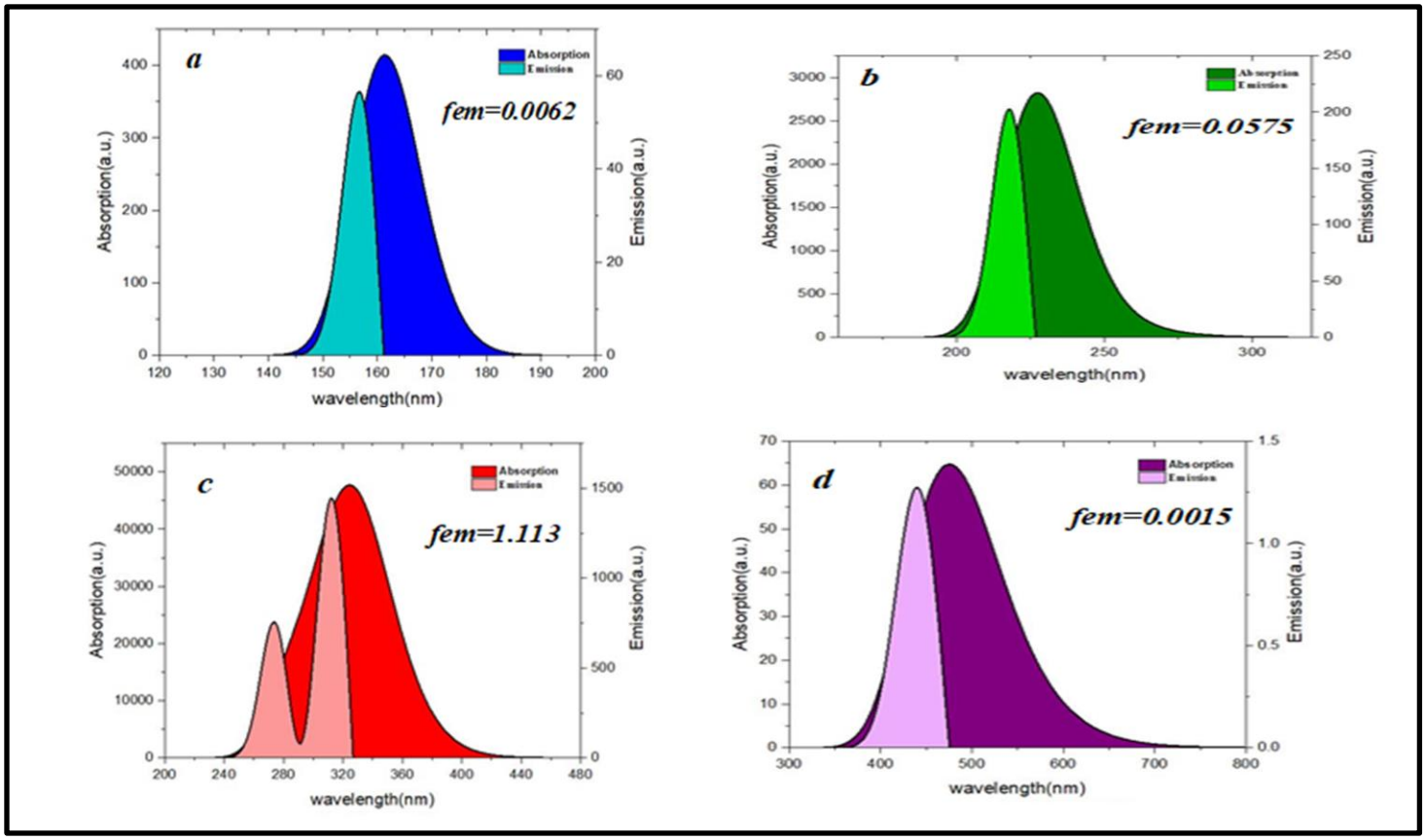

Figure (3.8): UV-Vis spectra for (a) PEG, (b) PEG- ZnO,(c) PEG- Dye and(d) PEG- ZnO-Dye.

Figure (3.8) and Table(3.6) demonstrates that the absorption intensity changes dramatically as the atom number changes. Absorption intensity (ε) value of PEG polymer is (400a.u), PEG-ZnO (2850 a.u.) ,PEG-Dye($4.5*10^4$) and its decreased strongly in the case of PEG-ZnO-Dye(65a.u.) as well as , It is possible to discern a sharp shift in the absorption peaks, since PEG polymer absorption at (161.4 nm). On the other hand, absorption of the PEG-ZnO at (225.34 nm), absorption of PEG-Dye(327nm) and of PEG-ZnO-Dye(500nm) Consequently, the absorption peak position moved to a longer wavelength as the atomic number of the nanocomposite was increased, resulting in a dramatic transition from the ultraviolet to the visible spectrum.

The second important result is exhibited in Figure 3.8, which shows (*fem*) as a function of the wavelengths. heights (*fem*) was in the case of (PEG-Dye(1.1137) the sequence of the absorption intensity, PEG-Dye > PEG-ZnO > PEG > PEG-ZnO-Dye and the emission oscillator strength (*fem*) order is PEG-Dye(1.113) > PEG-ZnO(0.0575) > PEG(0.0062) > PEG-ZnO-Dye(0.0015). From these result PEG-Dye nanocomposite was capable of serving as laser active medium.

3-4-3PMMA Polymer and its Nanocomposites

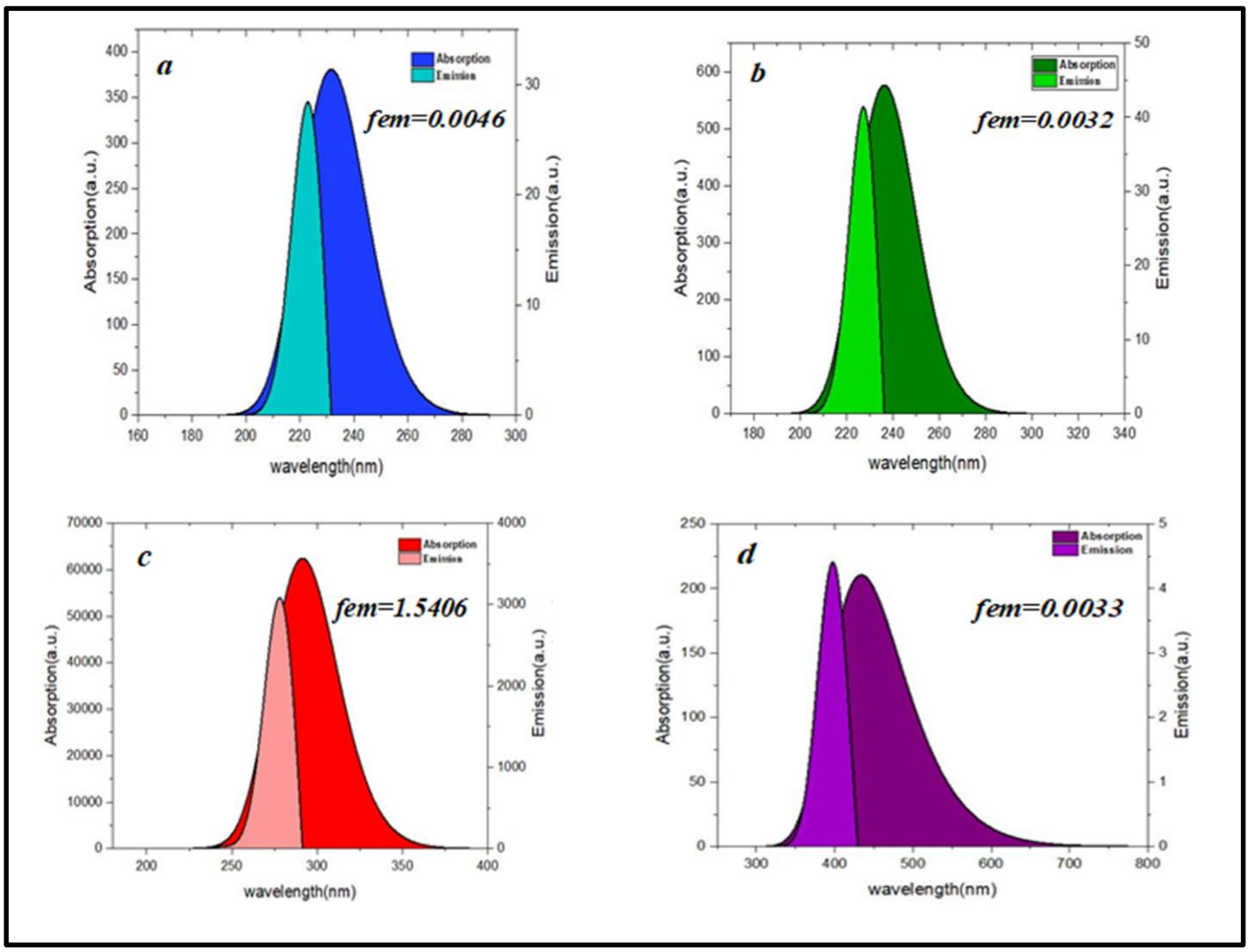

Figure (3.9): UV-Vis spectra for (a)pure PMMA, (b)(PMMA-ZnO), (c)(PMMA-Dye)and (d)(PMMA-ZnO-Dye).

Figure (3.9) and Table(3.6), we see the UV-Vis spectra of both PMMA and its nanocomposites.. PMM polymer absorption intensity (ε) is (380 a.u), PMMA-ZnO (550 a.u.) ,PMMA-Dye($6.4*10^4$) and its decreased in the case of PMMA-ZnO-Dye(422a.u.) as well as , PMMA polymer absorption at (233.47nm). on the other hand, intensity of absorption (ε) of PMMA-ZnO at (235.34 nm), absorption intensity(ε) of PMMA-Dye(291.44nm) and of PMMA-ZnO-Dye(422nm). The second important result is exhibited in Figure3.9, illustrated (f_{em}) with respect to wavelengths. The heights (f_{em}) was in the case of (PMMA-Dye(1.54).

The order of the absorption intensity (ε) is PMMA-Dye($6.4*10^4$) > PMMA-ZnO(550) > PMMA (380)> PMMA-ZnO-Dye(230) and the emission oscillator strength (f_{em}) order is PMMA-Dye(1.540)> PMMA-ZnO(0.0109) > PMMA(0.0046) > PMMA-ZnO-Dye(0.0033). From these results the structures and materials that can serve as an active laser medium was PMMA-Dye .

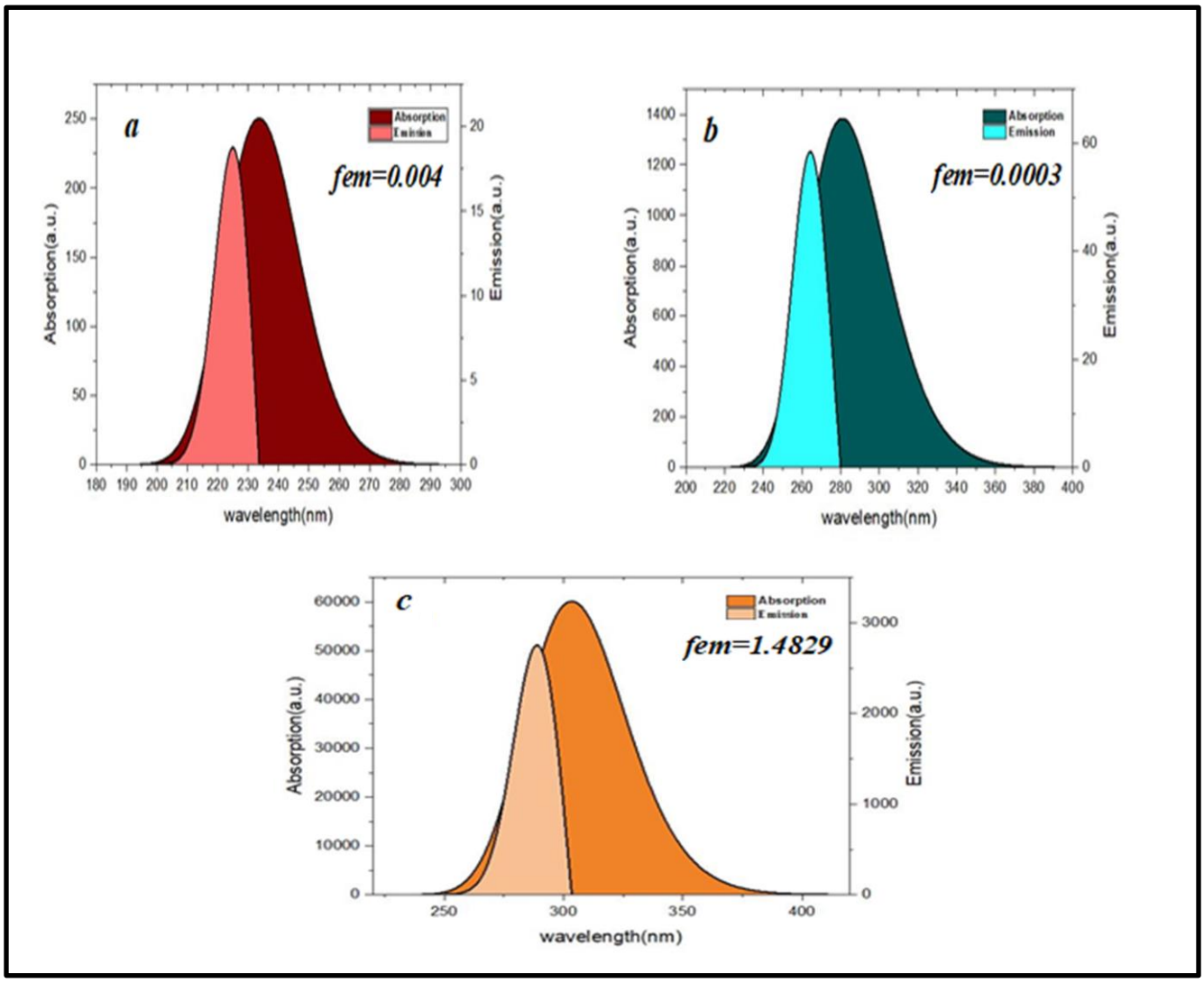

Figure (3.10): UV-Vis spectra for (a) PMMA-3Br, (b)PMMA-6Br,and(c) PMMA-3Br-Dye.

Figure (3.10),illustrate UV-Vis spectra of PMMA and its nanocomposites after the addition of Br nanocomposite. Figure showed that the maximum absorption intensity were in UV spectrum at (234.83 nm) for (PMMA-3Br), (290nm) for PMMA-6Br and(303.47 nm) for PMMA-3Br-Dye.

The value of the absorption intensity (ε) for the PMMA polymer molecule is(380a.u)., PMMA-3Br (250a.u.) ,PMMA-6Br(1380a.u.) and its increased in the case of PMMA-3Br-Dye($6*10^4$a.u.), due to adding of (Br NPS) to pure (PMMA) since the excitations of occupation level to the virtual level at these energies.

emission oscillator strength (f_{em}) sequence is PMMA-Dye-3Br(1.48)> PMMA-6Br(0.0134) > PMMA(0.0046) > PMMA-3Br(0.004). From these results PMMA-3Br-Dye nanocomposite could be used as an active laser medium.

Table3.6. The Absorption spectra calculations of the polymers and its nanocomposite

composite	Absorption peak position (nm)	Absorption Intensity	Oscillator strength
PVA	180	1000	0.0184
PVA-ZnO_2	262	750	0.0117
PVA-Dye	260	55000	1.03
PVA-Dye-ZnO_2	291.6	50000	1.2
PEG			
PEG	161.4	400	0.0062
PEG-ZnO2	225.34	2850	0.0575
PEG-Dye	327 286.46	45000 15000	1.1137 0.328
PEG-Dye-ZnO2	500	65	0.0015
PMMA			
PMMA	233.47	380	0.0046
PMMA-ZnO	235.34	550	0.0109
PMMA-Dye	291.44	64000	1.5406
PMMA-ZnO-Dye	422	230	0.0033
PMMA-3Br	234.83	250	0.004
PMMA-6Br	273.63	1380	0.0134
PMMA-3Br-Dye	303.47	60000	1.4829

3.4.4 UV-Vis Spectrum and Oscillator strength of pure Dye (Tetramethyl-p-quaterphynel).

UV-Vis spectra Dye(p-quaterphynel) illustrated in figures (3-11). It showes that absorption peak in UV region at (315 nm) for Dye, the oscillator strength intensity around(1.85)

In the Ultraviolet-Visible region the high absorption assigned to the energy of photon enough to react with atoms, thus the electron excites from a lower to higher energy level.

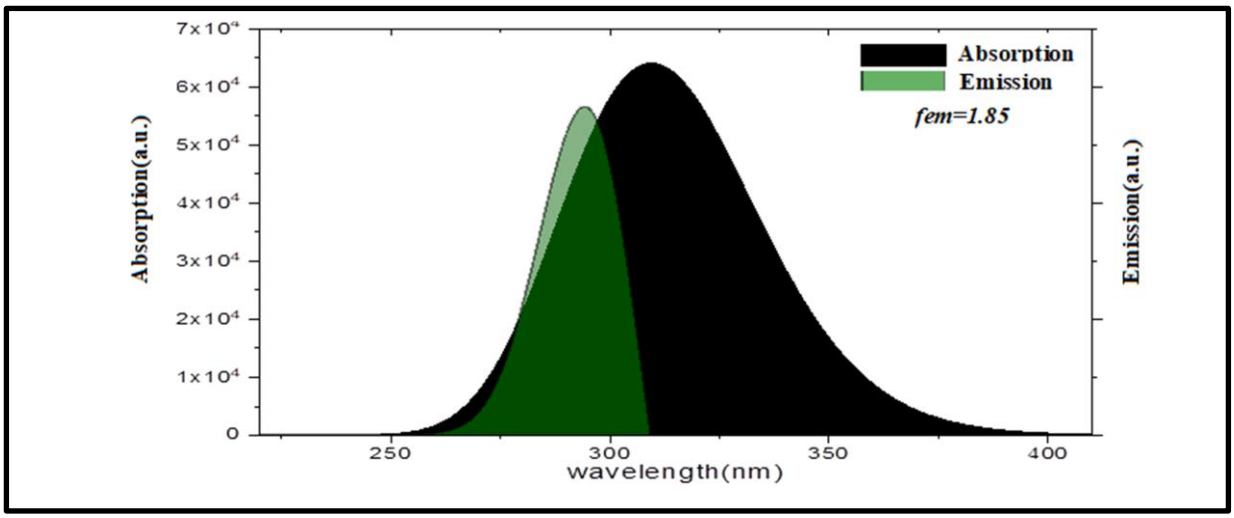

Figure (3.11): UV-Vis spectra for the pure Dye(Tetramethyl-p-quaterphynel).

3.5 Electronic States and Energy Gap.

By employing the DFT the electronic properties of Polymerse and thier nanocomposites were calculated. Electronic state energies ,(HOMO and LUMO) and the energy gap E_{gap}(eV) were computed. according to Koopman,s theorem,

these variables are include the ionization energy I_E(eV), electron affinity E_A in(eV), electrochemical hardness H in(eV), electronic softness S in$(eV)^{-1}$ and electrophilic index ω in(eV) were calculated.

Table 3.7 Illustrates the calculations of E_{HOMO} (High Occupied Molecular Orbital) Energy, E_{LUMO} (Low Unoccupied Molecular Orbital) energy and the energy gap E_{gap} for Polymer and its nanocomposite.

Molecular	HOMO(eV)	LUMO(eV)	Eg (eV)
PVA			
PVA	-6.9034	0.5633	7.4667
PVA-ZnO2	-6.532	-0.7110	5.821
PVA-Dye	-6.0030	-0.8550	5.1480
PVA-Dye-ZnO2	-5.5508	-1.4710	4.0797
PEG			
PEG	-6.7562	1.5012	8.2575
PEG-ZnO2	-6.3674	-0.5431	5.8242
PEG-Dye	-5.4585	-1.2808	4.1777
PEG-Dye-ZnO2	-5.3687	-2.5524	2.8163
PMMA			
PMMA	-7.4422	-0.4063	7.0359
PMMA-ZNO	-6.5344	-0.5793	5.9551
PMMA-DYE	-5.7323	-1.0727	4.6596
PMMA-DYE-ZNO	-5.3821	-1.1932	4.1889
PMMA-3Br	-7.1987	-0.8890	6.3097
PMMA-6Br	-7.0275	-1.9437	5.0838
PMMA-DYE-3Br	-5.9168	-1.4261	4.4906

The calculated values of E_{gap} in Table 3.7showe that, polymers and polymers nanocomposite have various electronic properties, energy gap in all polymers – nanocomposite got reduced due to adding ZnO and Dye since the electrons in the valence band can more easily access the conduction band localized levels due to dye and ZnO generation of new levels in the band gap[64-66] . in the cas of PVA nanocomposite PVA-ZnO2-Dye has the lowest energy gap (4.0797 eV). The order of energy gap is as:

PVA-ZnO_2–Dye(4.0798eV)< PVA-Dye(5.1480eV) < PVA-ZnO_2(5.821eV) < PVA(7.4667eV).

In the case of PEG nancomposite PEG-ZnO-Dye has the lowest energy gap(2.81eV). The order of energy gap is as:

PEG-ZnO-Dye(2.816eV)<PEG-Dye(4.177eV)<PEG-ZnO(5.824eV)< PEG(8.257eV).

For PMMA nanocomposite PMMA-ZnO-Dye and PMMA-3Br-Dye have the lowest energy gap(4.188eV) and (4.4eV) respsctively. The order of energy gap is as:

PMMA-ZnO-Dye(4.188eV)<PMMA-Dye(4.659eV)<PMMA-ZnO(5.955eV) <PMMA(7.035eV)

PMMA-3Br-Dye(4.490eV)<PMMA-Dye(4.659eV)<PMMA-6Br(5.083eV)
<PMMA-3Br(6.309eV)<PMMA(8.257eV).

In general, new electronic applications for the studied composites can be obtained due to the lowering energy gap. From Figures (3.12- 3.15) showed the HOMO and LUMO distribution for the polymers and composites under consideration.

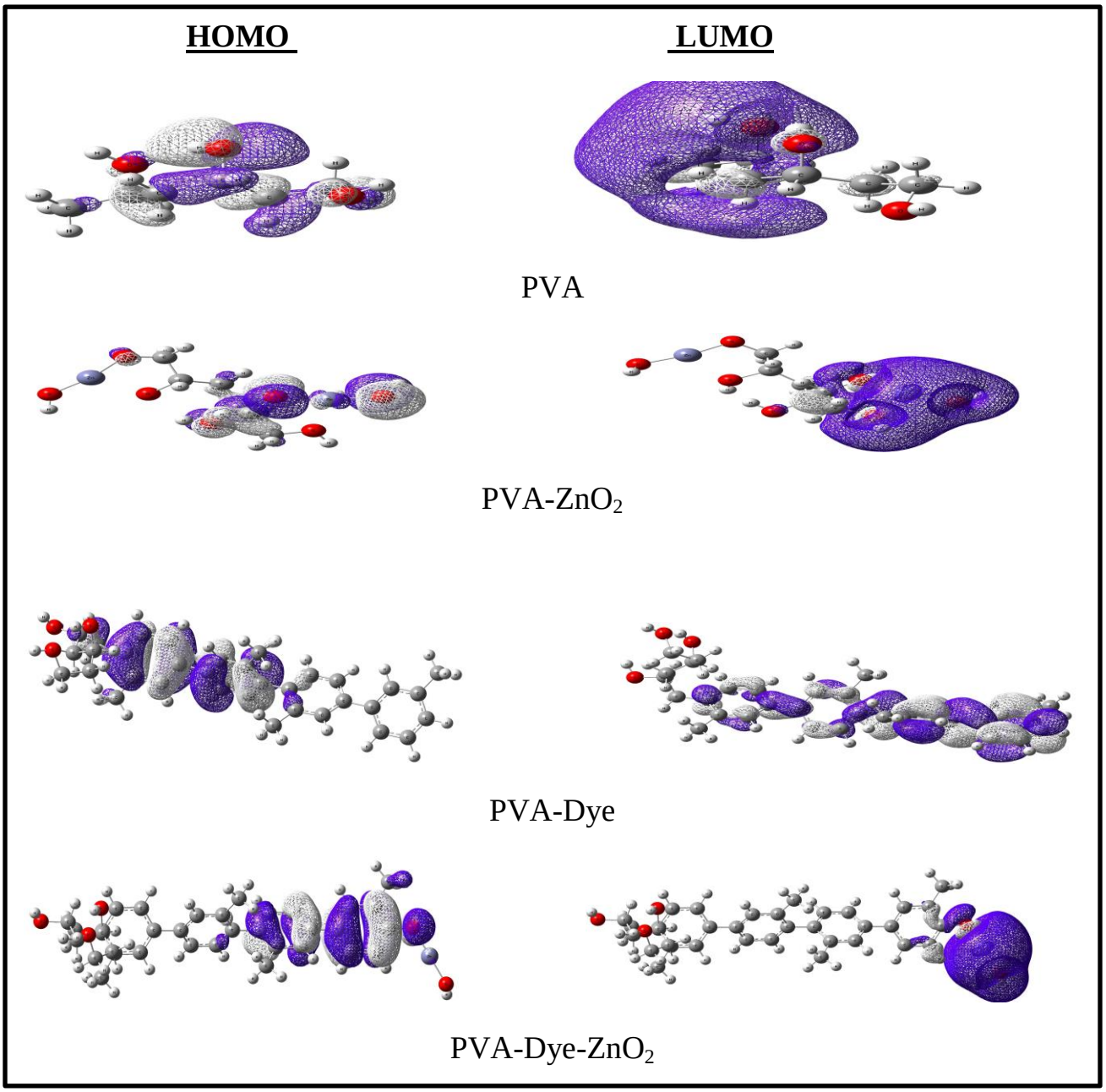

Figure (3.12):The distribution of HOMO and LUMO for (PVA and PVA- nanocomposites).

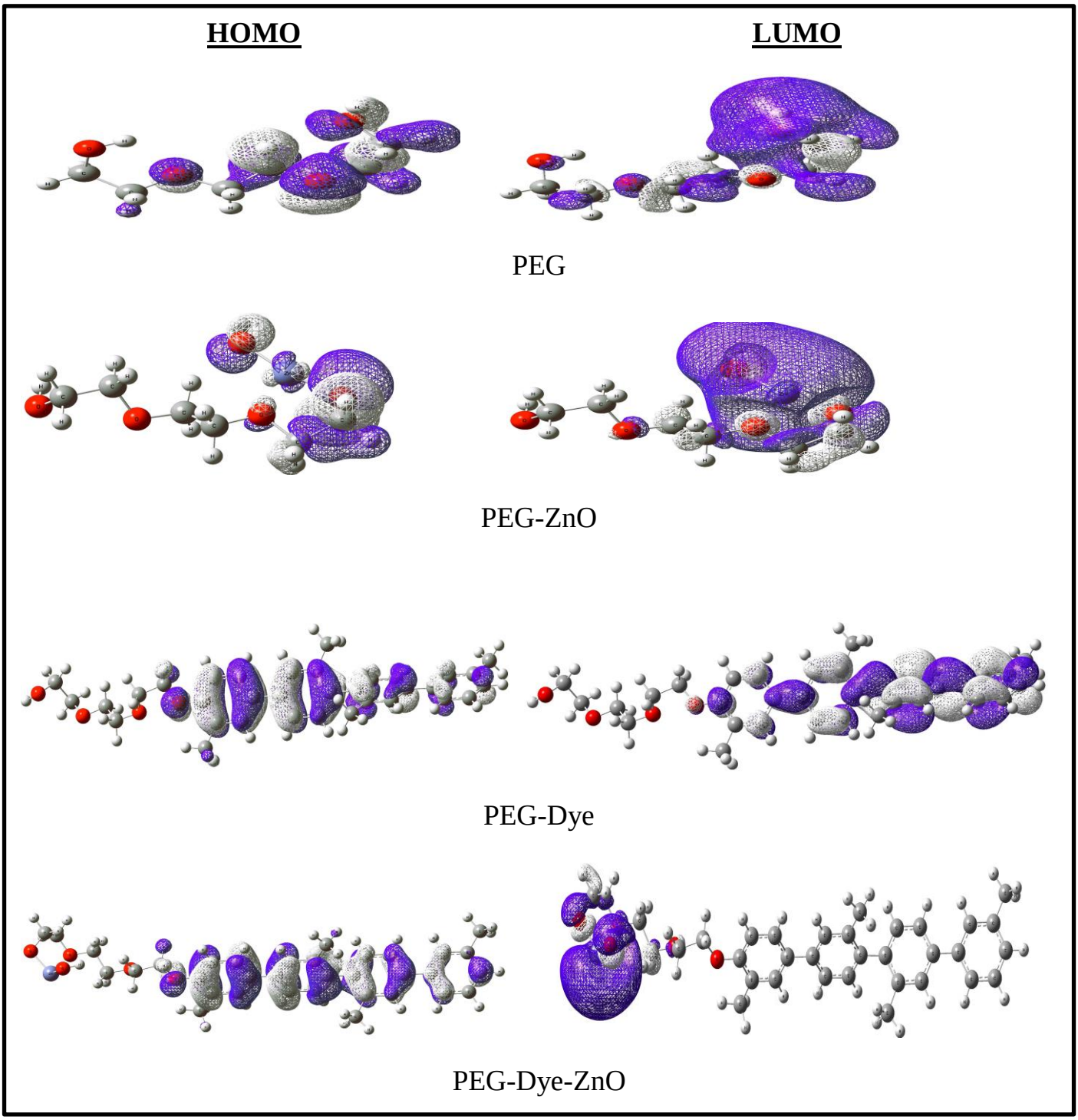

Figure(3.13): The distribution of HOMO and LUMO for (PEG and PEG-nanocomposites).

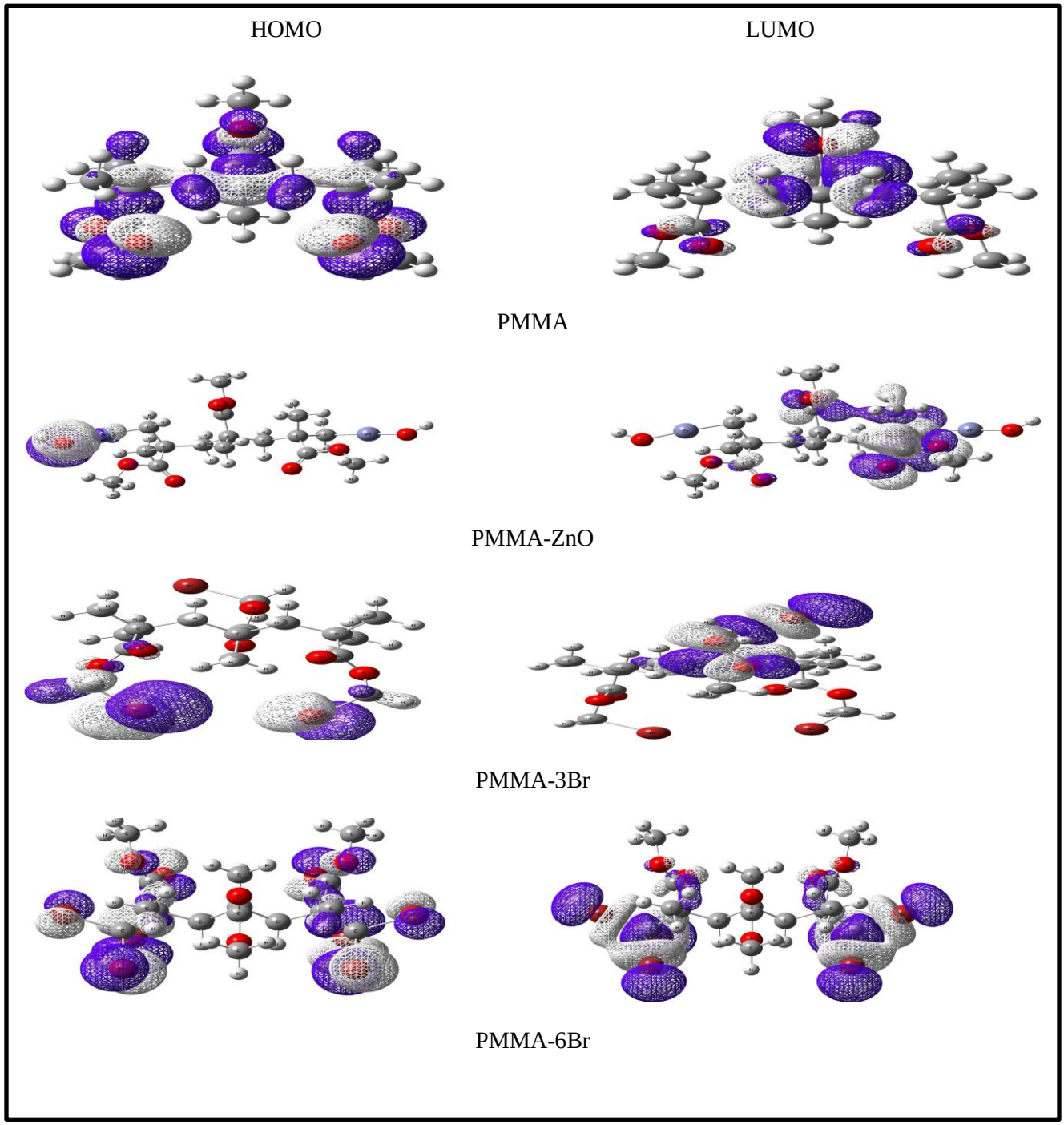

Figure (3.14):The distribution of HOMO and LUMO for (PMMA ,PMMA-ZnO and PMMA-Br nanocomposites).

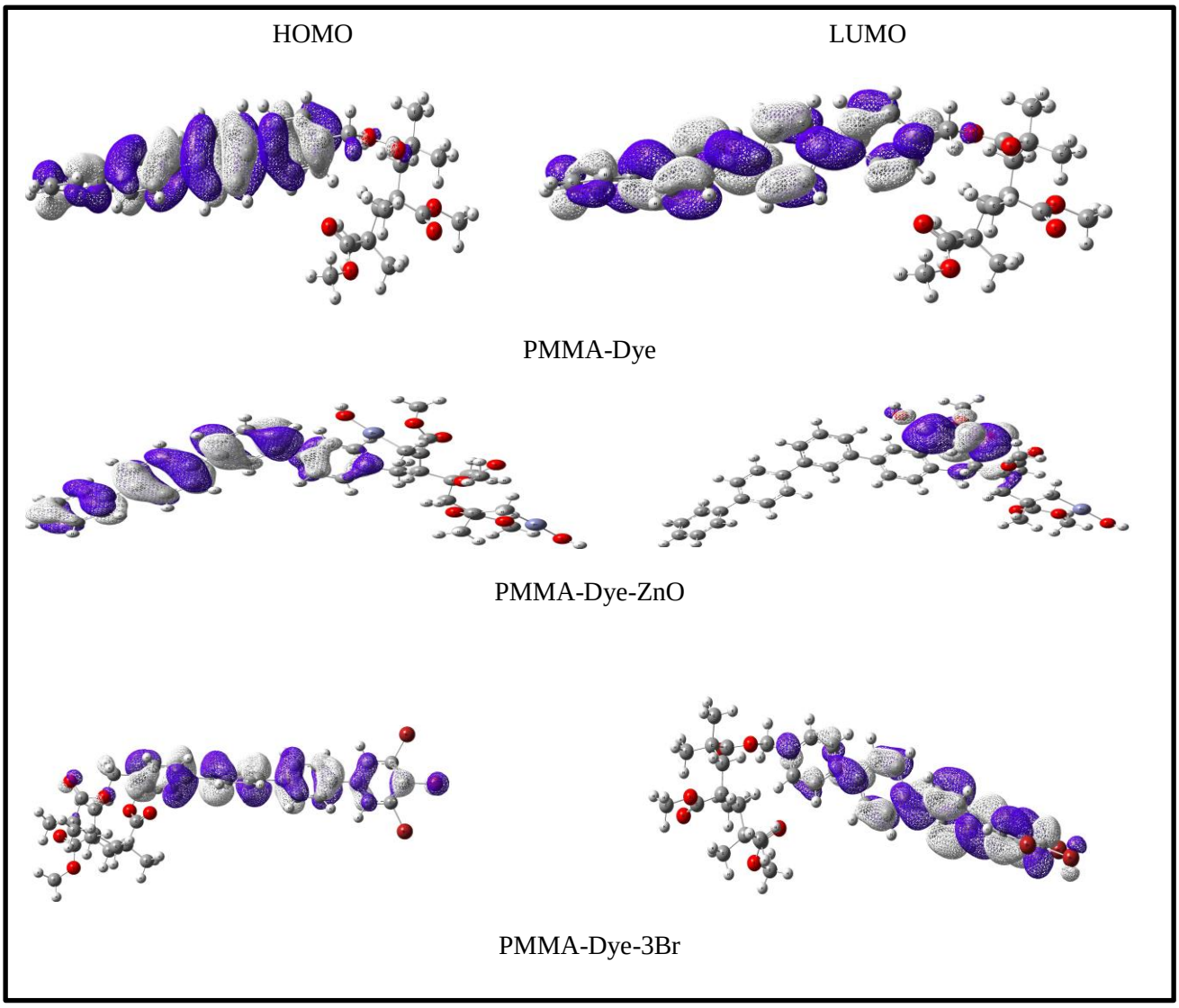

Figure (3.15):The distribution of HOMO and LUMO for (PMMA -Dye- nanocomposites).

3.6 Electronic Properties

Table 3.8 illustrates the values of some electronic properties from the time-independent DFT calculations by employing the B3LYP basis sets which calculated.

Ionization energy I_E and Electron affinity E_A for Polymers and its nanocomposite are calculated according to Koopman[s] theorem, those values showed that polymers;(PVA, PEG and PMMA) in compered with their nanocomposite, has the largest I_E in which is needed to high energy required to donate an electron and become a cation, relative to that required of other transitions, while (polymer-ZnO-Dye) has the lowest I_E. On the other hand, PVA-ZnO_2-Dye,PEG-ZnO-Dye and PMMA-6Br has the largest value of E_A in which such nanocomposite In comparison to the others, has high ability to receiving an electron to become an anion. In general, results of I_E and E_A for polymer-ZnO-Dye are suitable to appeared in many electronic applications.

Table 3.8 Illustrates the values of some electronic properties

Molecular	I_E(eV)	E_A(eV)	H (eV)	Sof$(eV)^{-1}$	ω(eV)	E_N(eV)
PVA						
PVA	6.9034	-0.5633	3.7333	0.1339	1.3459	3.1701
PVA-ZnO2	6.532	0.7110	2.9359	0.1703	2.2651	3.647
PVA-Dye	6.0030	0.8550	2.5740	0.1942	2.2840	3.4290
PVA-Dye-ZnO2	5.5508	1.4710	2.0399	0.2451	3.0214	3.5109
PEG						
PEG	6.7562	-1.5012	4.1287	0.1211	0.8361	2.6275
PEG-ZnO2	6.3674	0.5431	2.9121	0.1717	2.0498	3.4553
PEG-Dye	5.4585	1.2808	2.0889	0.2394	2.7179	3.3697
PEG-Dye-ZnO	5.3687	2.5524	1.4082	0.3551	5.5697	3.9606
PMMA						
PMMA	7.4422	0.4063	3.5180	0.1421	2.1887	3.9242
PMMA-ZNO	6.5344	0.5793	2.9776	0.1679	2.1245	3.5569
PMMA-DYE	5.7323	1.0727	2.3298	0.2146	2.4845	3.4025
PMMA-DYE-ZnO	5.3821	1.1932	2.0944	0.2387	2.5803	3.2876
PMMA-3Br	7.1987	0.8890	3.1548	0.1585	2.5917	4.0438
PMMA-6Br	7.0275	1.9437	2.5419	0.1967	3.9578	4.4856
PMMA-DYE-3Br	5.9168	1.4261	2.2453	0.2227	3.0017	3.6714

The calculated values of the electronic softness S is a reflection to the small separation between the valence band and conduction band in the polymer-nanocomposite under study. The results of S indicate to small excitation energies were required for an electron transfer from the valence band to conduction band .

The hardness decrease with addition nanoparticles to the pure Polymer, therefore all the nanocomposites are softer, and this reduces the resistance of a species to lose electrons[101,134 ,135]

From Table 3.8, The Polymer-nanocomposite have high values of electrophilic index ω, therefore, these complexes have ability to interacts with other surrounding species or molecules .

3.7 Density of States (DOS)

Figures (3-16) and (3-17) presented Density of states(DOS) for polymers and their nanocomposites were calculated as a function of energy by the density functional theory.

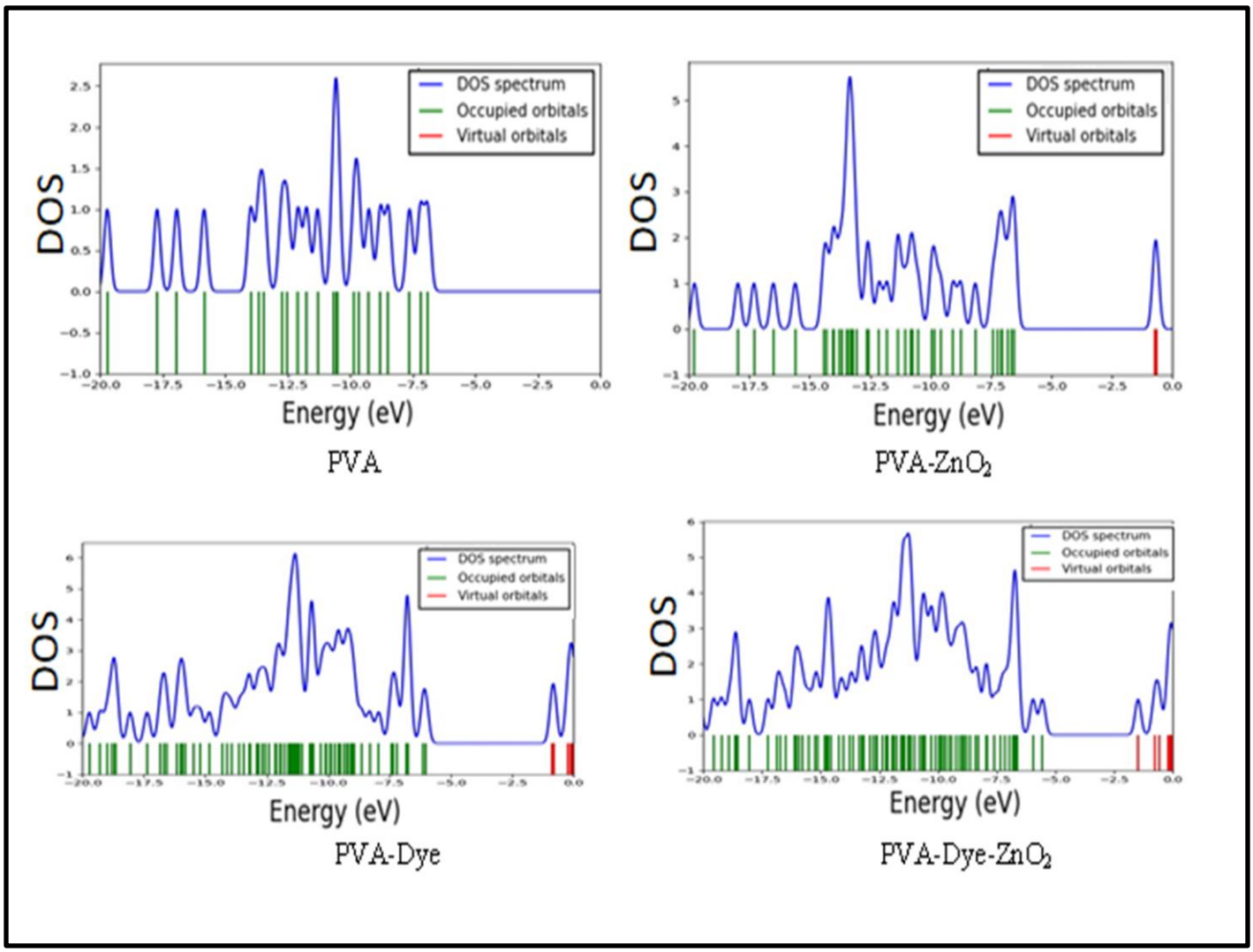

Figure (3.16): Density of state versus energy for PVA and PVA nanocomposites by DFT.

The results demonstrated that in all structures, the degeneracy of occupied molecular orbitals HOMO is greater than that of unoccupied molecular orbitals LUMO. According to the figures, the DOS was distributed more in the conduction band than in the valence band; this behavior is owing to the fact that the energies of LUMO are bigger than those of HOMO. In compared to pure polymers, electrons in nanocomposites can easily transition from the valence to conduction

band because the DOS in the conduction band is greater than the DOS in the valence band. This causes the nanocomposites to behave appropriately when interacting with other species.

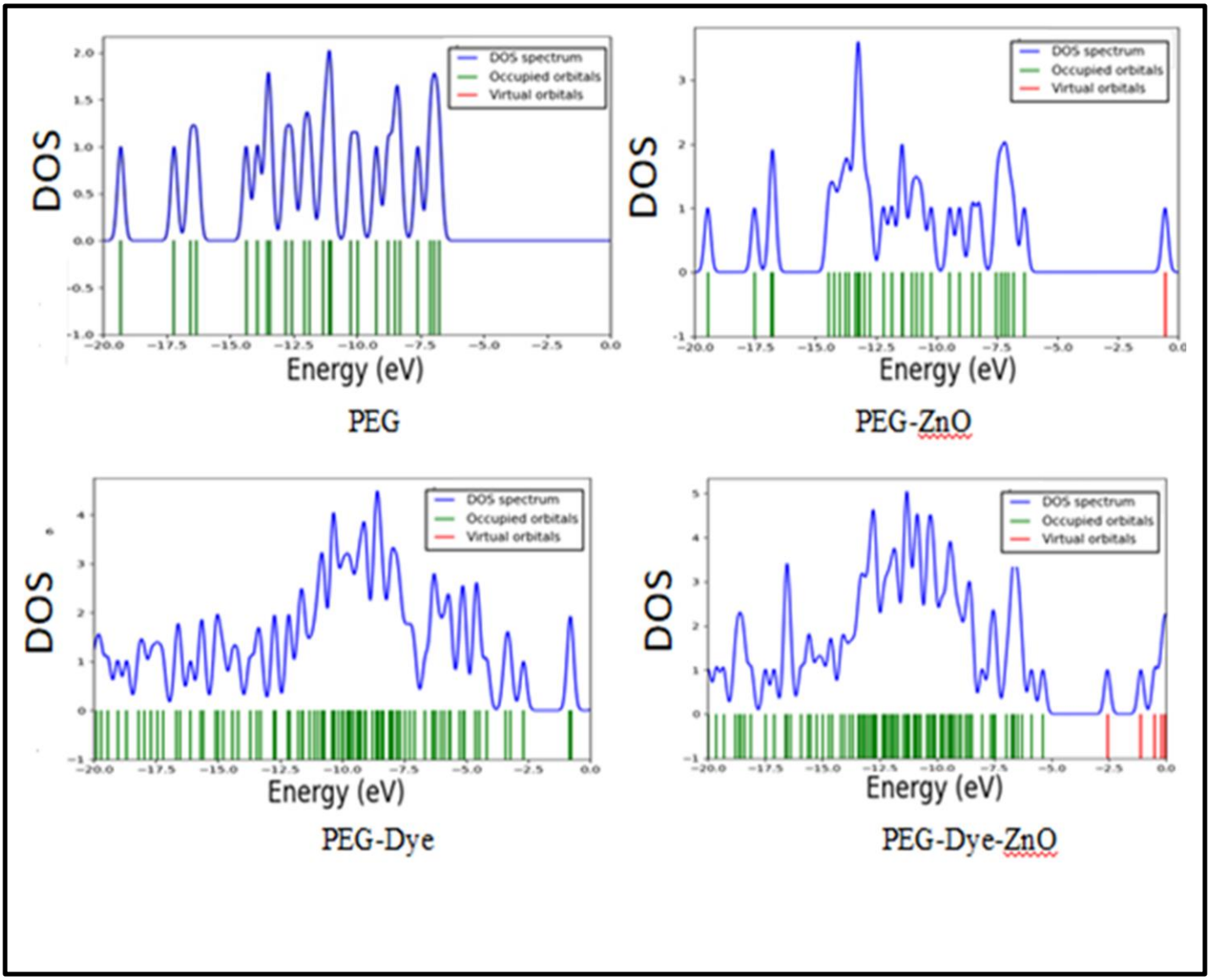

Figure (3.17): Density of state versus energy for PEG and PEG nanocomposites by DFT.

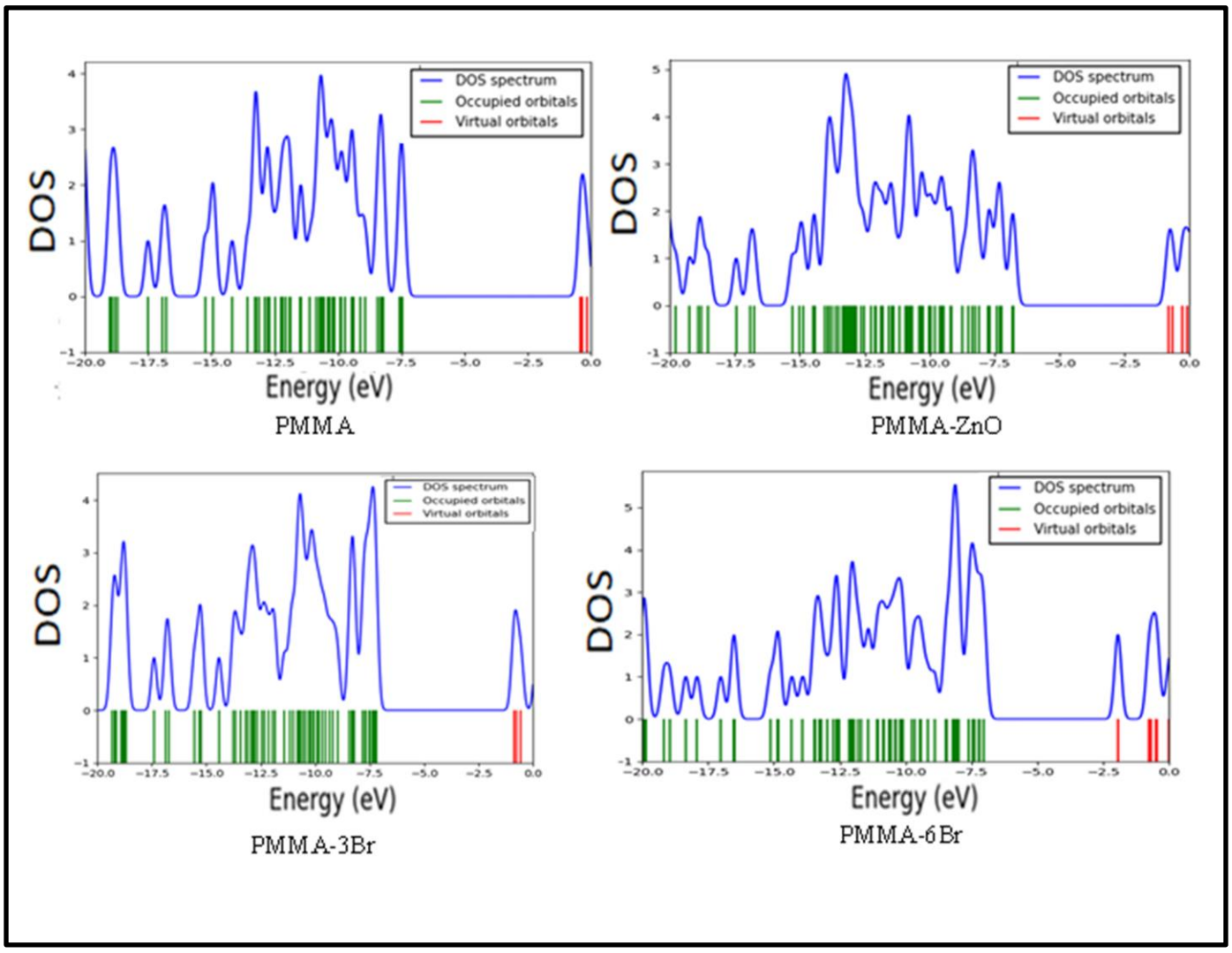

Figure (3.18): Density of state versus energy for PMMA and PMMA –ZnO and PMMA-Brnanocomposites by DFT.

As seen in Figure(3.19) for PMMA-Dye-ZnO, in this nanocomposite have doublet state in which the number of degeneracy of α and β occupied orbitals are greater than that the unoccupie orbitals. This property gave the complex to have high ability to an electron transfer from the valence band to conuction band.

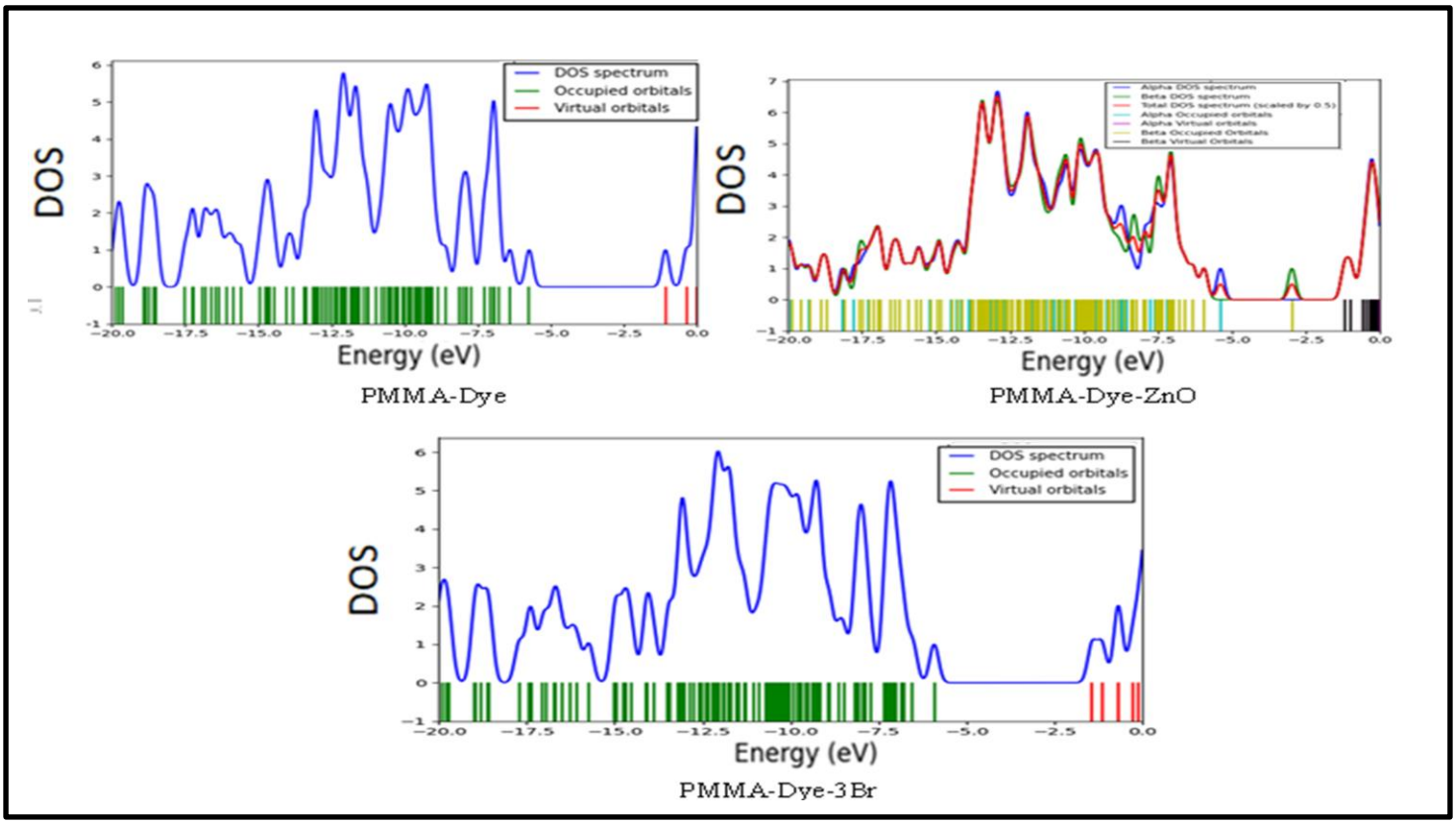

Figure (3-19):Density of state versus energy for PMMA and PMMA –Dye nanocomposites by DFT

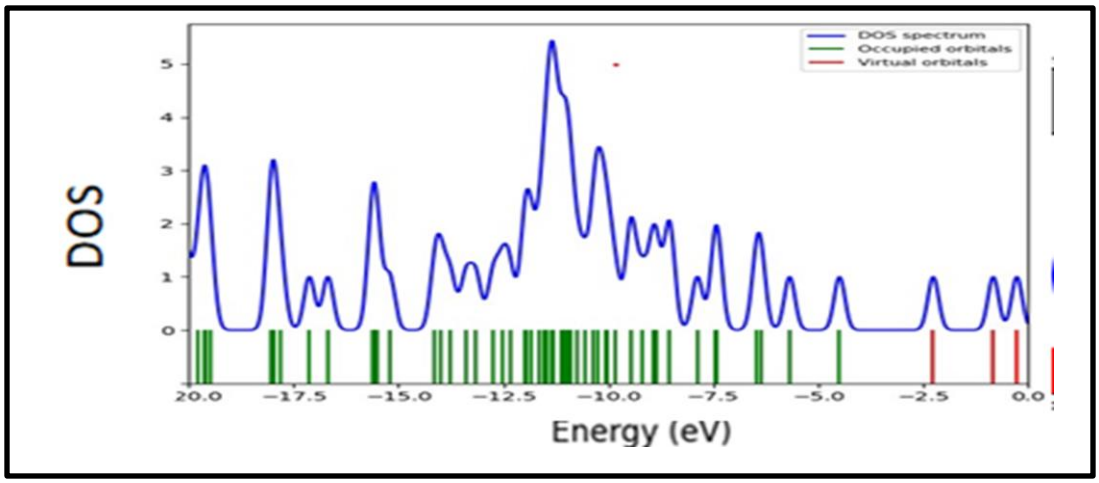

Figure (3-20):Density of state versus energy for Dye by DFT.

Chapter Four

Results and Discussion

Electrical Properties

4.1 Introduction

This chapter percent the electrical properties of Polymer-Dye(P-quaterphynel) nanocomposites. The mentioned properties were calculated as functions for energy and temperature. For the relaxation of the polymer-Dye nanocomposite under study SIESTA(Spanish Initiative for Electronic Simulation with Thousands of Atoms) have been used by employing the Generalized Gradient Approximation/Double Zeta Density Functional Theory GGA/DZ-DFT. For calculating the electrical properties for the studied nanocomposites Gollum program was employed. Initially, each one of the polymer-Dye nanocomposits was placed between two gold electrodes, then the nanocomposite plus restricted layers of the electrodes were allowable for a second time to create the relax structures.

4.2 Geometrical Optimization and Structural Properties

Figure 4.1 shows the optimized structures of the polymers-dye(tetramethyl-p quaterphynel) nanocomposite. After determination of the suitable distance Each nanocomposites was connected at the terminal ends to gold electrodes via carbon

atoms as anchors group. calculations using a combination of DFT and a non-equilibrium Green's function formalism were used in order to more accurately assess these molculer junction characteristics and behavior. Eight layers of (111)-oriented bulk gold with each layer consisting of 6×6 atoms and a layer spacing of 0.235 nm were used to create the molecular junctions, as shown in Figure(4.1).

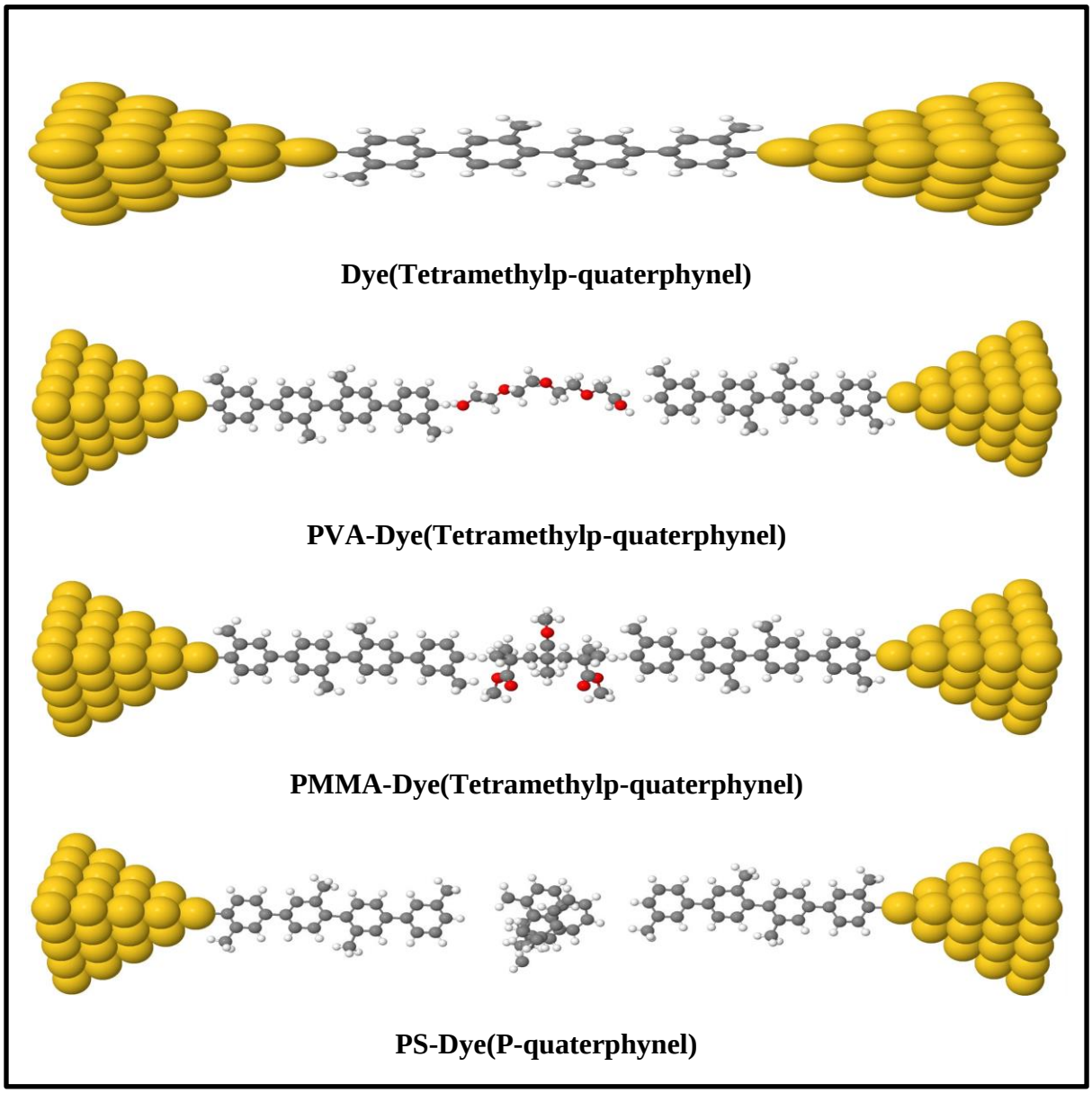

Figure (4.1): optimized molecules structures of Dye and Polymers-Dye.

Figure 4.1 shows optimized molecules under study in this thesis. Different molecular lengths and types of polymers serve to distinguish these molecules' structural characteristics. since the shortest molecule (Dye) has a molecule length of 1.637 nm, while the longest one (PVA) posses 5.044 nm. Table 4.1 displays each structural component in detail.

Table 4.1. The structural aspect of all molecules. L (C…C), is the molecule length, D (Au…Au), is the molecular length. X is the bond length (Au…C). Z (D – 0.25), is the theoretical electrodes separation. C–C is the carbon-carbon single bond.

Molecule	L (nm)	D (nm)	X (nm)	Z (nm)	C–C (nm)
Dye	1.637	2.117	0.241	1.867	0.149
PMMA	4.583	5.063	0.241	4.813	0.149
PVA	5.044	5.524	0.241	5.274	0.149
PS	4.734	5.214	0.241	4.964	0.149

4.2.1 Results of Conductance and Thermopower Properties

A one-dimensional structure with a randomly dispersed region will be used to represent the transmission coefficient T(E) at a molecular junction of electrons with energy moving from one electrode to another.

T(E) is a charestristic of the whole structure, which contian the electrodes, the nanocomposite, and the comunicated between the electrods and the nanocomposite.

However, a graph of T(E) vs E will show the isolated molecule's energy-level structure if the contact between the electrodes is poor, . If the isolated molecule possesses energy levels E, T(E) will display a serice of peaks (i.e. resonances) at energies around the levels E.

The effect of altering the polymer type of the nanocomposite on the results presente in Figures (4-2).

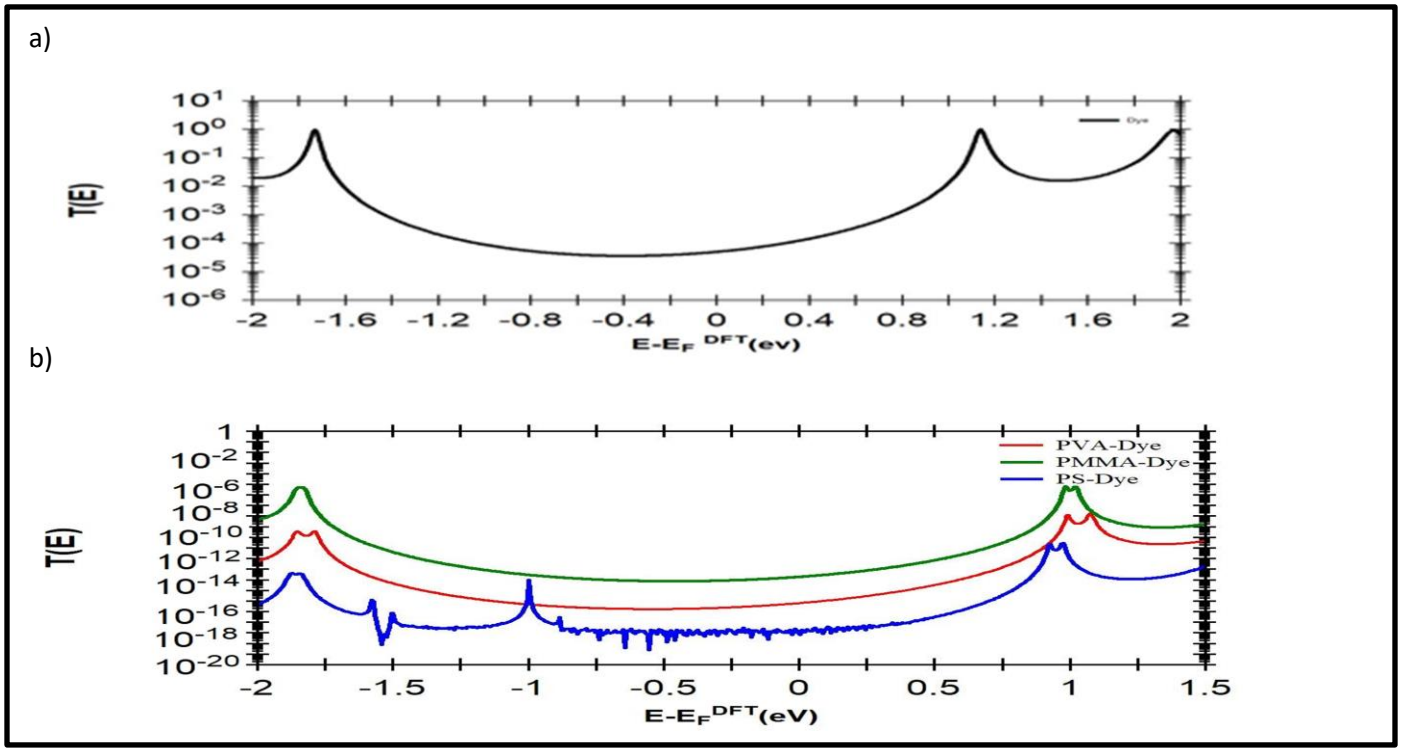

Figure(4.2):Transmission coefficient T(E) as a function of the Electron energy for a)Dye(Tetramethylp-quaterphynel) and b)polymers-Dye nanocomposite .

Depending on the aspects of the electrons path and quantum size effects these results could be explain, Since the molculaues length increased the length of the electrons' path, which in turn increased the tunneling distance, the transmission coefficient value decreased.. In contrast, with increasing of the molecular length the width of the HOMO-LUMO gap becomes narrow, which attributed to the quantum size role.

According to this, the shortest molecule dye (Tetramethyl p-quaterphynel) (2.117 nm) as shown in Figure (4.1), exhibits the highest transmission as shown in Figure (4.2)and the widest HOMO-LUMO gap , while the molecule PVA-Dye (5.524 nm) presented the lowest transmission than PMMA-Dye and Dye[136] ,also when compared with PS-Dye (5.214) its show lowest transmission coefficient and there is a rubbish in the transmission curve this can be explained due to that, when electrons travels through it suffer from scattering as well as when comparing with other polymers (PVA and PMMA) we can notice that the way that PS was contacted to Dye totally different thus it effect on the transmission curve and other properties, also we predicate there is another factor has been contributed on all result which is the Polymer type.

Another important result in PS-Dye curve shows, there is one resonance peak in the transport spectra for the structure there is one resonance peak in the

transport spectra for the structure , and this is a result of a destructive quantum interference between the discrete and continuous states .The order of the transmission is $T(E)_{Dye} > T(E)_{PMMA\text{-}Dye} > T(E)_{PVA\text{-}Dye} > T(E)_{PS\text{-}Dye}$.

worthy of note to mention that the HOMO and LUMO peak of polymer-Dye molecules in figure (4.2) is split into two peaks. This result due to the spin role [136].

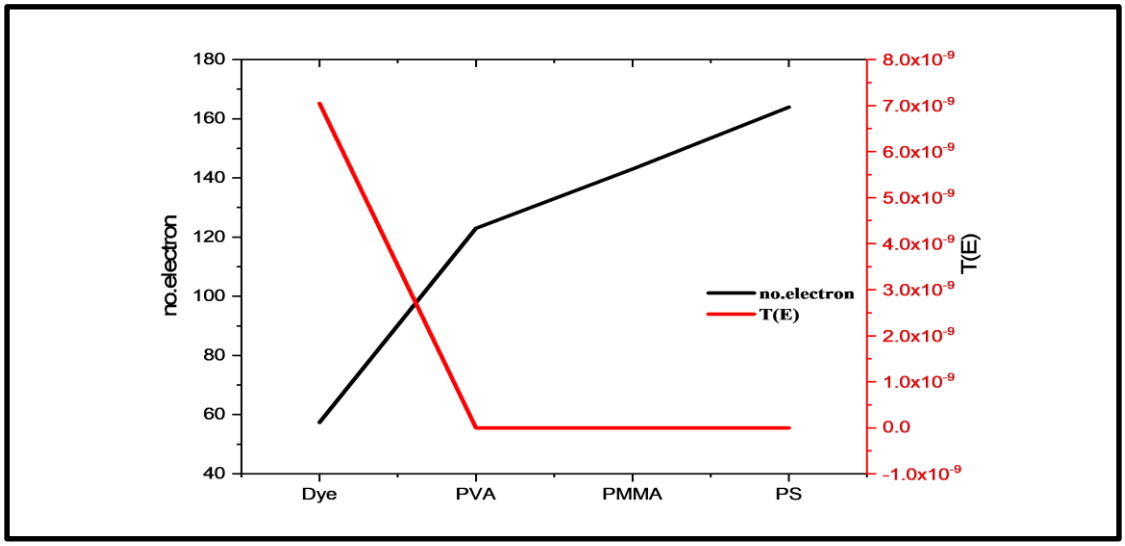

Figure 4.3. The transferred electrons from nanocomposites (Γ), and the electronic transmission coefficient of all nanocomposites

A very important result is shows Figure 4.3 , as it is familiar that increase in the transmission coefficient T(E) is due to the rising of number transferred electrons(Γ), but completely the opposite is provided by the results shown in Figure (4.3),where Dye that have the minimum Γ value, gives the maximum transmission coefficient. The opposite is true for Dye-PS, which has the maximum

value of Γ and the minimum value for the transition coefficient. These transport electrons of nanocomposit Dye, Dye-PVA, Dye-PMMA and Dye-PS could be wasted by recombination process.

Table 4.2. Γ is the transferred electrons. T(E) is the transmission coefficient.

NANOCOMPOSITE	Γ	T(E)
Dye	57.38	7.4691E-9
PVA-Dye	123	6.06644E-17
PMMA-Dye	143	1.89178E-14
PS-Dye	163.9	8.6596E-20

The most important feature for the electronic applications are Electrical conductance and thermopower. Here we are clearly show that the strong relation between these properties, because the high conductance result in low thermopower and vice versa, as presented in figures 4.3a,b,c.

Calculated thermopower values were negative and ranging between -0.178×10^{-4} Mvk^{-1} for Ps-Dye to -0.378×10^{-4} μVK^{-1} for PVA-Dye and positive for Dye 0.249×10^{-4} μVK^{-1} as shown in figure 4.4c and Table 4.2. These results demonstrate that the occupied molecular orbitals play an important role in determining the electrons transport mechanism which is a LUMO-dominated,as well as the value and sign of thermopower for all nanocomposite.

Figure 4.4d present the electronic figure of merit, which defined as ,quantity used to characterize the performance of a device, system or method, relative to its alternatives, the highest figure of merit value PVA-Dye nanocomposite (0.544×10-1), while the lowest value PS-Dye (0.1212×10-1) . These results prove that the calculated conductance value (see Figure 4.3b. certainly , the result of conductance (G), thermopower (S) and electronic figure of merit (ZTe), shown in Figures (4.3)a,b,c and d respectively, refer to a presence a relation between these factors. because the high G results in a low S, which leads to low ZTe.

Table 4.3. Thermopower (S). Electrical conductance (G/G0). Electronic figure of merit (ZTe). Threshold voltage (Vth).

Nanocomposite	S (μVK^{-1})	G/G_0	ZT_e	V_{th}(V)
Dye	0.249×10^{-4}	0.92×10^{-4}	0.243×10^{-1}	0.66
PMMA-Dye	-0.32×10-4	0.196×10-13	0.394×10-1	0.775
PVA- Dye	-0.378×10^{-4}	0.63×10^{-16}	0.54×10^{-1}	1.68
PS-Dye	-0.178×10^{-4}	0.154×10^{-18}	0.121×10^{-1}	1.554

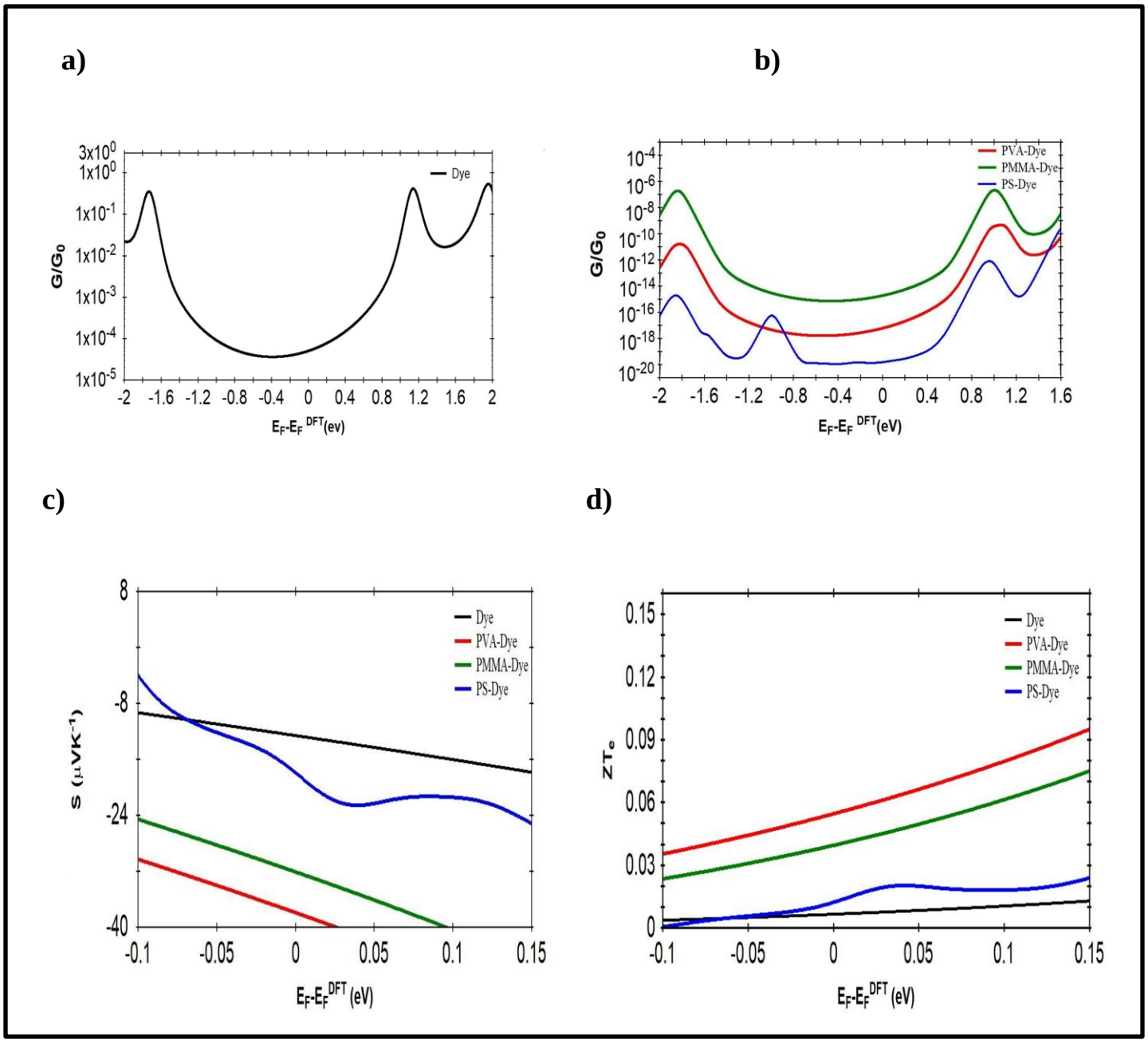

Figure (4-4):Electrical conductance as a function of the Fermi energy for a)Dye b)Polymer-Dye(Tetramethylp-quaterphynel) molecules c)thermoelectric power(polymers-dye and d)Figure of mert(polymers-dye).

Figure 4.5a,b,c shows molecular junctions with current-voltage (I–V) characteristics curves these results shows one of the most important physical parameters to determine and predicate the appropriate application, such as a field-effect transistor (FET), diodes and light emitting diodes which is threshold voltage (V_{th}). Threshold voltage is the minimum required voltage at which the device starts to turn on. to predict correct circuit behavior from a circuit simulator accurate modeling of threshold voltage is important . Figure 4.5a ,b,c show that the V_{th} of these nanocomposite is between 0.66 V to 1. 68 V (see Table 4.4).

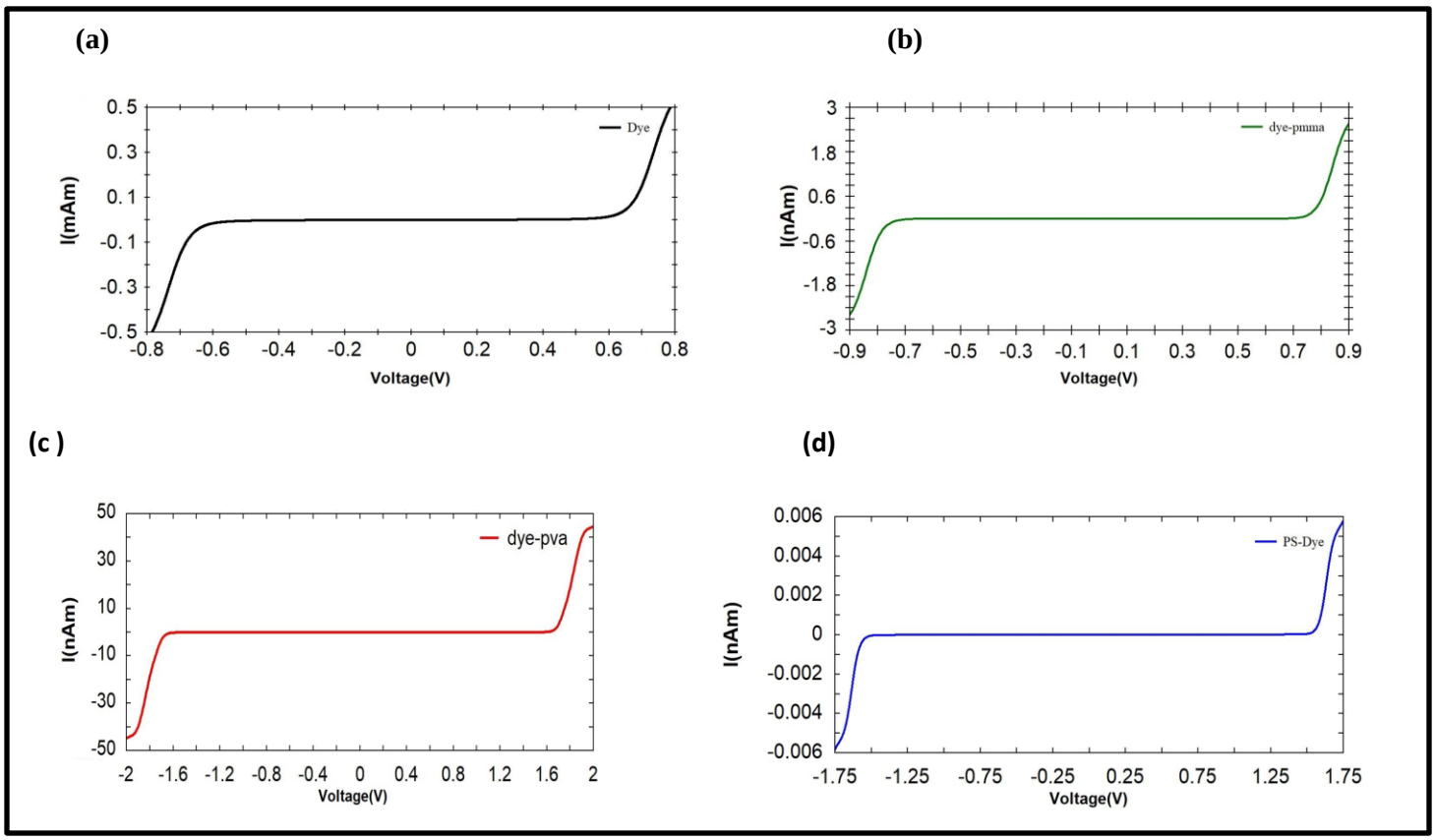

Figure(4.5):Current-Voltage characteristic of (a)Dye,(b)Dye-PVA (c) Dye-PMMA ,and (d)Dye-PS.

Chapter Five

Conclusions and Future Works

5.1 Conclusions

The conclusions of the present study can be summarized as follows:

1. This study used B3LYP/DFT to study the geometry optimization of polymer nanocomposites, the study found that polymer nanocomposites can be used for optoelectronic applications. This work provides new data for these nanocomposites, as no previous reference data was available.

2. The polymer-dye nanocomposite based on PVA, PEG, and PMMA can be a powerful device for optoelectronic applications, particularly for laser active mediums. This is because these structures have a high value of the emission oscillator strength (fem).

3. The addition of nanoparticles to the polymer affects the calculation of the HOMO, LUMO, and energy gap. The presence of nanoparticles decreases the energy gap of the studied polymer (PVA, PEG, and PMMA). PVA-ZnO nanocomposites have the smallest energy gap, which makes them a potential candidate for new electronic materials.

4. All the studied nanocomposites need a small amount of energy to become cations. This is because the ionization potential decreases with an increase in the number of atoms. However, the electronic affinity increases with an increase in the number of atoms.

5. The hardness decreases with an increase in the number of atoms. Therefore, all the nanocomposites are softer than pure polymer. This reduces the resistance of a species to lose electrons.

6. Adding polymer to dye minimizes T(E) due to an increase in the molecular length.

7. Adding metal oxide nanoparticles and dye increases the DOS. This is because adding dye or metal oxide nanoparticles causes an additional state.

8. The thermoelectric properties of polymer-dye junctions with different polymers (PVA, PMMA, PS) show that the existence of destructive quantum interference as an anti-resonance decreases the thermopower and figure of merit. However, it is a powerful strategy to enhance the electrical conductance. The position of the anti-resonance is not only an important factor to determine the sign of Seebeck coefficient, but also it is a useful technique to predict the value of Fermi energy.

9. The I-V characteristics show that Vth increases by adding polymers to dye. This shows that polymer effects overcome the dye.

In summary, this study has shown that polymer nanocomposites have potential applications in optoelectronics and thermoelectrics.

5.2 Future Works

1.Study of mechanical properties of (Polymer-ZnO) And (Polymer-ZnO-Dye) Nanocomposites.

2.Study of the effect of ZnO NPS on the electrical and thermal properties of (dye-Polymer-Dye) and (Polymer-ZnO) nanocomposites.

3.Study of the electronic and optical properties of Polymer with other metal oxides.

References

[1] Patra, J. K., & Baek, K. H.. "Comparative study of proteasome inhibitory, synergistic antibacterial, synergistic anticandidal, and antioxidant activities of gold nanoparticles biosynthesized using fruit waste materials", International journal of nanomedicine, 11,4691–4705, (2016).

[2] Q.Mary,"the future with nanotecnology", University of London,Group Report, (2011).

[4] Shukla, A. K., & Iravani, S., "Metallic nanoparticles: green synthesis and spectroscopic characterization" Environmental Chemistry Letters, 15(2), 223-231, (2017).

[5] Paul, D. R., & Robeson, L. M., "Polymer nanotechnology: nanocomposites", Polymer, 49(15), 3187-3204, (2008).

[6] J. Bhaiswar, M. Salunkhe, S. Dongre and B. Kumbhare, "comparative study on thermal stability and optical properties of PANI/CdS and PANI/PbS nanocomposite",IOSR Journal of Applied Physics, International Conference on Advances in Engineering Technology-2014 (ICAET-2014),80,79-82, (2013).

[7] Sharma, S. K., Prakash, J., Sudarshan, K., Sen, D., Mazumder, S., & Pujari, P. K., "Structure at Interphase of Poly (vinyl alcohol)–SiC Nanofiber Composite and Its Impact on Mechanical Properties: Positron Annihilation and Small-Angle X-ray Scattering Studies. Macromolecules, 48(16), 5706-5713, (2015).

[8] Ningaraju, S., Prakash, A. G., & Ravikumar, H. B., "Studies on free volume controlled electrical properties of PVA/NiO and PVA/TiO2 polymer nanocomposites",Solid State Ionics, 320, 132-147, (2018).

[9] J. Bhaiswar, M. Salunkhe, S. Dongre and B. Kumbhare,"Comparative study on thermal stability and optical propertiesof PANI/CdS nanocomposite",IOSR Journal of APPLIED Physics, International Conference on Advances in Engineering Technology-2014 (ICAET-2014),80,79-82, (2014).

[10] Sangawar, V., & Golchha, M., "Evolution of the optical properties of Polystyrene thin films filled with Zinc Oxide nanoparticles", Int. J. Sci. Eng. Res, 4(6), 2700-2705, (2013).

[11] Xiang, Q., Yu, J., & Jaroniec, M. "Graphene-based semiconductor photocatalysts", Chemical Society Reviews, 41(2), 782-796, (2012).

[12] Karabulut, S., "Metathesis chemistry: from nanostructure design to synthesis of advanced materials" (Vol. 243). Springer Science & Business Medi, ISBN 978-1-4020-6091-5,504 pages, (2007).

[13] Hermann, K., & Witko, M., "Theory of physical and chemical behavior of transition metal oxides: vanadium and molybdenum oxides. In Oxide surfaces",9,136-198, (2001).

[14] Sherrill, A. B., & Barteau, M. A., "Principles of reactivity from studies of organic reactions on model oxide surfaces". Chem Inform, 32(35), 409-442. (2001).

[15] Camargo, P. H. C.,"Satyanarayana, K. G., & Wypych, F. Nanocomposites: synthesis, structure, properties and new application opportunities". Materials Research, 12(1), 1-39,(2009).

[16] S. Mussa and F. Basheer, " Material Technology", Tripoli, (2003).

[17] D. Lukhassen and A. Meide ,"A advanced materials and structures and them fabrication process", 3th Edition, Narvik university college, HIN, (2003).

[18] Hdidar, M., Chouikhi, S., Fattoum, A., Arous, M., & Kallel, A. "Influence of TiO_2 rutile doping on the thermal and dielectric properties

of nanocomposite films based PVA. Journal of Alloys and Compounds", 750, 375-383,(2018).

[19] Jang, J. H., & Han, J. I. "Cylindrical relative humidity sensor based on poly-vinyl alcohol (PVA) for wearable computing devices with enhanced sensitivity. Sensors and Actuators", A: Physical, 261, 268-273, (2017).

[20] Rathod, S. G., Bhajantri, R. F., Ravindrachary, V., Sheela, T., Pujari, P. K., Naik, J., & Poojary, B. "Pressure sensitive dielectric properties of TiO_2 doped PVA/CN-Li nanocomposite", Journal of Polymer Research, 22(6), 1-14,(2015).

[21] Sirait, M., Gea, S., & Motlan, E. M., "Effect of mixed nanoparticles ZnS and polyvinyl alcohol (PVA) against nanocomposite mechanical properties of PVA/ZnS". American Journal of Physical Chemistry, 3(1),5-8,(2014).

[22] Kumar, N. B., Crasta, V., & Praveen, B. M. "Advancement in microstructural, optical, and mechanical properties of PVA (Mowiol 10-98) doped by ZnO nanoparticles", Physics Research International, Volume 2014, Article ID 742378, 9 pages, (2014).

[23] U. Ali, K. J. B. A. Karim and N. A. Buang, "A Review of the properties and applications of poly (methyl methacrylate) (PMMA)", Polymer Reviews, 55, 678-705, (2015).

[24] B. Cheng, J. Zhao, L. Xiao, Q. Cai, R. Guo, Y. Xiao and S. Lei, "PMMA interlayer-modulated memory effects by space charge polarization in resistive switching based on CuSCN-nanopyramids/ZnO-nanorods p-n heterojunction", Scientific Reports, 5,17859, (2015).

[25]D. H. Lee, J. M. Kim, K. T. Lim, H. J. Cho, J. H. Bang and Y. S. Kim, "Investigation of charge trapping mechanism for nanocrystal-based organic nonvolatile floating gate memory devices by band structure analysis electronic", Matterials Letters,12, 376-382, (2016).

[26]J. Jian, H. Chang, A. Vena and B. Sorli, Microsyst, "Study and design of resistive switching behaviors in PMMA-based conducting-bridge random-access memory (CBRAM) devices", Microsystem Technologies, 23, 1719-1725, (2015).

[27]S. L. Hsu, "Polymer data handbook", Oxford university press, 1102, (1999).

[28] "Common Plastic Resins Used in Packaging". Introduction to Plastics Science Teaching Resources. American Chemistry Council, Inc. Retrieved 24 December(2012).

[29] "Polystyrene (C8H8)n - Properties, Structure, Molecular Weight, Uses". BYJUS. Retrieved 18 June (2022).

[30] George A. & Digenis, Alexander G., "Method of fixing radioactive tritiated water in a stable tritiated polystyrene product", issued (2017).

[31] Bailey FE, Koleske JV). "Polyoxyalkylenes". Ullmann's Encyclopedia of Industrial Chemistry. Weinheim: Wiley-VCH (2000).

[32] Wei-Chi Laia , Wen-Bin Liaua,b,*, Tai-Tso Lina, "The effect of end groups of PEG on the crystallization behaviors of binary crystalline polymer blends PEG/PLLA",Polymer 45 3073–3080,(2004).

[33] Ganji M, Docter M, Le Grice SF, Abbondanzieri EA, "DNA binding proteins explore multiple local configurations during docking via rapid rebinding". Nucleic Acids Research. 44 (17): 8376–84 September (2016).

[34] Sheftel VO, "Indirect Food Additives and Polymers: Migration and Toxicology", CRC. pp. 1114–1116, (2000).

[35] S. Tasch, C. Brandstaetter, F. Meghdadi, G. Leising, G. Froyer, L. Athouel, Adv. Mater 9 ,(1997).

[36] M. Era, T. Tsutsui, S. Saito, Appl. Phys. Lett. 67 ,(1995)

[37] D.J. Gundlach, Y.Y. Lin, T.N. Jackson, D.G. Schlom, Appl. Phys. Lett. 71 ,(1997)

[38] Seliskar, C. J.; Landis, D. A.; Kauffman, J. M.; Aziz, M. A.; Steppel, R. N.; Kelley, C. J.; Qin, Y.; Ghiorghis, A. Characterization of New Excimer Pumped UV Laser Dyes 3. p-Quinqui-, Sexi-, Octi- and Deciphenyls. Laser Chem., 13, 19−28,(1993).

[39] Rinke, M.; Gü sten, H.; Ache, H. J., "Photophysical Properties and Laser Performance of Photostable UV Laser Dyes.2. Ring-Bridged P-Quaterphenyls",J. Phys. Chem, 90, 2666−2669, (1986).

[40] Schneider, D. J.; Landis, D. A.; Fleitz, P. A.; Seliskar, C. J.; Kauffman, J. M.; Steppel, R. N., "Characterization of New Excimer Pumped UV Laser Dyes I. p-Terphenyls", Laser Chem, 11, 49-62, (1991).

[41] Fleitz, P. A.; Seliskar, C. J.; Steppel, R. N.; Kauffman, J. M.; Kelly, C. J.; Ghiorghis, A., "Characterization of New Excimer Pumped UV Laser Dyes 2. p-Quaterphenyls", Laser Chem., 11, 99−107,(1991).

[42] Banerjee, M.; Shukla, R.; Rathore, R. Synthesis, " Optical, and Electronic Properties of Soluble poly-p-phenylene Oligomers as Models for Molecular Wires",J. Am. Chem. Soc, 131, 1780−6, (2009).

[43] Exciton, Exalite Datasheets; Vol. 13, (2012).

[44] Finnerty, J. J.; Koch, R. ,"Accurate Calculated Optical Properties of Substituted Quarter phenyleneNanofibers", J. Phys. Chem. A 114, 474−80, (2010).

[45] Jiang,a Yuan-Yuan Liu,a Xu Liu,a He Lin,a Kun Gao,a Wen-Yong Lai and Wei Huang ab,"Organic solid-state lasers: a materials view and future development", The Royal Society of Chemistry , (2020).

[46] B. H. Soffer and B. B. McFarland, Appl. Phys. Lett. 10,266–267,(1967).

[47] A. S. D. Sandanayaka, T. Matsushima, F. Bencheikh, S. Terakawa, W. J. Potscavage, C. Qin, T. Fujihara, K. Goushi, J.-C. Ribierre and C. Adachi, Appl. Phys. Express, 12, 061010,(2019).

[48] Bahaa H. Rabee, Majeed Ali Habeeb, Ahmad Hashim," Preparation of (PS-PMMA-ZnCl2) Composites and Study their Electrical and Optical Properties", International Journal of Science and Research (IJSR), Volume 3 Issue 10, October (2014).

[49] A.A. Attia a, M.M. Saadeldin, H.S. Soliman , A.-S. Gadallah , K. Sawa by, " Structural and optical properties of p-quaterphenyl thin films and application in organic/inorganic photodiodes", Optical Materials xxx 1-6,(2016).

[50] Hegedűs, P., Szabó-Bárdos, E., Horváth, O., Szabó, P., & Horváth, K. ,"Investigation of a TiO2 photocatalyst immobilized with poly (vinyl alcohol) ". Catalysis Today, 284, 179-186, (2017).

[51] Xiang, A., Liu, D., Tian, H., & Varada Rajulu, A. "Improved mechanical and wear resistance properties of silicon carbide/poly (vinyl alcohol) composites by silane coupling agents", Polymer Composites, 39(11), 3849-3857, (2018).

[52] Pham, N. K., Vu, N. H., Van Pham, V., Ta, H. K. T., Cao, T. M., Thoai, N., & Tran, V. C.,"Comprehensive resistive switching behavior of hybrid polyvinyl alcohol and TiO2 nanotube nanocomposites identified by combining experimental and density functional theory studies", Journal of Materials Chemistry C, 6(8), 1971-1979,(2018).

[53] Sihama Issa Salih , Jawad Kadhim Oleiwi and Arkan Saad Mohamed," Investigation Of Mechanical Properties Of Pmma Composite Reinforced With Different Types Of Natural Powders", Vol. 13, No. 22, November ,(2018).

[54] S. Ahmed, M. Hussein, S. Hadi and S. A. Mohammed, "Study the effect of thickness on optical properties of polymer PMMA thin films

preparated by spin coating method", Journal of University of Babylon, 27, 4, (2019).

[55] AnghamHazim ,Ahmed Hashim, and Hayder M. Abduljalil, " Novel (PMMA-ZrO2-Ag) Nanocomposites: Structural, Electronic, Optical Properties as Antibacterial for Dental Industries", International Journal of Emerging , Volume 7, No.8 August, (2019).

[56] S. A. Hussain, A. H. O. Alkhayatt, E. A. Mahdi and F. A. Najim, "Preparation of composite polymethylmethacrylate /silver (PMMA/Ag) films and studying the effect of silver nanoparticles on their optical properties", Test Engineering and Management, 83, 574-585, (2020).

[57] Hind Ahmed and Ahmed Hashim ," Design and characteristics of novel PVA/PEG/Y2O3 structure for optoelectronics devices", Journal of Molecular Modeling (2020).

[58] AnghamHazim, Hayder M. Abduljalil and Ahmed Hashim2," First Principles Calculations of Electronic, Structural and Optical Properties of (PMMA–ZrO2–Au) and (PMMA–Al2O3–Au) Nanocomposites for Optoelectronics Applications", Transactions on Electrical and Electronic Materials,(2021).

[59] Ameen Alwan Mohaimeed," Study the Influence of TiO2-Nanoparticles Doped in Polyvinyl Alcohol by Measuring Optical Properties of PVA Films", Iraqi Journal of Nanotechnology, synthesis and application 3 59-70,(2022).

[60] Ameen Alwan Mohaimeed and Bahaa H. Rabee," nfluence of Berry dye on some properties of nanocomposite(PVA/TiO2) films", Optical and Quantum Electronics ,(2023).

[61] Matthew Robert Davis, "Computational studies of noncovalent interactions in ligand-gated ion channels - and - Synthesis and characterization of red and near infrared cyanine dyes", PhD , California Institute Of Technology Pasadena, California, (2018).

[62] D. Young, "Computational Chemistry: A Practical Guide for Applying Techniques to Real-World Problems", NY: John Wiley & Sons, Inc., New York, (2001).

[63] Y. Wang, "Theoretical Studies on Water Splitting Using Transition Metal Complexes" Ph.D. Thesis, Royal Institute of Technology Stockholm, Sweden, 2014.

[64] E. Schrodinger, "An Undulatory Theory of The Mechanics of Atoms and Molecules" The Physics Review, Vol. 28, pp. 1049-1070, (1926).

[65] P. A. Cox, "Introduction to Quantum Theory and Atomic Structure", Oxford University Press Inc., New York, (1996).

[66] D. W. Rogers, "Computational Chemistry Using the PC", Third Edition, John Wiley & Sons, Inc., Hoboken, New Jersey, (2003).

[67] F. Jensen, "Introduction to Computational Chemistry", Second Edition, John Wiley & Sons, Ltd, , Denmark, (2007).

[68] W. J. Hehre, "A Guide to Molecular Mechanics and Quantum Chemical Calculations", Wavefunction, Inc., Printed in the United States of America, (2003).

[69] C. J. Cramer, "Essentials of Computational Chemistry: Theories and Models", Second Edition ,John Wiley & Sons Ltd., The Atrium, Southern Gate, Chichester, England, (2004).

[70] P. A. Cox, "Introduction to Quantum Theory and Atomic Structure", Oxford University Press Inc., New York, (1996).

[71] M. Mueller, "Fundamentals of Quantum Chemistry: Molecular Spectroscopy and Modern Electronic Structure Computations", Kluwer Academic/Plenum Publishers, New York, (2001).

[72] D. W. Rogers, "Computational Chemistry Using the PC", Third Edition, John Wiley & Sons, Inc., Hoboken, New Jersey, (2003).

[73] C. J. Cramer, "Essentials of Computational Chemistry: Theories and Models", Second Edition ,John Wiley & Sons Ltd., The Atrium, Southern Gate, Chichester, England, (2004).

[74] P. Hohenberg and W. Kohn, physical Review 136, 864, (1964).

[75] B. K. Lipkowitz, R. Larter, R. T. Cundari and D. B. Boyd, "Reviews in computational chemistry", 21, John Wiley and Sons, Inc., Hoboken, New Jersey, (2005).

[76] D. Young, "Computational Chemistry: A Practical Guide for Applying Techniques to Real-World Problems", NY: John Wiley & Sons, Inc., New York, (2001).

[77] M. Fayngold and V. Fayngold, "Quantum Mechanics and Quantum Information", Published by Wiley-VCH Verlag GmbH & Co. KGaA, Weinheim, Germany, 2013.

[78] R. O. Jones, "Density functional theory: Its origins, rise to prominence, and future", Reviews of Modern Physics, Vol. 87, pp. 897-923, (2015).

[79] W. Koch and M. C. Holthausen, "A Chemist's Guide to Density Functional Theory", Second Edition, Wiley-VCH Verlag GmbH, Weinheim, (2001).

[80] P. Piecuch, J. Maruani, G. Delgado-Barrio and Stephen Wilson, "Advances in the Theory of Atomic and Molecular Systems, Conceptual and Computational Advances in Quantum Chemistry", Springer Dordrecht Heidelberg London New York, (2009).

[81] A. Gonis, "The Pursuit of Fallacy in Density Functional. Theory: The Quest for Exchange and Correlation, the Rigorous Treatment of Exchange in the Kohn-Sham Formalism and the Continuing Search for Correlation", World Journal of Condensed Matter Physics, Vol. 4, pp. 200-225, (2014).

[82] A. F. Oliveira, G. Seifert, T. Heinec and H. A. Duarte, "Density-Functional Based Tight-Binding: an Approximate DFT Method", Journal Braz. Chem. Soc., Vol. 20, pp. 1193-1205, (2009).

[83] J. Kohanof, "Elements of first-principles electronic structure calculations : Theory and Computational Methods", Cambridge University Press, (2006).

[84] J. P. Perdew, A. Ruzsinszky, L. A. Constantin, Jianwei Sun, and G.I. Csonka, "Some Fundamental Issues in Ground-State Density Functional Theory: A Guide for the Perplexed", Journal Chemical Theory Computation., Vol. 5, pp. 902-908, (2009).

[85] K. Capelle, "A Bird's-Eye View of Density-Functional Theory", Brazilian Journal of Physics, Vol. 36, pp. 1318-1343, (2006).

[86] S. Botti, "Applications of Time-Dependent Density Functional Theory", Physica Scripta. Vol. 109, pp. 54-60, (2004).

[87] M. Petersilka, U. J. Gossmann, and E. K. U. Gross, "Excitation Energies from Time-Dependent Density-Functional Theory", Physical Review Letters, Vol. 76pp. 1212-1215, (1996).

[88] C. Fiolhais F. Nogueira and M. Marques, "A Primer in Density Functional Theory", Springer-Verlag Berlin Heidelberg New York, (2003).

[89] P. Samal, "Studies in Excited-State Density-Functional Theory", Ph.D. Thesis, Indian Institute of Technology, India, (2006).

[90] A. L. Miguel Marques, C. A. Ullrich, F. Nogueira, A. Rubio and K. Burke K.U. Eberhard, "Time-Dependent Density Functional Theory", Springer, Berlin Heidelberg, (2006).

[91] R. J. Reimers, "Computational Methods for Large Systems: Electronic Structure Approaches for Biotechnology and Nanotechnology", Published by John Wiley & Sons, Inc., Hoboken, New Jersey, (2011).

[92] W. Koch and M. C. Holthausen, *"A Chemist's Guide to Density Functional Theory"*, Second Edition, Wiley-VCH Verlag GmbH, Weinheim, (2001).

[93] Y. Li and C. A. Ullrich, *"Time-dependent V-representability on lattice* systems", The Journal of Chemical Physics, Vol. 129, pp. 1-9, (2008).

[94] I. C. Gerber and J. G. Angyan, "Hybrid functional with separated range", Chemical Physics Letters, Vol. 415, pp. 100-105, (2005).

[95] V. Sahni, "Quantal density functional theory II: approximation methods and applications", Springer-Verlag, Berlin Heidelberg, (2010).

[96]M. Mueller, "Fundamentals of Quantum Chemistry: Molecular Spectroscopy and Modern Electronic Structure Computations", Kluwer Academic/Plenum Publishers, New York, (2001).

[97] M. Schlipf, "Heyd-Scuseria-Ernzerhof Screened-Exchange Hybrid Functional for Complex Materials: All-Electron Implementation and Application", Reihe Schlüssel technologien, Key Technologies Band, Vol. 58, (2013).

[98] V. Sahni, *"Quantal Density Functional Theory II: Approximation Methods and Applications"*, Springer Verilog, Berlin Heidelberg, (2010).

[99] P. J. Stephens, F. J. Devlin, C. F. Chabalowski and M. J. Frisch, "Ab Initio Calculation of Vibrational Absorption and Circular Dichroism Spectra Using Density Functional Force Fields", The Journal of Physical Chemistry, Vol. 98, pp. 11624-11627, (1994).

[100] A. M. Pier and N. Kumar. “Quantum transport in mesoscopic systems: complexity and statistical fluctuations”, A Maximum Entropy

Viewpoint (Mesoscopic Physics and Nanotechnology) Reissue Edition, Oxford University Press on Demand, p. 416, (2010).

[101] A. Szabo and N. S. Ostlund, "Modem quantum chemistry: Introduction to advanced electronic structure theory", Dover Publication, Inc. Mineola, New York, p. 484, (2012).

[102] N. E. Economou, "Green's functions in quantum physics", Book, 3rd Edition, Springer Series in Solid-State, p. 474, (2006).

[103] W. J. Hehre, "A Guide to Molecular Mechanics and Quantum Chemical Calculations", Wave function, Inc., Printed in the USA, p. 796, (2013).

[104] R. Landauer, "Spatial variation of currents and fields due to localized scatterers in metallic conduction", IBM Journal of Research and Development, Vol.1(3), pp. 223-231, (1957).

[105] M. Buttiker, Y. Imry, R. Landauer, and S. Pinhas. "Generalized many channel conductance formula with application to small rings", Physical Review B, Vol. 31(10), pp. 6207-6215, (1985).

[106] R. Mera-Adasme , F. Mendizabal, C. Olea-Azar, S. Miranda-Rojas and P. Fuentealba, "A Computationally Efficient and Reliable Bond Order Measure", Journal American Chemica Society, Vol. 115(17), 4397–4405, (2011).

[107] E. Artacho, J. Gale, A. Garc, J. Junquera, P. Ordej, D. anchez-Portal and J. Soler, "SIESTA-trunk-462", Book, User's Guide, CIC-Nanogune and University of Cambridge, Fundaci on General Universidad Autonoma de Madrid, p. 141, (2014).

[108] E. Artacho, E. Anglada, O. Dieguez, J. D. Gale, A. Garcia, J. Junquera, R. M. Martin, P. Ordejon, J. M. Pruneda, D. Sanchez-Portal and J. M. Soler, “The SIESTA Method; Developments and Applicability”, IOP Science, Journal of Physics, Condensed Matter, Vol. 20(6), pp. 1−6, (2008).

[109] V. Nagarajan and R. Chandiramouli, "Quantum Chemical Studies on ZrN Nanostructures", International Journal of Chem. Tech. Research, Vol.6, pp. 21-30, (2014).

[110] L. G. Zhuo, W. Liao, and Z. X. Yu, "A Frontier Molecular Orbital Theory Approach to Understanding the Mayr Equation and to Quantifying Nucleophilicity and Electrophilicity by Using HOMO and LUMO Energies", Asian Journal of Organic Chemistry, Vol. 1, pp. 336-345, (2012).

[111] R. D. Bach, G. J. Wolber, and H. B. Schlege, "The Origin of the Barriers to Thermally Allowed, Six-Electron, Pericyclic Reactions: The Effect of HOMO-HOMO Interactions on the Trimerization of Acetylene", Journal American Chemical Society, Vol. 107, pp. 2838-2841, (1985).

[112] E. N. Zarkadoula, S. Sharma, J. K. Dewhurst, E. K. U. Gross and N. N. Lathiotakis, "Ionization potentials and electron affinities from

reduced-density-matrix functional theory", Physical Review A, Vol. 85, pp. 1-7, (2012).

[113] A. Szabo and N. S. Ostlund, "Modem quantum chemistry: Introduction to advanced electronic structure theory", Dover Publication, Inc. Mineola, New York, (1997).

[114] C. Zhan, J. A. Nichols and D. A. Dixon, "Ionization Potential, Electron Affinity, Electronegativity, Hardness, and Electron Excitation Energy: Molecular Properties from Density Functional Theory Orbital Energies", Journal Physical and Chemistry A, Vol. 107, pp. 4184-4195, (2003).

[115] Y. Karzazi, M. E. Belghiti1, F. El-Hajjaji and B. Hammouti," Density Functional Theory modeling and Monte Carlo simulation assessment of N-Substituted Quinoxaline Derivatives as Mild Steel Corrosion Inhibitors in acidic medium", Journal Mater. Environ. Sci., Vol. 7, pp. 3916-3929, (2016).

[116] A. Hinchliffe, "Molecular Modelling", John Wiley & Sons Ltd, England, (2003).

[117] O. A. Kolawole and S. Banjo, "Theoretical Studies of Anti-corrosion Properties of Triphenylimidazole Derivatives in Corrosion Inhibition of Carbon Steel in Acidic Media via DFT Approach", Analytical & Bioanalytical Electrochemistry, Vol. 10, pp. 136-146, (2018).

[118] D. M. York, "A Generalized Formulation of Electronegativity Equalization from Density-Functional Theory", International Journal of Quantum Chemistry: Quantum Chemistry Symposium, pp. 385-394, (1995).

[119] R. G. Pearson, "Chemical hardness and density functional theory", Journal Chemical Sciences., Vol. 117, pp. 369-377, (2005).

[120] R. V. Reyes and A. Aria, "Evaluation of group electronegativities and hardness (softness) of group 14 elements and containing functional groups through density functional theory and correlation with NMR spectra data", Journal Ecl. Quim., Sao Paulo, Vol. 33, pp. 69-76, (2008).

[121] L. Toukal, S. Keraghel, F. Benghanem and A. Ourari, "Electrochemical, Thermodynamic and Quantum Chemical Studies of Synthesized Benzimidazole Derivative as an EcoFriendly Corrosion

Inhibitor for XC52 Steel in Hydrochloric Acid", International Journal of Electrochemical Science, Vol. 13, pp. 951-974, (2018).

[122] M. A. Hossain, J. Jewaratnam, A. Ramalingam, J. N. Sahud and P. Ganesan, "A DFT method analysis for formation of hydrogen rich gas from acetic acid by steam reforming process", Journal the Science and Technology of Fuel and Energy, Vol. 11, pp. 49-60, (2018).

[123] T. Forbes, "Engineering System Dynamics", second edition, Taylor and Francis Group, France, (2007).

[124] J. David, "Introduction to Quantum Mechanics", second edition, Pearson Education International, America, (1995).

[125] D. K. C. Mac Donald, Thermoelectricity, Dover Publications, Inc., New-York, pp. 1–24, (2006).

[126] H. Vander, Journal of IEEE, Vol. 7, PP.97–126, (2006).

[127] A. D. Polyanin and V. F. Zaitsev, "Exact Solutions for Ordinary Differential Equations", Chapman & Hall/CRC Press, Boca Raton, second edition, (2003).

[128] A. D. Polyanin, " Linear Partial Differential Equations for Engineers and Scientists", Chapman & Hall/CRC Press, Boca Raton, (2002).

[129] M. J. Frisch, G. W. Trucks, H. B. Schlegel J. V. Ortiz, J. Cioslowski, and D. J. Fox, "Gaussian 09, revision A. 02 Gaussian, Inc", Wallingford CT., (2009).

[130] M. D. Hanwell, D. E. Curtis, D. C. Lonie, T. Vandermeersch, E. Zurek and G. R. Hutchison, "Avogadro: an advanced semantic chemical editor, visualization, and analysis platform", Journal of Cheminformatics Vol. 4(17), (2012).

[131] M. D. Hanwell, D. E. Curtis, D. C. Lonie, T. Vandermeersch, E. Zurek and G. Hutchison , "Avogadro: an advanced semantic chemical editor, visualization, and analysis platform", BMC Part of Springer Nature, Journal of Cheminformatcs, Vol. 4(17), (2012).

[132] D.D. Roy , A.K. Todd and M.M. John, "Gauss View 5.0.8. Gaussian, Inc.", Gaussian, Inc., Wallingford, (2009).

[133] E. Artacho, J. Gale, A. Garc, J. Junquera, P. Ordej, D. anchez-Portal and J. Soler, "SIESTA-trunk-462", Fundaci on General Universidad Aut onoma de Madrid, (2013).

[134] Angham Hazim Hussein," Theoretical and Experimental Studies on Structural and Optical Properties of New Nanocomposites for Using in Biomedical Applications",PhD.2020

[135] Hind A. Mohammed Roof Yasin," Characterization and Simulation of Poly Vinyl-Alcohol / Nanocomposites and Their Applications",PhD,2019

[136] Saba Razaq Salman, "Theoretical Investigation of Optoelectronic properties of a Promising Laser Active Medium,PhD,2022.

الخلاصة

تم فحص الهيكل الالكتروني لمركبات البوليمر النانوية المقترحة حديثا بشكل نظري باستخدام نظرية الكثافة الوظيفية DFT وذلك بتطبيق مستوى الدالة الهجينة B3LYP .

لحساب الخصائص الهيكلية والكهربائية والبصرية تم استخدام نظرية الكثافة الوظيفية في برنامج الكاوسيين وكذلك تم استخدام الطريقة المعتمدة على الزمن لحساب الاطياف فوق البنفسجية- المرئية للمركبات النانوية تحت الدراسة.

أظهرت النتائج أن مركبات البوليمر النانوية لديها فجوة طاقة منخفضة وهذا يعني ان الالكترونات الموجودة في المركب النانوي بالإمكان أثارتها بسهولة مما يؤدي الى تحسين الخصائص الكهربائية والبصرية.

يشير انخفاض فجوة الطاقة الى سلوكيات الكترونية مختلفة على سبيل المثال يشير هذا التغير الى انخفاض الصلادة وزيادة المرونة للمركبات النانوية, وهذا يشير إلى أن الجسيمات النانوية تتفاعل مع البوليمر بطريقة تغير البنية الإلكترونية للمادة.

كما تم توضيح الخصائص الإلكترونية والكهروحرارية لمركب صبغة-بوليمر-صبغة وهذا مهم لمستقبل الالكترونيات الجزيئية, حيث يمكن أن يؤدي الى تطوير أجهزة جديدة ذات اداء محسن.

ولتحقيق هذا الامر تم استخدام برنامج سياستا ودالة نظرية النقل الشكلية الوظيفية لـجريين

باختصار استخدمت هذه الدراسة نظرية كثافة الحالات لدراسة التركيب الالكتروني لمركبات البوليمر النانوية وللمركب بوليمر –صبغة- بوليمر , حيث أظهرت النتائج ان هذه المواد لديها القدرة على تحسين الخواص الكهربائية والبصرية وكذلك السلوك الكهرو حراري.

جمهورية العراق

وزارة التعليم العالي والبحث العلمي

جامعة بابل/ كلية العلوم للبنات

قسم فيزياء الليزر

تحليل نظري لخواص بوليمرات نانوية في تطبيقات البصريات الالكترونية

اطروحة

مقدمة إلى مجلس كلية العلوم للبنات - جامعة بابل

وهي جزء من متطلبات نيل درجة الدكتوراه في علوم فيزياء الليزر وتطبيقاته

من قبل

وسن مبدر خلخال

بكالوريوس علوم فيزياء الليزر /2011

ماجستير علوم فيزياء الليزر وتطبيقاته / 2015

بأشراف

أ. د.غالب عبد الوهاب علي الدهش

1444هـ **2023 م**